Theoretical and Experimental Investigations on Solar Distillation of İYTE Gülbahçe Campus Area Seawater

By

Pınar İlker ALKAN

A Dissertation Submitted to the
Graduate School In Partial Fulfillment of the
Requirements for the Degree of

MASTER OF SCIENCE

MS Program: Energy Engineering

İzmir Institute of Technology
İzmir, Turkey

April 2003

We approve the thesis of **Pınar İlker ALKAN**

Date of Signature

..... 18.04.2003
Prof. Dr. Ing. Gürbüz ATAGÜNDÜZ
Supervisor
Department of Mechanical Engineering

..... 18.04.2003
Prof. Dr. Necdet ÖZBALTA
Co-Supervisor
Department of Mechanical Engineering

..... 18.04.2003
Prof. Dr. Ali GÜNGÖR
Department of Mechanical Engineering

..... 18.04.2003
Assoc. Prof. Dr. Barış ÖZERDEM
Department of Mechanical Engineering

..... 18.04.2003

Assist. Prof. Dr. Gülden GÖKÇEN
Department of Mechanical Engineering

..... 18.04.2003
Prof. Dr. Ing. Gürbüz ATAGÜNDÜZ
Head of Interdisciplinary
Energy Engineering (Energy and Power Systems)

ACKNOWLEDGEMENT

I am greatly grateful to my director of thesis Prof.Dr.-Ing Gürbüz Atagündüz for his precious instruction. His dynamic thinks, his broad and profound knowledge and his patient instruction have given me a great help.

I would also express thanks to my co-adviser of thesis Prof.Dr. Necdet Özbalta for his instruction, suggestions and comments.

I want to thank the Mechanical Engineering Workshop Personnel for construction of solar still and İzmir Institute of Technology Research Fund for their financial support to complete this study.

I would also express thanks to Assoc.Prof.Dr. Uğur Sunlu for his help to analyze distilled water.

I am deeply grateful to
Prof. Dr.-Ing. Gürbüz ATAGÜNDÜZ
Prof. Dr. Necdet ÖZBALTA
Prof. Dr. Ali GÜNGÖR
Assoc. Prof. Dr. Barış ÖZERDEM
Assist. Prof. Dr. Gülden GÖKÇEN
for examination of the thesis.

I would like to give my special thanks to Tolga Ayav for his support and helps. I would also thank to all my friends especially Farah Tatar and Nurdan Yıldırım.

Especially, I would like to give my special thanks to my mother and my father whose patience enabled me to complete this work.

ABSTRACT

The world demand for potable water is increasing steadily with growing population. Water desalination using solar energy is suitable for potable water production from brackish and seawater.

In this study, a solar distillation in a single basin is studied theoretically and experimentally in İzmir Institute of Technology Gülbahçe Campus area. The still was constructed using a 2100 mm x 700 mm base area, and the glass cover of still inclined at 38^{0}. Temperatures of glass cover, seawater inside the still, seawater interface, inside moist and ambient air and humidity was recorded continuously and distilled water was measured for each hour.

Afterwards, to obtain extra solar energy, the aluminum reflector (2100 mm x 500 mm) was assembled to the still and effect of the reflector on the still productivity was examined.

And also in this study, theoretical study was examined to describe the energy balances for the glass cover, seawater interface, black plate at the bottom and overall still and also to find still productivity.

ÖZ

Artmakta olan dünya nüfusu ile birlikte kullanılabilir su ihtiyacı da gittikçe artmaktadır. Güneş enerjisi kullanarak deniz suyu veya tuzlu sudan, kullanılabilir su eldesi uygun bir yöntemdir.

Bu çalışmada, bir basit sera tipi güneş enerjili damıtıcı üzerine teorik ve deneysel çalışmalar İzmir Yüksek Teknoloji Enstitüsü Gülbahçe Kampüsü'nde yapılmıştır. Damıtıcı 2100 mm x 700 mm alan üzerine kurulmuş ve damıtıcının cam örtüsü 38^0 eğimle yerleştirilmiştir. Cam örtü sıcaklığı, damıtıcı içindeki su sıcaklığı, su yüzey sıcaklığı, iç ve dış hava sıcaklıkları ve havadaki nem oranı her saat için ölçülmüştür.

Alüminyum reflektör (2100 mm x 500 mm), ekstra güneş enerjisi elde etmek amacıyla damıtıcıya monte edilmiş ve reflektörün damıtıcı verimliliği üzerindeki etkisi incelenmiştir.

Ayrıca bu çalışmada, cam örtü, denizsuyu yüzeyi, siyah taban ve tüm damıtıcı için enerji denkliklerini tanımlamak ve damıtıcı verimliliğini bulmak için teorik bir çalışma yapılmıştır.

TABLE OF CONTENTS

LIST OF FIGURES

LIST OF TABLES

NOMENCLATURE

ϑ_g: Temperature of glass cover, ^0C

ϑ_b: Temperature of bottom, ^0C

ϑ_r: Temperature of inside moist air, ^0C

ϑ_i: Seawater interface temperature, ^0C

ϑ_l: Temperature of the liquid at the bottom, ^0C

ϑ_a: Temperature of ambient air, ^0C

T_{sky}: Sky temperature, ^0K

I_s: Solar Intensity, W/m^2

$q_{k,l}$: Heat Transfer from the liquid at the bottom into the atmosphere through the bottom area, W/m^2

$q_{k,b}$: Heat transfer from the bottom into the atmosphere, W/m^2

$q_{k,air}$: Heat transfer from the inside moist air through the circumferential area into the atmosphere, W/m^2

$q_{h,g}$: Convective heat transfer from the glass cover into the atmosphere, W/m^2

$q_{g,s}$: Net radiative heat transfer from the glass cover into the sky, W/m^2

d_g: Transmittance of glass

r_g: Reflectivity of glass

m^*_{cw}: Mass flow rate of condensed water, kg/m^2s

$m^*_{m,air}$: Mass flow rate of moist air, kg/m^2s

h_r: Convective heat transfer coefficient at moist air, $W/m^2\,^0K$

h_a: Convective heat transfer coefficient at ambient air, $W/m^2\,^0K$

k_l: Overall heat transfer coefficient for heat transfer from the liquid at the bottom into the atmosphere through the bottom area, $W/m^2\,^0K$

k_r: Overall heat transfer coefficient for heat transfer for heat transfer from the inside moist air through the circumferential area into the atmosphere, $W/m^2\,^0K$

k_b:Overall heat transfer coefficient for heat transfer from the bottom into the atmosphere, $W/m^2\,^0K$

λ: Thermal conductivity, W/m^0K

A_b: Bottom area covered by the seawater, m^2

A_g: Glass cover surface area, m^2

$A_{k,air}$: Circumferential area of the solar still covered by the inside moist air, m^2

$A_{k,l}$: Circumferential area of the solar still covered by the seawater, m^2

ρ: Density, kg/m^3

w : Wind velocity, m/s

h_M: Mass transfer coefficient for non permeable plane, m/s

$h_{M,h}$: Mass transfer coefficient for semi permeable plane, m/s

β : Thermal expansion coefficient, ^0K

Chapter 1

INTRODUCTION

Today fresh water demand is increasing continuously, because of the industrial development, intensified agriculture, improvement of standard of life and increase of the world population. Only about 3 % of the world water is potable and this amount is not evenly distributed on the earth. On deserts and islands where underground water is not readily obtainable and the cost of shipping the places is high it is worthwhile to take into consideration of producing potable water from saline water, using solar energy that is in abundance in deserts.

Large quantities of fresh water are required in many parts of the world for agricultural, industrial and domestic uses. Lack of fresh water is a prime factor in inhibiting regional economic development. The oceans constitute an inexhaustible source of water but are unfit for human consumption due to their salt content, in the range of 3 % to 5 %. Seawater and sometimes brackish water desalination constitute an important option for satisfying current and future demands for fresh water in arid regions. Desalination is now successfully practiced in numerous countries in the Middle East, North Africa, southern and western US, and southern Europe to meet industrial and domestic water requirements.

The supply of drinking water is a growing problem for most parts of the world. More than 80 countries, which between then have 40 % of the world's population, are being suffered from this problem. In order to solve this problem, new drinking water sources should be discovered and new water desalination techniques be developed. In many countries, fossil fuel burning water desalination systems are currently used. These systems can range up to 10 ton/day in capacity. The main water desalination or purification methods are distillation, reverse osmosis and electrodialysis. For bigger systems, reverse osmosis and electrodialysis are more economical, but for smaller ones, simple solar stills could be preferred because of their low costs. These days, in a number of countries including West-Indian Islands, Kuwait, Saudi Arabia, Mexico and Australia, these type of distillation units exist.

Desalination has become increasingly important in providing an economically viable solution to the problem of decreasing fresh water resources. There are many

factors to take into consideration to make a new technology “sustainable.” As we begin the 21st century, we must look towards cleaner sources of energy. Fossil fuel resources will soon be expired due to our rate of consumption. Cleaner energies such as natural gas, solar power, and photovoltaic technology must be integrated into desalination technology.

Solar desalination is a process where solar energy is used to distill fresh water from saline, brackish water for drinking purposes, charging of the batteries and medical appliances, etc. In recent years desalination of water has been one of the most important technological work undertaken in many countries. Many areas in Middle East and elsewhere have little or no natural water supplies which can be used for human consumption and, hence, depend heavily on water produced by desalination. Several methods of solar water desalination are known. Many workers indicate that the utilization of solar energy for water desalination is becoming more attractive as the cost of energy is continuously increases. Solar desalination is particularly important for locations where solar intensity is high and there is a scarcity of fresh water. The methods of solar water desalination are classified according to the way in which solar energy is used; the best-known method is the direct use of solar energy.

Small production systems as solar stills can be used if fresh water demand is low and the land is available at low cost. High fresh water demands make industrial capacity systems necessary. These systems consist of a conventional seawater distillation plant coupled to a thermal solar system. This technology is known as indirect solar desalination. Many small size systems of direct solar desalination and several pilot plants of indirect solar desalination have been designed and implemented. Nevertheless, in 1996 solar desalination was only 0.02 % of desalted water production.

Another advantage of desalination is that it will never run out its “raw material.” Because the facility is located right next to the ocean, and the ocean is so vast. Because of this, desalination is a “drought-proof” resource that is constantly able to produce fresh water regardless of the amount of rainfall. This is a great advantage if the desalination process is located in an agricultural area.

Chapter 2

PROPERTIES OF WATER

2.1.Product Water

Most people assume that the different standardizing bodies drew up their standards after studying how much of each of the various chemicals it was desirable to have present. Unfortunately, apart from a few well-known toxic elements, chemical standards for water are based on non-medical parameters such as corrosion, taste, and scale formation.

Despite this exclusiveness, product water should comply with purity standards similar to those in Table 2.1.

Table 2.1. Purity Standards of Water[1]

Substance	Concentration*, mg/l		Troubles	Approximate Concentration in seawater, mg/l
	Maximum acceptable	Maximum allowable		
Total solids	500	1500		36000
Chloride	200	600	Taste and corrosion	19800
Sulphade	200	400	Gastro-intestinal irritatio	2760
Calcium	75	100	Scaling	420
Magnesium	30	150	Taste and scaling	1330
Fluoride	0,7	1,7	Fluorosis	1,5
Nitrate	< 50	100	Methaemoglobinaemia	small
Copper	0,05	1,5	Taste	0,01
Iron	0,1	1	Taste and discoloration	0,02
Sodium chloride	250	...		30000
Hydrogen (in pH units)	7.0 -8.5	6.5 - 9.2		

*International Standards for Drinking Water, World Health Organization, and/or European Standards for drinking Water

2.2. Feed Water

The composition of the feed water is important for many reasons. The principal ones are as follows:

- It is required in the production of the physical property data used for design purposes. These data are generally related to the total quantity of dissolved in the water, and only related to a much lesser extent to the proportions of the different ions.
- In design for operation without the formation of scale, the composition of scale-forming ions such as calcium, magnesium, sulfate, and bicarbonate is important. The total quantity of salts dissolved in the water is only relevant in that it alters the solubility or activity of the scale forming compounds. Thus brackish water may have only one-third of the salinity of seawater but may contain a high concentration of calcium-ions and produce larger amounts of scale.
- It is required when the desalination process is being selected. In general, the efficiencies of distillation processes such as electrodialysis and reverse osmosis are strongly dependent on salinity. Hence the membrane processes are more widely used with brackish water and less widely with seawater.

2.2.1.Brackish Water

From desalination point of view feed water means seawater, brackish water, or contaminated fresh water. With brackish or contaminated feed waters it is necessary to determine the composition of the individual ions. The salinities of typical samples are indicated in Table 2.2.

Table 2.2. Typical Water Supplies[1]

Water sample	Total dissolved solids, mg/l
Well water	300-500
Typical river water	200-750
Typical brackish water	1500-6000
Typical seawater	36000
Water for irrigation	1000

2.2.2.Seawater

Water is probably the most efficient solvent known to man and consequently the oceans contain traces, at least, of every naturally occurring element. Table 2.3 gives the major components of seawater.

Various forms of circulation are present, and over many centuries this mixing has brought the oceans to a stage where for all practical purposes the relative composition of seawater is constant. This does not imply that all samples have the same composition, but merely that all ions are present in the same ratios and that the only variation is in the amount of pure water present. One this was established it meant that if the percentage composition of any one ion was measured then the amount of all other ions could be accurately found by calculation.

Table 2.3. Major Components of Seawater[1]

Ion	Concentration, g/kg of seawater	
	Salinity 35 g/kg	Chlorinity 19 g/kg
Sodium	10.759	10.561
Magnesium	1.294	1.272
Calcium	0.413	0.4
Potassium	0.387	0.38
Strontium	0.0135	0.013
Boron	0.004	0.004
Chloride	19.354	18.98
Sulphate	2.712	2.648
Bromide	0.067	0.065
Fluoride	0.0013	0.0013
Bicarbonate	0.142	0.139

2.3.Artificial Seawater

Although it is sometimes necessary to make measurements with natural seawater, most physical properties required in desalination can be determined from artificial seawater. Table 2.4 gives the composition of artificial seawater. Table 2.5 shows comparison of artificial and natural seawaters. [1]

Table 2.4. Composition of artificial Seawater

Compound	Quantity in g/l	
	IP/ASTM seawater	"Ca free" seawater
NaCl	24.53	26.9
$MgCl_2.6H_2O$	11.1	....
$MgCl_2$	....	3.2
Na_2SO_4	4.09	....
$MgSO_4$	....	2.2
$CaCl_2$	1.16	....
KCl	0.69	0.6
$NaHCO_3$	0.2	....
KBr	0.1	0.1
H_3BO_3	0.03	0.03
$SrCl_2.6H_2O$	0.04	....
NaF	0.003	0.003

Table 2.5. Comparison of Artificial and Natural seawaters

Ratio	Natural seawater	Artificial Seawater	
		IP/ASTM	"Ca-free"
Na/Cl	0.5556	0.5559	0.5573
Ca/Cl	0.021	0.016	....
Mg/Cl	0.067	0.067	0.067
K/Cl	0.02	0.02	0.018
SO_4/Cl	0.1395	0.1396	0.0925
Br/Cl	0.0034	0.0035	0.0037
Sr/Cl	0.0007	0.0005	....
F/Cl	7×10^{-5}	4×10^{-5}	4×10^{-5}
H_3BO_3/Cl	0.0014	0.0015	0.0016

Chapter 3

SOLAR RADIATION

The sun is a “more or less average” star with a mass equal to nearly one – third of a million Earths. Spectral measurements have confirmed the presence of nearly all the known elements in the sun. As is typical of many stars, about 94% of the atoms and nuclei in the outer parts are hydrogen, about 5.9 % are helium, and a mixture of all the other elements make up the remaining one – tenth of one percent. A gaseous globe with a radius of $7x10^5$ km, it has a mass about $2x10^{30}$ kg. This grater than the earth’s mass by a factor of about 330000. The total rate of energy output from the sun $3.8x10^{33}$ ergs/s ($3.8x10^{23}$ kW). At a mean distance of $1.496x10^8$ km from the sun, the earth intercepts about 1 part in 2 billion of this energy.

Most of the energy produced in the fusion furnace of the sun transmitted radially as electromagnetic radiation popularly called sunshine or solar energy. The sun radiates at an effective surface temperature about 5800 K.

Solar radiation is a general term for the electromagnetic radiation emitted by the sun. This radiation can be captured and converted to useful forms of energy such as heat and electricity, using a variety of technologies[3].

Solar radiation drives atmospheric circulation. Since solar radiation represents almost all the energy available to the earth, accounting for solar radiation and how it interacts with the atmosphere and the earth's surface is fundamental to understanding the earth's energy budget.

Solar radiation reaches the earth's surface either by being transmitted directly through the atmosphere direct solar radiation (direct beam or extraterrestrial radiation), or by being scattered or reflected to the surface diffuse solar radiation. About 50 percent of solar (or short-wave) radiation is reflected back into space, while the remaining short-wave radiation at the top of the atmosphere is absorbed by the earth's surface and re-radiated as thermal infrared (or long wave) radiation.

As sunlight passes through the atmosphere, some of it is absorbed, scattered, and reflected by air molecules, water vapor, clouds, dust, and pollutants from power plants, forest fires, and volcanoes. This is called diffuse solar radiation. The solar radiation that reaches the surface of the earth without being diffused is called direct beam solar

radiation. The sum of the diffuse and direct solar radiation is called global or total solar radiation. Atmospheric conditions can reduce direct beam radiation by 10 percent on clear, dry days, and by 100 percent during periods of thick clouds.

The third type of radiation that is sometimes present at the glazing of a solar collector or a window is reflected radiation. This is either diffuse or direct radiation reflected from the foreground onto solar aperture. The amount of reflected radiation varies significantly with the nature of foreground, being relatively higher for a light colored environment near the collector and relatively lower for a dark colored environment. The motion of the sun is important in determining the angle at which beam radiation strikes a surface. Therefore the first topic dealt with quantitavely has to do with the seasonal location of the sun relative to a viewer on the earth. [2]

Reflectivity of the surface is often described by the term surface albedo. The Earth's average albedo, reflectance from both the atmosphere and the surface, is about 30 %.

Figure 3.1 describes the modification of solar radiation by atmospheric and surface processes for the whole Earth over a period of one year. Of all the sunlight that passes through the atmosphere annually, only 51 % is available at the Earth's surface to do work. This energy is used to heat the Earth's surface and lower atmosphere, melt and evaporate water, and run photosynthesis in plants. Of the other 49 %, 4 % is reflected back to space by the Earth's surface, 26 % is scattered or reflected to space by clouds and atmospheric particles, and 19 % is absorbed by atmospheric gases, particles, and clouds [4].

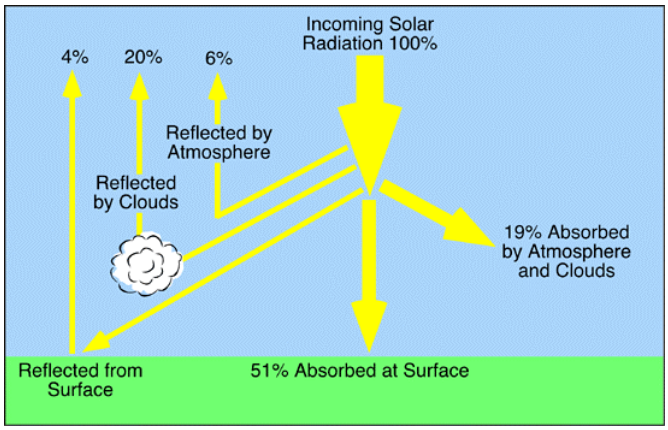

Figure.3.1. Modification of Solar Radiation by Atmospheric and Surface Processes[4]

Solar radiation is a term used to describe visible and near-visible (ultraviolet and near-infrared) radiation emitted from the sun. The different regions are described by their wavelength range within the broadband range of 0.20 to 4.0 μm (microns). Terrestrial radiation is a term used to describe infrared radiation emitted from the atmosphere. The following is a list of the components of solar and terrestrial radiation and their approximate wavelength ranges:

Ultraviolet: 0.20 - 0.39 μm
Visible: 0.39 - 0.78 μm
Near-Infrared: 0.78 - 4.00 μm
Infrared: 4.00 - 100.00 μm

Approximately 99% of solar, or short-wave, radiation at the earth's surface is contained in the region from 0.3 to 3.0 μm while most of terrestrial, or long-wave, radiation is contained in the region from 3.5 to 50 μm.

Outside the earth's atmosphere, solar radiation has an intensity of approximately 1370 watts/meter^2. This is the value at mean earth-sun distance at the top of the atmosphere and is referred to as the Solar Constant. On the surface of the earth on a clear day, at noon, the direct beam radiation will be approximately 1000 watts/meter^2 for many locations.

The availability of energy is affected by location (including latitude and elevation), season, and time of day. All of which can be readily determined. However, the biggest factors affecting the available energy are cloud cover and other meteorological conditions which vary with location and time.

The intensity of solar radiation striking a horizontal surface is measured by a pyranometer. The instrument consists of a sensor enclosed in a transparent hemisphere that records the total amount of short-wave incoming solar radiation. That is, pyranometers measure "global" or "total" radiation: the sum of direct solar and diffuse sky radiation. Incoming (or down welling) longwave radiation is measured with a pyrgeometer. Outgoing (upwelling) longwave radiation is measured in various ways, such as with pyrgeometers or with sensors that measure the temperature of the surface [5].

Chapter 4

DESALINATION TECHNIQUES

Desalting refers to a water treatment process that removes salts from water. It is also called desalination or desalinization, but it means the same thing. Desalting can be done in a number of ways, but the result is always the same: fresh water is produced from brackish water or seawater.

Throughout history, people have continually tried to treat salty water so that it could be used for drinking and agriculture. Of all the globe's water, 94 percent is salt water from the oceans and 6 percent is fresh. Of the latter, about 27 percent is in glaciers and 72 percent is underground. While this water is important for transportation and fisheries, it is too salty to sustain human life or farming. Desalting techniques have increased the range of water resources available for use by a community.

Until recently, only water with a dissolved solids (salt) content generally below about 1000 milligrams per liter (mg/l) was considered acceptable for a community water supply. This limitation sometimes restricted the size and location of communities around the world and often led to hardship to many that could not afford to live near a ready supply of fresh water. The application of desalting technologies over the past 50 years has changed this in many places. Villages, cities, and industries have now developed or grown in many of the arid and water-short areas of the world where sea or brackish waters are available and have been treated with desalting techniques.

This change has been very noticeable in parts of the arid Middle East, North Africa, and some of the islands of the Caribbean, where the lack of fresh water severely limited development. Now, modern cities and major industries have developed in some of those areas thanks to the availability of fresh water produced by desalting brackish water and seawater [6].

4.1.The Development of Desalting

Desalting is a natural, continual process and an essential part of the water cycle. Rain falls to the ground. Once on the ground, it flows to the sea, and people use the water for various purposes as it makes this journey. As it moves over and through the

earth, the water dissolves minerals and other materials, becoming increasingly salty. While in transit and upon arrival in the world's oceans or other natural low spots like the Dead Sea or the Great Salt Lake, a part of the water is evaporated water leaves the salt behind, and the resulting water vapor forms clouds that produce rain, continuing the cycle. It is shown in Figure 4.1.

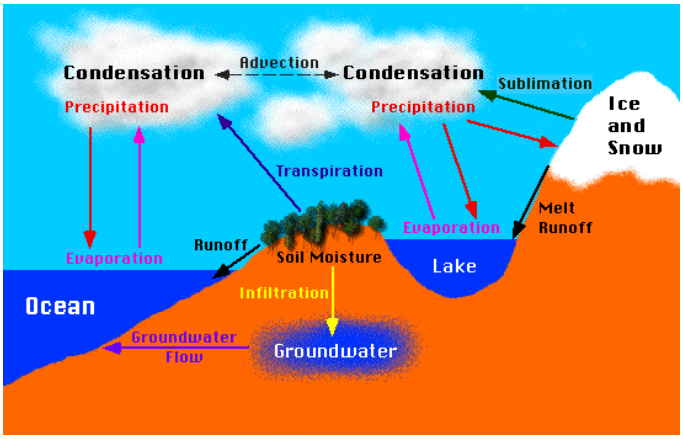

Fig.4.1. Natural Water Cycle [6]

A major step in development came in the 1940s, during World War II, when various military establishments in arid areas needed water to supply their troops. The potential that desalting offered was recognized more widely after the war and work was continued in various countries.

A desalting device essentially separates saline water into two streams: one with a low concentration of dissolved salts (the fresh water stream) and the other containing the remaining dissolved salts (the concentrate or brine stream). The device requires energy to operate and can use a number of different technologies for the separation. This process is shown in Figure 4.2 [6].

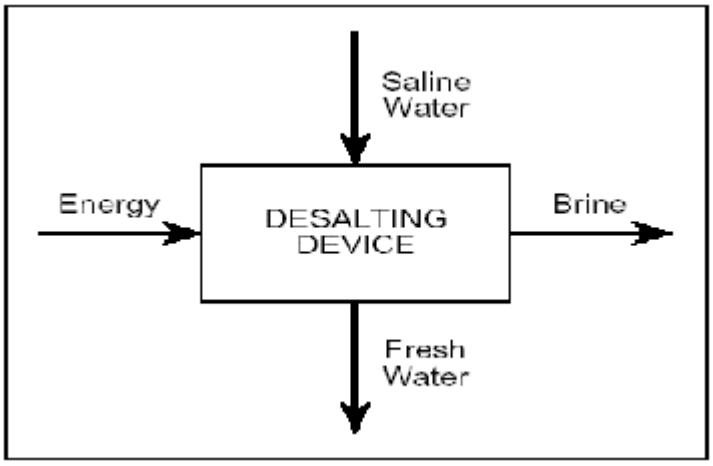

Figure 4.2. Diagram of Desalinaton Process[6]

Desalination can be achieved by using a number of techniques. These may be classified into the following categories:

- Phase change or thermal processes
- Membrane or single-phase processes

In Table 4.1, the most important technologies in use are listed. In phase change or thermal processes, the distillation of seawater is achieved by utilizing a thermal energy source. The thermal energy may be obtained from a conventional fossil-fuel source, nuclear energy or from a non-conventional solar energy source. In the membrane processes, electricity is used either for driving high-pressure pumps or for ionization of salts contained in seawater [7].

Table 4.1. Desalination Processes[7]

Thermal Processes	Membrane Processes
1.Multistage flash(MSF)	1.Reverse osmosis
2.Multiple effect boiling(MEB)	RO without energy recovery
3.Vapour Compression(VC)	RO with energy recovery(ER-RO)
4.Freezing	2.Electrodialysis(ED)
5.Solar stills	3.Ion exchange
conventional solar stills	
special stills	
wick-type stills	
multiple wick type stills	

4.2.Thermal Processes

About half of the world's desalted water is produced with heat to distill fresh water from seawater. The distillation process mimics the natural water cycle in that salt water is heated, producing water vapor that is in turn condensed to form fresh water. In a laboratory or industrial plant, water is heated to the boiling point to produce the maximum amount of water vapor.

To do this economically in a desalination plant, the applied pressure of the water being boiled is adjusted to control the boiling point because of the reduced atmospheric pressure on the water, the temperature required to boil water decreases as one moves from sea level to a higher elevation. Thus, water can be boiled on top of Mt. McKinley, in Alaska [elevation 6,200 meters (20,300 feet)], at a temperature about 16 °C (60.8 °F) lower than it would boil at sea level. This reduction of the boiling point is important in the desalination process for two major reasons: multiple boiling and scale control.

To boil, water needs two important conditions: the proper temperature relative to its ambient pressure and enough energy for vaporization. When water is heated to its boiling point and then the heat is turned off, the water will continue to boil only for a short time because the water needs additional energy (the heat of vaporization) to permit boiling. Once the water stops boiling, boiling can be renewed by either adding more heat or by reducing the ambient pressure above the water. If the ambient pressure were reduced, the water would be at a temperature above its boiling point (because of the reduced pressure) and would flash to produce vapor (steam), the temperature of the water will fall to the new boiling point. If more vapors can be produced and then condensed into fresh water with the same amount of heat, the process tends to be more efficient.

To significantly reduce the amount of energy needed for vaporization, the distillation desalting process usually uses multiple boiling in successive vessels, each operating at a lower temperature and pressure. Typically 8 tons of distillate can be produced from 1ton of steam. This process of reducing the ambient pressure to promote additional boiling can continue downward and, if carried to the extreme with the pressure reduced enough, the point at which water would be boiling and freezing at the same time would be reached.

Aside from multiple boiling, the other important factor is scale control. Although most substances dissolve more readily in warmer water, some dissolve more readily in cooler water. Unfortunately, some of these substances, like carbonates and sulfates, are found in seawater. One of the most important is calcium sulfate (CaSO4), which begins to leave solution when seawater approaches about 115 °C (203 °F). This material forms a hard scale that coats any tubes or surfaces present. Scale creates thermal and mechanical problems and, once formed, is difficult to remove. One way to avoid the formation of this scale is to control the concentration level of seawater and to control the top temperature of the process. Another way is to add special chemicals to the seawater that reduce scale precipitation and permit the top temperature to reach 110ºC. These two concepts have made various forms of distillation successful in locations around the world. The process that accounts for the most desalting capacity for seawater is multi-stage flash distillation, commonly referred to as the MSF process [8].

4.3.Membrane Processes

In nature, membranes play an important role in the separation of salts, including both the process of dialysis and osmosis, occurs in the body. Membranes are used in two commercially important desalting processes: electrodialysis (ED) and reverse osmosis (RO). Each process uses the ability of the membranes to differentiate and selectively separate salts and water. However, membranes are used differently in each of these processes.

ED is a voltage driven process and uses an electrical potential to move salts selectively through a membrane, leaving fresh water behind as product water.

RO is a pressure-driven process, with the pressure used for separation by allowing fresh water to move through a membrane, leaving the salts behind. Figure 4.3 shows the diagram of membrane process.

Scientists have explored both of these concepts since the turn of the century, but their commercialization for desalting water for municipal purposes has occurred in only the last 30 to 40 years [6,8].

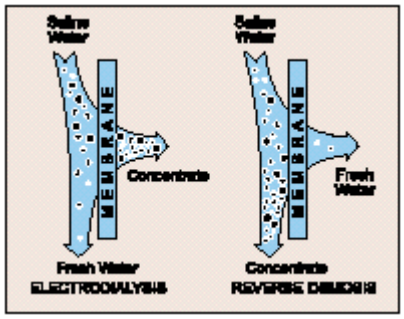

Figure 4.3. Diagram of membrane processes [6].

Membrane processes constitute a well-established technology for the desalination of brackish water. Recently, the use of membrane systems has increased substantially and is rapidly expanding its share of the desalination market for brackish water, wastewater reuse, and seawater [1].

Chapter 5

SOLAR DESALINATION

The use of direct solar energy for desalting saline water has been investigated and used for some time. During World War II, considerable work went into designing small solar stills for use on life rafts. This work continued after the war, with a variety of devices being made and tested.

These devices generally imitate a part of the natural hydrologic cycle in that the sun's rays heat the saline water so that the production of water vapor (humidification) increases. The water vapor is then condensed on a cool surface, and the condensate collected as fresh water product. An example of this type of process is the greenhouse solar still, in which the saline water is heated in a basin on the floor, and the water vapor condenses on the sloping glass roof that covers the basin. Figure 5.1 shows diagram of a solar still.

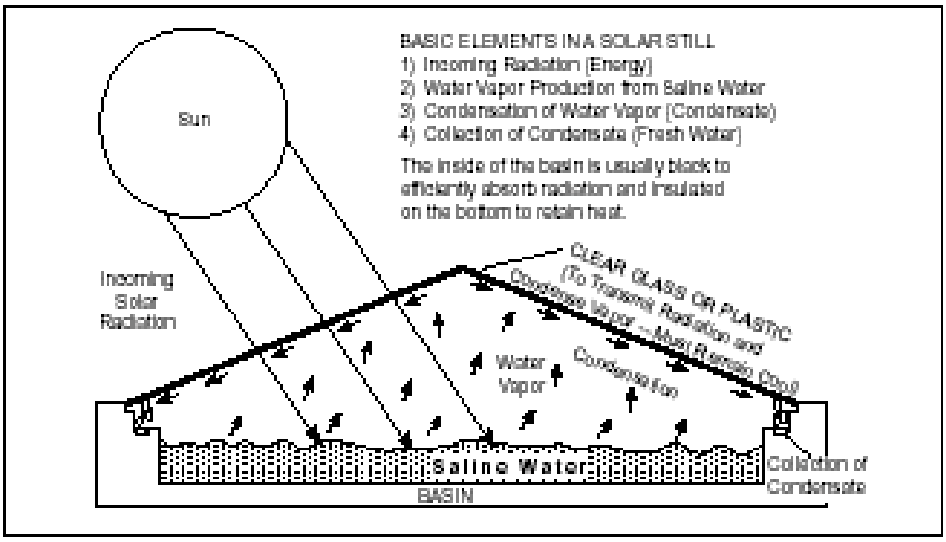

Figure 5.1. Diagram of a solar still [6]

Variations of this type of solar still have been made in an effort to increase efficiency, but they all share the following difficulties, which restrict the use of this technique for large-scale production:

- Large solar collection area requirements
- High capital cost
- Vulnerability to weather-related damage

A general rule of thumb for solar stills is that a solar collection area of about one square meter is needed to produce 4 liters of water per day (10 square feet/gallon). Thus, for a 4000 m^3/d facility, a minimum land area of 100 hectares would be needed (250 acres/mgd). This operation would take up a tremendous area and could thus create difficulties if located near a city where land is scarce and expensive [6].

5.1.Solar Desalination Systems

A representative example of direct collection systems is the conventional solar still, which uses the greenhouse effect to evaporate salty water. It consists of a basin, in which a constant amount of seawater is enclosed in a v-shaped glass envelope.

There are different types of solar stills built in different countries on the world, which in common have a saline water basin with a black bottom, a transparent cover and collecting pipes, which give the condensed water as end product. Sunlight heats the water in the basin. This heated water evaporates and recondenses on the underside of the sloping transparent cover and runs down into collecting through along the inside lower edges of the transparent cover, Figure 5.2. Usually the transparent cover is made of glass or plastic such as polyvinyl chloride or polyvinyl fluoride. The basin is covered with a thin black plastic film, like butyl caoutchouc and insulated against the heat losses into the ground [7].

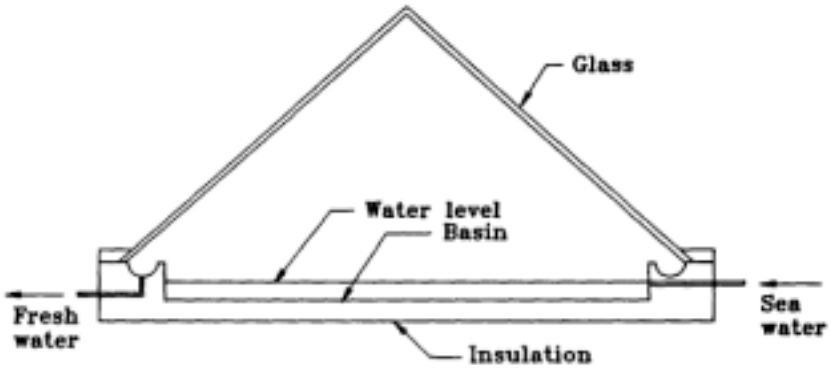

Figure 5.2. Schematic of a solar still [7]

A typical still efficiency, defined as the ratio of the energy utilized in vaporizing the water in the still to the solar energy incident on the glass cover, is 35%(maximum) and daily still production is about 3-4 l/m^2.

Several attempts have been made to use cheaper materials such as plastics. These are less breakable, lighter in weight for transportation, and easier to set up and mount. Their main disadvantage is there is their shorter life. Many variations of the basic shape have been developed to increase the production rates of solar stills. Some of the most popular are shown in Figure 5.3 [7].

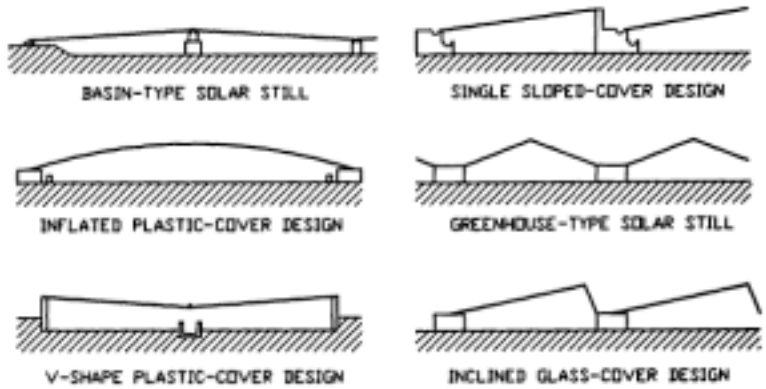

Figure 5.3. Common designs of solar stills [7]

On the islands where underground natural sources are not available and the cost of shipping water to the islands is high, plastic rooftop solar stills are convenient to use, Figure 5.4.

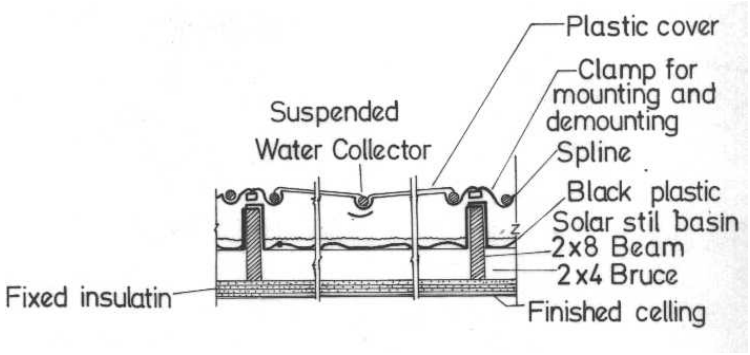

Figure 5.4. Plastic rooftop solar still [9]

This type of a solar still usually consists of a plastic cover, a black plastic solar still basin and a fixed insulation. The water depth should be no more than 2 cm., because of the weight, which brings an additional load to the roof of the building.

Figure 5.5 shows a lightweight collapsible solar still for only few gallons per day of fresh water production. These types of solar stills usually are used for emergency cases on islands, which are used as navy bases.

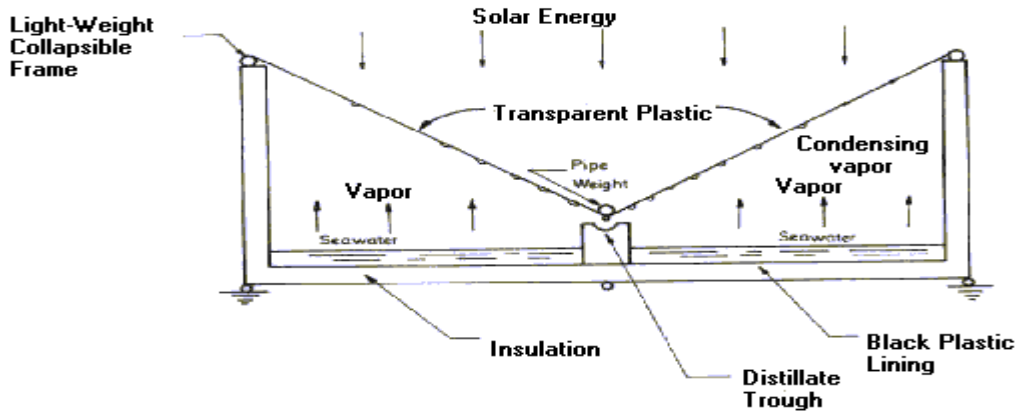

Figure 5.5. Light-weight Collapsible solar still [9]

Figure 5.6 gives the basic concept of a horizontal concentric tube solar still. This solar still utilizes air as working medium. Air carries the water vapor from the annular space between the clear outer and the inner tube through the inside of the inner tube where the water vapor condenses and gives up its heat of condensation directly to the seawater being sprayed on the outer surface of the inner tube. The water vapor will have the preferential tendency to condense on the inside surface of the clear outer tube.

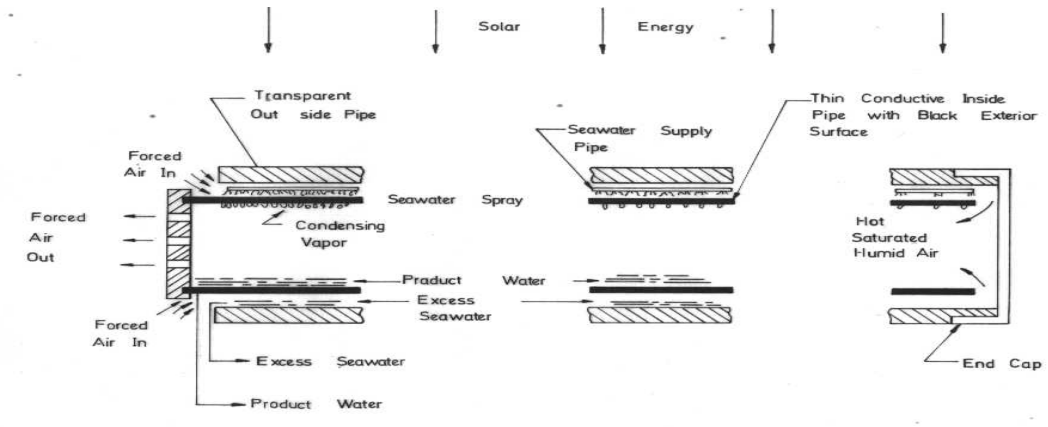

Figure 5.6. Horizontal concentric tube solar still [9]

Figure 5.7 shows high performance solar still. In this type of solar still the heat of condensation of water vapor is received by a working fluid, e.g., water can be used as a working fluid. As shown in Figure 5.7, the working fluid circulates around the solar still. Its temperature is minimum at point 1 and maximum at point 2, from where it flows down on an insulated inclined plane back to the heat exchanger. The heat exchanger is either a double plate or a double pipe type. In the latter case, the outer pipe has perforations on it. The seawater enters the annular space and evaporates on receiving heat from working fluid. The issuing vapor then rises and condenses on a glass plate as it gives up its heat to the working fluid [9].

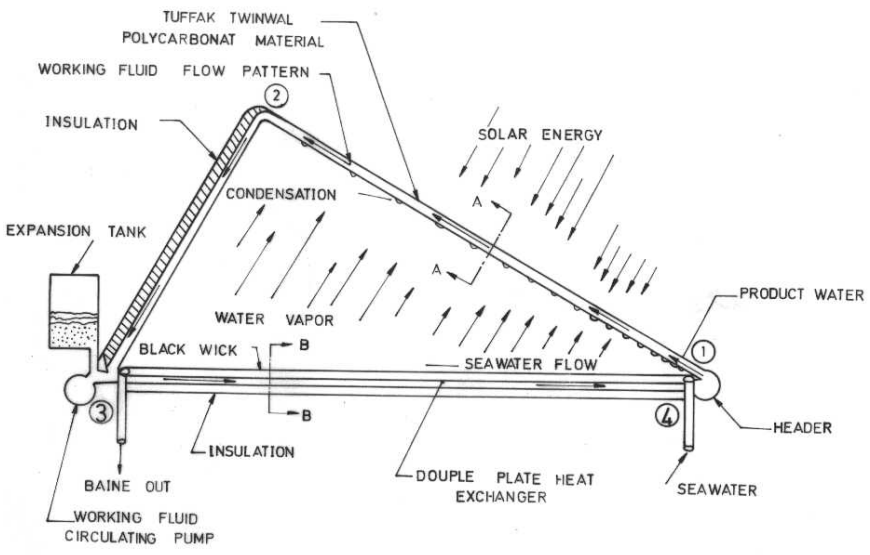

Figure 5.7. High performance solar still [9]

Figure 5.8 shows cylindrical parabolic type solar still. It has a parabolic reflector; the reflector was designed to concentrate the incident solar radiation on the black outside surface of a tray located on the focal line of the reflector [10].

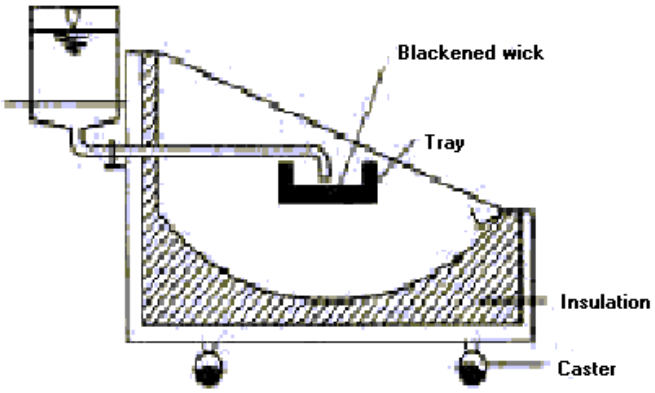

Figure 5.8. Cylindrical Parabolic type [10]

In double basin solar still the transparent glass cover and glass plate transmit solar radiation. The absorbing plate is then heated directly by solar radiation. The saline water feeds are introduced on the upper surfaces of both the absorbing and glass plates where some water evaporates, while the remainder is collected at the bottom and discarded as concentrated brine [11]. (Figure.5.9)

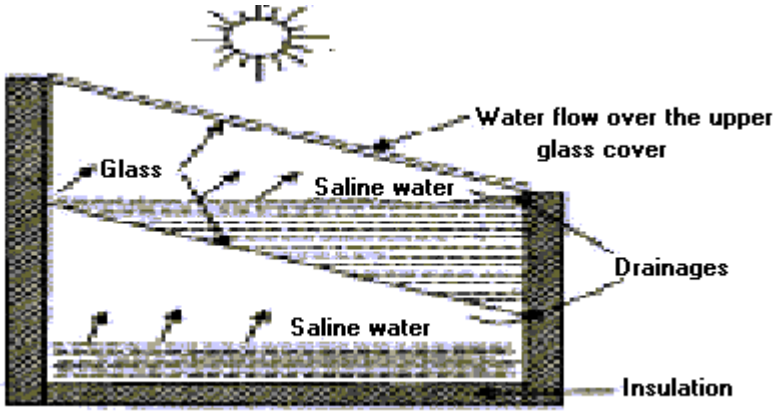

Figure.5.9. Stationary double-basin still with flowing water over upper basin [11]

Another type of solar still that is designed to operate with a very low heat capacity is the tilted-wick still. Figure 5.10 shows tilted wick solar still [12] .

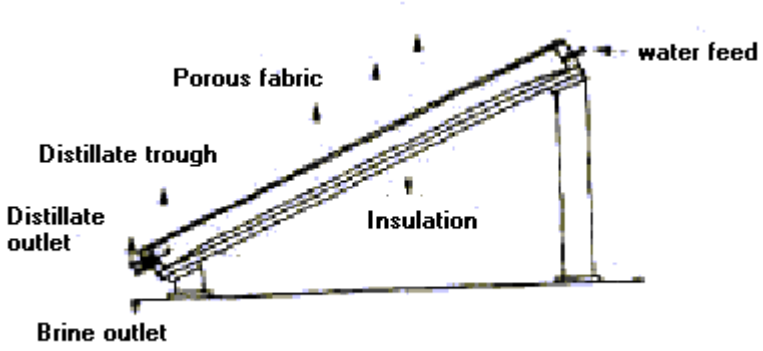

Figure 5.10. Tilted wick solar still [12]

5.2. Studies on Solar Desalination

The first solar distillation device having the capacity of about 23 m^3/d in clear weather, was designed and manufactured in 1872 near Las Salinas in northern Chile. The still used a shallow black basin to hold the salt water and absorb solar radiation: water vaporized from the brine, condensed on the underside of a sloped transparent cover, ran into troughs, and was collected in tanks at the end of the still. (Figure 5.11.)

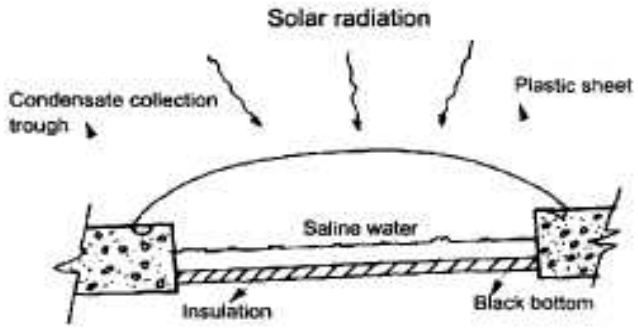

Figure 5.11. Simple Solar Still [12]

During World War II, efforts were increased to produce a solar still that could be used on life rafts for ships and aircraft. Telkes invented a small inflatable plastic unit for this purpose, and hundreds of thousands of the units were produced. Most stills built and studied since then have been based on the same concept, though with many variations in geometry, materials, methods of construction, and operation.

From 1958 to 1965 OSWs Solar Distillation Research Station in Florida tested a number of different types of solar stills, and it was concluded that high fixed charges associated with the cost of still construction would not be offset by the savings resulting from free solar energy.

Past research work has been focused on the construction cost obstacle of the solar still. However, various plastic films have been used instead of the more durable and expensive glass coverings.

The next stage was to improve the operating efficiencies of the various types of solar distillation devices. Several researchers have attempted to enhance the vapor condensation rate by forcing air circulation in stills and to increase the output of the stills by using latent heat of vaporization in either multi- effect systems or for preheating the brine [12].

Table 5.1 shows some solar stills in various countries in the world. This table shows that most of the stills were built during the period 1960-1980 [14].

Table 5.1. Some Basin Type Solar Stills in the World [14]

Country	Location	Year	Basin Area (m^2)	Productivity (m^3/day)(liter/m^2.day)		Cover
Australia	Muresk I	1963	372	0.83	2.30	Glass
	Muresk II	1966	372	0.83	2.30	Glass
	Coober Pedy	1966	3160	6.35	2.01	Glass
	Caiguna	1966	372	0.78	2.10	Glass
	Hamelin Pool	1966	557	1.21	2.17	Glass
	Griffith	1967	413	0.91	2.20	Glass
Chile	Las Salinas	1872	4460	14.76	3.31	Glass
	Quillagua	1968	100	0.40	4.0	Glass
	Quillagua	1969	103	0.40	3.88	Glass
Greece	Symi I	1964	2686	7.56	2.81	Plastic
	Aegina I	1965	1490	4.24	2.84	Plastic
	Salamis	1965	388	1.10	2.83	Plastic
	Patmos	1967	8600	26.11	3.04	Glass
	Kimolos	1968	2508	7.57	3.02	Glass
	Nisyros	1969	2005	6.06	3.02	Glass

India	Bhavnagar	1965	377	0.83	2.20	Glass
Mexico	Natividad Island	1969	95	0.38	4.0	Glass
	Puerta Chale	1974	300	1.00	3.33	Glass
	Punta Chucca	1974	470	1.50	3.19	Glass
Pakistan	Gwadar II	1972	9072	27.0	2.98	Glass
Spain	Las Marinas	1966	868	2.57	2.96	Glass
Tunisia	Chakmou	1967	440	0.53	1.20	Glass
	Mahdia	1968	1300	4.16	3.20	Glass
U.S.A	Daytona Beach	1959	224	0.53	2.37	Glass
	Daytona Beach	1961	246	0.57	3.20	Glass
	Daytona Beach	1961	216	0.38	1.76	Plastic
	Daytona Beach	1963	148	0.61	4.12	Plastic
U.S.S.R	BalchardenTurkmena	1969	600	1.62	2.70	Glass
WestIndies	Petit St.	1967	1710	4.92	2.88	Plastic
	Vincent Haiti	1969	223	0.76	3.41	Glass

Minasian at al, in 1995, evaluated the possibility of increasing the productivity of the conventional basin type solar still by using a cylindrical parabolic reflector while solving the most important maintenance problem usually encountered in the basin type solar still, i.e. salt accumulation. In this study, the productivity of the conventional basin type solar still has been increased by using a stainless steel cylindrical parabolic reflector. The reflector concentrates the incident solar radiation on the black outside surface of a tray located on the focal line of the reflector. Results of the study showed that the productivity of the new proposed still were 25-35 % greater than the productivity of the conventional basin type solar still [10].

Elkader represented the experimental results carried out with a solar still with inclined evaporating yute to study the effects of air gap, base slope angle and glass cover slope angle on the performance of the still. In order to investigate the parameters involved in the still, three models have been designed, manufactured and tested against some experimental measurements on a still having 1m x 1m-basin area. The models have been designed in a way that it can give different base slope angle and glass slope angle. A comparison between the three models has been made for three glass slope angles. The test results show that the model with the base slope of 15^{0} and glass slope

of 35 ^{0} gave the best results. It gave a daily-desalinated water quantity of 5.6-liter/m^2 day[14].

In a conventional solar still the production of fresh water in bright sunny weather and with warm air temperature is about 5-5.5-liter/m^2 day, according to the depth of the water in the solar still. In some devices it is possible to obtain efficiencies of up to 0.50 and 0.60. The aim of this research was to increase distillation productivity by utilizing the latent heat released by the condensing water steam. For this purpose Cappelletti built a solar still characterized by two basins (B_1 and B_2) superimposed upon each other. The building materials were a sheet of black Plexiglas for the bottom of the solar still, a sheet of transparent Plexiglas for all boxes, and a sheet of black polystyrene used as insulating material. The solar still was hermetically sealed to reduce the leakage of vapor to the surroundings. The greatest quantity of fresh water obtained by the tested solar still was 1.7-1.8 liter/m^2 day. This result was achieved in the third week of July when solar radiation was 27-28 MJ/m^2 day. The efficiency of the tested solar still was about 0.16 [15].

In 1996, another solar distillation system has been established. The system was consisting of two flat plate solar collectors, which have selective surfaces, a storage tank and a basin-type solar still. During daytime, water was circulated naturally through collectors and stored in the tank, and during night-time, this stored energy was used to heat-up water in the basin. This system gave up to 100 % more yield when compared with a conventional still [16].

Kumar at al., presented the annual performance of an active solar still. Analytical expressions for water and glass cover temperatures and yield have been derived in terms of design and climatic parameters. Numerical computations have been carried out for Delhi climatic conditions (latitude: 28 ^{0} 35' N, Longitude: 77 ^{0} 12' E). It has been observed that for given parameters, the annual yield is optimum when the collector inclination is 20^{0} and the still glass cover inclination is 15 ^{0} [17].

Boukar and Harmim have been to study the effect of desert climatic conditions on the performance of a simple basin solar still and a similar one coupled to a flat plate solar collector. Tests were conducted at the solar station of Adrar, an Algeria Saharan Site. The performance of the simple still is compared with the coupled one. They were tested for all day productivity under clear sky conditions, with different depth levels of brackish water for winter and summer period and for a three months round test from

January to March 2000. Data were taking during all type of sky conditions. A three months round study showed that the productivity of the simple basin and similar coupled to a flat plate solar collector strongly depends on the solar radiation and ambient temperature. The daily still productivity in summer period varies from 4.01 to 4.34 liter/m^2day for simple basin solar still and from 8.02 to 8.07 liter/m^2day for the coupled one [18].

Another study was presented a modeling and experimental research of solar distillation applied to the Sahara arid regions by Bouchekima at al. The aim of this work was an improvement of the efficiency and production rate of fresh water by using solar distiller with capillary film. This solar distiller was designed and patented by R. and C. Ouahes and P. Le Goff. It was made of identical evaporation-condensation cells. The brine to be evaporated was a thin film impregnating a fabric assumed to be very thin and adhering by capillary forces to the wall of the plate. Its advantage resides in the reuse of latent heat of steam condensed in the one stage, for water evaporation in the subsequent stage. The study on the performance of this solar still has been conducted under the actual insulation at the South of Algeria: in an experimental station near Touggourt (Algerian Sahara). In this arid land, there is brackish underground water; therefore, solar desalination is necessary to produce drinking water. Figure 5.12 shows the principles of capillary film distiller [19].

.

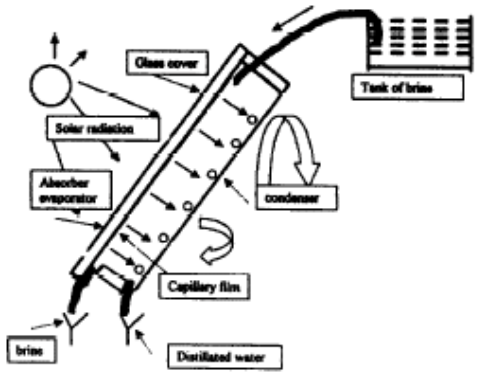

Figure 5.12. Principles of capillary film distiller [19].

Another study is an experimental study on solar distillation in a single slope basin still by surface heating the water mass. An experimental study was conducted in a single slope basin solar still after introducing a floating perforated and folded aluminum

sheet over the water surface, which concentrates heat energy at the surface layer, prevents the whole water mass from getting heated up by convection (by preventing/reducing transmission of radiation through the water body to the bottom liner) and allows evaporated water particles from the covered segments to escape out into the air gap through the holes on it. The distillate yield was found to have improved considerably, especially when the water depth was high. The study also indicated some design features that would further enhance the improvement in output due to the modification made [20].

5.3.Parameters Affecting the Output of a Solar Still

The productivity of a still is under the effect of three groups of conditions. These are ambient conditions, Operating conditions and Design conditions. Ambient conditions are ambient temperature, insolation, and wind velocity. Operating conditions are depth of water, the orientation of the still and inlet temperature of water, etc. Design conditions are the selection of the material of the still and cover, slope of the cover, distance between the water and the cover (gap distance) and numbers of covers used, etc. It is clear that ambient conditions are not under control, and a optimum design must satisfy the requirements of the operating conditions and design conditions [13].

5.3.1.Effect of Wind Velocity

Wind velocity has little effect on productivity, but even low wind speeds increases the production rates as compared to zero wind conditions. The fact is high wind velocity will increase the heat loss by convection from the cover to the ambient. This causes a decrease in the condensing surface temperature and accordingly increases the yield of a still. The numerical calculations showed that when the wind velocity changes from 1 to 9 m/s, the productivity decreases by 13 % [21].

5.3.2.Effect of Water Depth

The depth of water in the basin affects the performance of a still considerably. At low water depths, the thermal capacity will be lower and hence the increase in water temperature will be faster resulting in higher outputs. Water depth becomes important

especially in the morning when low energy from the sun is available and it is required to heat the water quickly to producing fresh water. Hence the only solution is to operate the still at lower depths. An increase in the water depth from 1.27 cm to 30 cm reduces the output by 30% [13].

5.3.3.Effect of Ambient Air Temperature

The effect of ambient temperature variations on solar still productivity is examined by the several researchers. The numerical results showed that a slight increase of 3 % in the solar still productivity is obtained by increasing the ambient temperature by 5 ^{0}C [21].

5.3.4.Effect of the Gap Distance

Reducing the gap distance between the evaporating surface and the condensing cover improves the still performance. The effect of the gap distance is much important than the effect of the cover slope. Reducing the gap distance will reduce the height of the walls of the still and hence will reduce the shadowing effect of these sides. Also less time is elapsed by the saturated air to reach the condensing surface and therefore continuous and quicker air movement in the still is established. Reducing the gap distance from 13.0 cm to 8 cm for the same cover slope increases the output by 11.0 %[13].

5.3.5.Effect of Number of Covers

Number of transparent covers used in a solar still does not increase the output, because it increases the temperature of the inner cover (condensing surface). But it also keeps the still airtight. Due to double glass cover reduction of 25-35 % of the output was noticed. Also uses a double glass cover increases the initial cost of the still [13].

5.3.6.Other Effects

Some other effects may be mentioned like the degree of salinity of water. As salt concentration of the water is increased, the yield of the still decreases, also with time if the salt sticking to the absorbing plate is not removed completely, this will reduce the efficiency of the absorbing plate. Also salty water damages the materials of the still by

corrosion. In some experiments to increase the absorbtivity of water in the basin and hence the output of the still, the water is colored with some dyes or charcoal pieces are added. Charcoal pieces have the properties of wettability, large absorption coefficient for solar radiation and that they scatter rather than reflect the solar radiation. It was concluded that their effect is most noticed in the mornings and on cloudy days when the value of the solar radiation is low. However, the presence of the charcoal pieces reduces the start–up time of evaporation [13].

5.4. Materials of a Solar Still

The research and development work done up to date has yield more useful information on the materials of solar stills. One of the most important component being the cover of the still, the material of the cover should be selected properly. The choice of the transparent cover is between glass and plastic. Glass covers are preferred against the plastic ones, but the main advantage of plastic against glass is that plastic is cheaper. Basin liner material must absorb solar radiation and must be water tight. Because a still may run dry, this material should withstand high temperatures. Asphalt mats have been used to line large deep basin steels. For shallow basins, liners of black butyl rubber sheet and black polyethylene sheet are preferred. Butyl rubber has the ability to withstand high temperatures. Sealing of the transparent cover to prevent vapor leakage is very important. The most effective sealant material used so far is silicon rubber sealant which remains elastic for long time. Other sealants have been used such as tars and tapes. These materials deteriorate in time and become brittle so that cracks are formed and hence permit leakage of vapor. It has been observed that the use of galvanized iron as a distillate channel is not a good choice since it corrodes badly in contact with saline water. Aluminum may be used as distillate channel but it also corrodes at high temperatures.

Chapter 6

THEORETICAL & EXPERIMENTAL ANALYSIS OF SOLAR STILL

6.1. Principles of Solar Still

In a simple solar still, solar radiation passes through the glass cover. The passed solar energy is partially absorbed in the thin seawater layer, and is absorbed by black cover on the basin. Thus, seawater and basin are heated by the solar energy. Heat is conducted from the black surface into the seawater. Thus the temperature of the seawater increases. Vaporization takes place at the interface, seawater surface-air inside of the solar still, at the interface temperature, ϑ_i. Interfacial area, sea water surface is semi permeable. A plane is called semi permeable when the mass flux of one component is zero. Such a plane is, for instance, the surface of water, which evaporates into an adjoining air stream because water but no air passes through the surface. Thus, at the interface the saturated air at the temperature, ϑ_i, is transported by diffusion due to the partial pressure difference and convection due to the natural convection of the humid air from the interface into the air inside of the solar still with the temperature, ϑ_r. Of course at steady state or quasi-steady state conditions the air inside of the solar still is also saturated at the temperature, ϑ_r. Therefore, the humid saturated air inside of the solar still will condense at the glass cover, which has a lower temperature, ϑ_g then the air temperature inside solar still, ϑ_r. Heat of condensation heats the glass cover and glass cover in heat exchange with surrounding and air inside of the still by convection and radiation. The condensate flows down, it is collected along the glass cover and collected in a channel at the end of the glass cover on south side of the still. And then it collects in a storage bottle outside of the still.

In order to be able to calculate the daily produced condensed water, energy balance method will be applied.

6.2. Energy and Mass Balance Method

The performance of a solar still is generally expressed as the quantity of water evaporated by unit area of the basin in one day cubic meters or liters of water per square meter of the basin area per day. This performance of a solar still can be predicted by writing the energy and mass balance equations on the various components of the still.

A. Theoretical Treatment of Solar Still without Reflector

The whole system is a quasi-steady state condition and temperatures will be assumed not to change in one hour interval of time. Energy balance equations for the whole still, glass cover, seawater interface and black plate at the bottom can be written as follows:

Energy Balance for the Whole Still

The energy balance of the whole still should be considered. From Figure 6.1., it can be seen that the energy input to the still and the heat transfer from the still to the atmosphere.

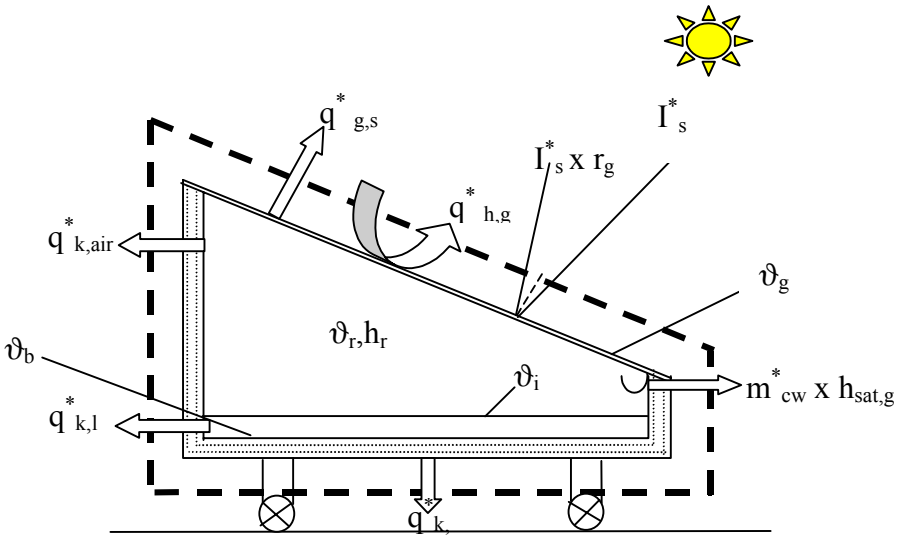

Figure 6.1. Illustration of the Overall Energy Balance

$$I^*_s\ A_g = I^*_{s,}r_g\ A_g + q^*_{g,s}\ A_g + q^*_{h,g}\ A_g + q^*_{k,air}\ A_{k,air} + q^*_{k,l}\ A_{k,l} + q^*_{k,b}\ A_b + (m^*_{cw} x\ h_{sat,g})$$

[j/s] (6.1)

$$I^*_s\ A_g/A_b = I^*_{s,}r_g\ A_g/A_b + q^*_{g,s}\ A_g/A_b + q^*_{h,g}\ A_g/A_b + q^*_{k,air}\ A_{k,air}/A_b + q^*_{k,l}\ A_{k,l}/A_b + q^*_{k,b}\ A_b/A_b + (m^*_{cw} x\ h_{sat,g})/A_b$$

[j/m^2 s] (6.2)

I^*_s is the solar radiation intensity and r_g is the reflectivity of the glass cover for visible light.

Considering the heat transfer from the cover to the atmosphere by convection:

$$q^*_{h,g} = h_g (\vartheta_g - \vartheta_a) \quad (6.3)$$

where ϑ_g is the glass temperature. h_g is the convective heat transfer coefficient and is given by the following formula:

$$h_g = 5.7 + 3.8w \quad (6.4)$$

where the forced convection coefficient dependent on the wind velocity, w(m/s).

Radiative heat transfer from the glass cover to the atmospheric air is given by the following formula:

$$q^*_{g,s} = \varepsilon_g C_s [(T_g/100)^4 - (T_{sky}/100)^4] \quad (6.5)$$

where emisivity of the glass, ε_g, is 0.88 for infrared radiation, the constant, C_s, is 5.667 W/m^{2}K^4 and T_{sky} is the sky temperature. Generally for practical purposes the average sky temperature during operations hours can be assumed as about 20 ^{0}C below the ambient temperature , i.e. $T_{sky} = T_a - 20^0$C [16].

The conductive heat transfer from the bottom to the atmosphere may be formulated as:

$$q^*_{k,b} = k_b (\vartheta_b - \vartheta_a) \quad (6.6)$$

where $\frac{1}{k_b} = \frac{1}{h_{in}} + \sum \frac{\delta_i}{\lambda_i} + \frac{1}{h_a}$

Considering the heat transfer from the circumferential area of the still by conduction; From inside moist air to the atmosphere,

$$q^*_{k,air} = k_r (\vartheta_r - \vartheta_a) \text{ where } \frac{1}{k_r} = \frac{1}{h_r} + \sum \frac{\delta_i}{\lambda_i} + \frac{1}{h_a} \quad (6.7)$$

From liquid to the atmosphere,

$$q^*_{k,l} = k_l (\vartheta_l - \vartheta_a) \text{ where } \frac{1}{k_l} = \frac{1}{\infty} + \sum \frac{\delta_i}{\lambda_i} + \frac{1}{h_a} \text{ and } \vartheta_l = (\vartheta_i + \vartheta_b)/2 \quad (6.8)$$

$h_{sat,g}$ is the enthalpy of water at saturation temperature ϑ_g and m^*_{cw} is the mass flow rate of condensed water.

Energy Balance for Glass Cover

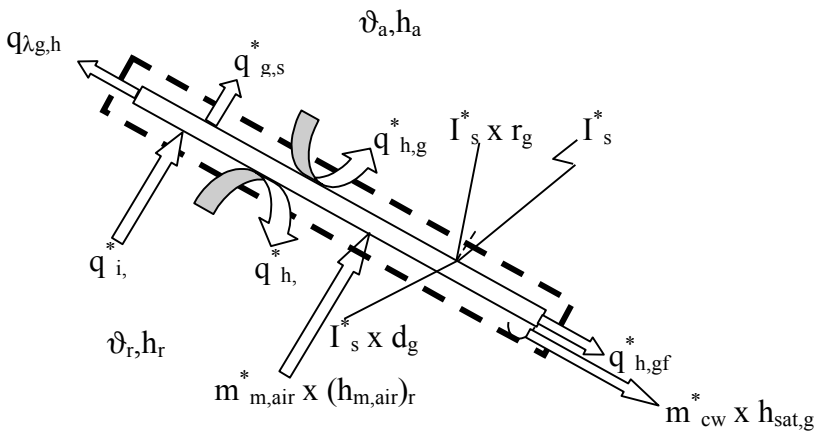

Figure 6.2. Energy Balance for Glass Cover

From Figure 6.2, the energy balance equation of glass cover is;

$$I^*_s A_g + q^*_{i,g} A_g \cos\beta + q^*_{h,r} A_g + m_{m,air} h_{m,air,r} = I^*_{s,r_g} A_g + I^* d_g A_g + q^*_{g,s} A_g + q^*_{h,g} A_g + q^*_{\lambda,gh} A_{\lambda,gh} + q^*_{h,gf} A_{h,gf} + m^*_{cw} h_{sat,g} \quad [\text{j/s}] \quad (6.9)$$

$$I^*_s\ A_g/A_b + q^*_{i,g}\ A_g/A_b\ \cos\beta + q^*_{h,r}\ A_g/A_b + (m_{m,air}\ h_{m,air,r})/A_b = I^*_{s,r} g\ A_g/A_b + I^* d_g\ A_g/A_b + q^*_{g,s}\ A_g/A_b + q^*_{h,g}\ A_g/A_b + q^*_{\lambda,gh}\ A_{\lambda,gh}/A_b + q^*_{h,gf}\ A_{h,gf}/A_b + (m^*_{cw}\ h_{sat,g})/A_b \quad [\text{j/m}^2\text{ s}] \quad (6.10)$$

where $q^*_{i,g}$ is the radiative heat flux from the water surface to the glass, $q^*_{h,r}$ is the convective heat flux from the water surface to the glass and $h_{m,air}$ is the enthalpy of water at saturation temperature ϑ_r and $m^*_{m,air}$ is the mass flow rate of moist air.
$q^*_{\lambda,gh}$ and $q^*_{h,gf}$ are the heat losses from the back and front borders of the glass and for calculations they can be neglected.

Between an optical permeable and non permeable walls (water surface is assumed to be a non permeable wall because transmittance of water equals zero for infrared radiation) , radiative heat transfer from the water to the glass is:

$$q^*_{i,g} = \frac{((\frac{T_i}{100})^4 - (\frac{T_g}{100})^4) + ((1-\varepsilon_g)/\varepsilon_g) d_g (\frac{T_i}{100})^4)}{\frac{1}{\varepsilon_g c_s} + \frac{1}{\varepsilon_w c_s} - \frac{1}{c_s} + \frac{1-\varepsilon_p-\varepsilon_g}{\varepsilon_w \varepsilon_g c_s} d_g} \quad (6.11)$$

where ε_g is the emissivity of water and d_g is the transmittance of water for infrared radiation [23].
Convective heat transfer from the water to the glass is:

$$q^*_{h,r} = h_r\ (\vartheta_r - \vartheta_g) \quad (6.12)$$

where h_r is the convective heat transfer coefficient.

Calculation of convective heat transfer coefficient, h_r:
According to Churchill, Nusselt number is formulated as,

$$Nu = 0.766\ [\ Ra\ f_2(Pr)\ ]^{1/5} \quad \text{for} \quad Raf_2(Pr) \le 7 \times 10^4 \quad (6.13)$$

and

$$Nu = 0.15\ [\ Ra\ f_2(Pr)\ ]^{1/3} \quad \text{for} \quad Raf_2(Pr) \ge 7 \times 10^4 \quad (6.14)$$

where $f_2(Pr) = [\ 1+(0.322/Pr)^{11/20}]^{-20/11}$

it can be tabulated for different prandtl numbers as,

Pr	0.01	0.70	7	100	∞
$f_2(Pr)$	0.0242	0401	0.736	0.927	1

Grashof number, Gr, is given by the following formula:

$$Gr = \frac{g\ell^3}{\nu^2}\beta\Delta T \tag{6.15}$$

where g is the gravitational acceleration in m/s^2, ν is the momentum diffusivity in m^2/s, ℓ is the characteristic length in m, and it can be calculated by:

$$\ell = \frac{A}{U} \tag{6.16}$$

where A is the surface area and U is the circumference of the participating heat transfer area whose projected in down stream direction.

β is the thermal expansion coefficient is,

$$\beta = -\frac{1}{\rho}\left(\frac{\partial\rho}{\partial T}\right)_p \tag{6.17}$$

This thermodynamic property of the fluid provides a measure of the amount by which density changes in response to a change in temperature at constant pressure. If it is expressed in the following approximate form,

$$\beta\Delta T = -\frac{1}{\rho}\frac{\rho_\infty - \rho_0}{\rho_\infty} \quad \text{valid for } \beta\,\Delta T << 1 \tag{6.18}$$

ρ_o = inside density

ρ_∞ = outside density of the boundary layer

Free convection effects obviously depend on the expansion coefficientβ. The manner in which β is obtained depends on the fluid. For ideal gas,

$$\beta = \frac{1}{273}\ \left[K^{-1}\right] \tag{6.19}$$

and for reference point T_∞,

$$\beta = \frac{1}{T_\infty} \quad [K^{-1}] \tag{6.20}$$

Rayleigh number is calculated by Ra=Gr Pr.

For all calculations physical and transport properties will be in $T_{m,}$

$$T_m = \frac{T_0 + T\infty}{2} \tag{6.21}$$

Convective heat transfer coefficient can be calculated by;

$$h_r = \frac{Nu\lambda}{\ell} \tag{6.22}$$

λ is the thermal conductivity of air at T_m [24].

Energy Balance for Seawater interface

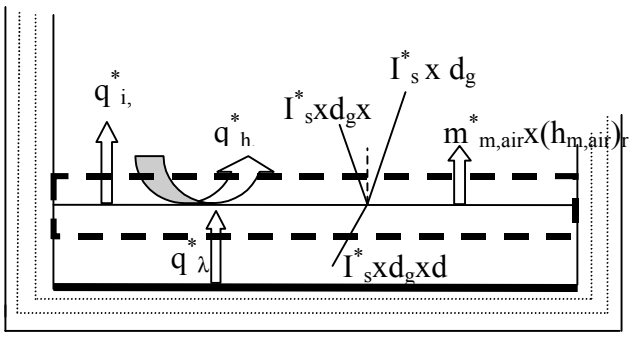

Figure 6.3. Heat Transfer Modes for Seawater Interface

By referring to Figure 6.3., the energy balance for seawater interface can be written as follows:

$$I^*_s\, d_g\, A_g + q^*_\lambda\, A_b = I^*_{s,}\, d_g\, r_w\, A_b + I^*_{s,} d_g\, d_w\, A_b + q^*_{i,g}\, A_b + q^*_{h,r}\, A_b + m_{m,air}\, h_{m,air,i} \text{ [kj/s]} \tag{6.23}$$

$$I^*_s\, d_g\, A_g/A_b + q^*_\lambda\, A_b/A_b = I^*_{s,}\, d_g\, r_w\, A_b/A_b + I^*_{s,} d_g\, d_w\, A_b/A_b + q^*_{i,g}\, A_b/A_b + q^*_{h,r}\, A_b/A_b + (m_{m,air}\, h_{m,air,I})/A_b \quad [\text{ j/m}^2\text{s}] \tag{6.24}$$

where d_w is the transmittance of water, r_w is the reflectivity of water for visible light. $h_{m,air}$ is the enthalpy of water at saturation temperature ϑ_i and $m^*_{m,air}$ is the mass flow rate of moist air.

The conductive heat transfer from the bottom to the seawater interface is:

$$q_{\lambda} = \lambda_w/\delta_w(\vartheta_b - \vartheta_i) \tag{6.25}$$

And the heat transfer from seawater interface to the glass cover is:

$$q_{h,r} = h_r(\vartheta_i - \vartheta_r) \tag{6.26}$$

Energy Balance for Black Plate

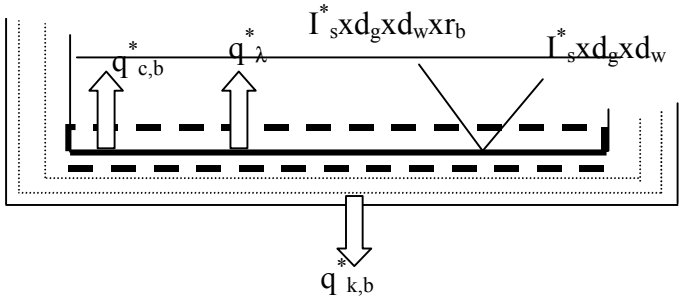

Figure 6.4. Energy Balance for Black Plate

According to Figure 6.4. the energy balance for black plate can be written as follows:

$$I^*_s\, d_g\, d_w\, A_b - I^*_s\, d_g\, d_w\, r_b\, A_b = q^*_{\lambda}\, A_b + q^*_{k,b}\, A_b - q^*_{c,b} A_b \quad [\text{j/s}] \tag{6.27}$$

$$I^*_s\, d_g\, d_w\, A_b/A_b - I^*_s\, d_g\, d_w\, r_b\, A_b/A_b = q^*_{\lambda}\, A_b/A_b + q^*_{k,b}\, A_b/A_b - q^*_{c,b} A_b/A_b \; [\text{j/m}^2\text{s}] \tag{6.28}$$

Where r_b is the reflectivity of black plate. $q^*_{c,b}$ is the convective heat transfer from bottom to the seawater;

$$q^*_{c,b} = h_{cb}(\vartheta_b - \vartheta_i) \tag{6.29}$$

the seawater depth in the still is very thin. Because of this convective heat transfer from black plate to the seawater can be neglected.

Reynolds analogy holds mass transfer coefficient is:

$$h_M = \frac{h}{\rho c_p} \quad [\text{ m/s}] \tag{6.30}$$

and then mass flow rate of evaporated water mass will be calculated according to the semi-permeable plane theory. For this purpose first of all the mass flux for a non permeable plane according to the Reynolds analogy is calculated. Using this value, the mass transfer coefficient for semi permeable plane will be as follows,

$$h_{M,h} = h_M \frac{P}{p_i - p_r} \ell n \frac{P - p_r}{P - p_i} \tag{6.31}$$

and then mass flow rate of evaporated water mass is,

$$m^*_{vapour} = h_{M,h} \frac{1}{RT} (p_{v,w} - p_{v,air}) A_b \quad [\text{ kg/s}] \tag{6.32}$$

Solutions of Energy Balance Equations

By the theoretical investigation of the solar still under consideration the following assumptions are made:

- The whole system is in a quasi-steady state condition
- Heat loss by radiation from the circumferential area is neglected
- At the base of the still, temperature of the walls equals to water temperature, and the water temperature is the average of the interface temperature, ϑ_I and the bottom temperature, ϑ_b.
- The wind speed is assumed to be constant during the experiment.

According to these assumptions, equations (6.2), (6.10), (6.24) and (6.28) was solved simultaneously.

Solutions of these non-linear equations simultaneously, yield the following temperatures:

Glass cover: ϑ_g

Inside air temperature: ϑ_r

Interface temperature: ϑ_i

Bottom temperature: ϑ_b

According to these temperatures, the evaporated water rate can be calculated.

B. Solar Stills with Reflector

In this study, vertical aluminum plate reflector, which has dimensions 2100 mm x 500 mm, was used to get extra solar energy. The solar radiation coming from sun to the reflector reflects to the glass cover and then enters the solar still as extra solar energy. Measurements were carried out with reflector and "fictive sun method" was used for calculation of extra solar energy gain. In fictive sun method, the shade of the reflector on the tilted surface will be calculated using the beams coming from the fictive sun.

The experiments was carried out in İzmir with a latitude of $\phi = 38.46^0$.The reflector and solar still are south facing and the surface azimuth angle is zero.

The amount of the solar energy of the reflected beams can be calculated as follows: firstly, the angle of incidence can be calculated according to Benford and Boch:

$$\cos\theta = \sin\delta \sin\phi \cos\beta - \sin\delta \cos\phi \sin\beta \cos\gamma + \cos\delta \cos\phi \cos\beta \cos\omega + \cos\delta \sin\phi \sin\beta \cos\gamma \quad \cos\omega + \cos\delta \sin\beta \sin\gamma \sin\omega \qquad (6.33)$$

where θ: Angle of incidence. It is the angle between the beam radiation on a surface and the normal to that surface.

δ: Declination. It is the angular position of the sun at solar noon with respect to the plane of the Equator, north positive; $-23{,}45° < \delta < +23{,}45°$.

ϕ: Latitude. It is angular location north or south of the Equator, north positive; $-90° < \phi < +90°$.

β: Slope. It is the angle between the incline surface and the horizontal plane.

γ: Surface azimuth angle. It is the angle in the horizontal plane between the projection of the surface normal vector of the inclined surface and the south indicating line according to a reference point; $-180° < \gamma < +180°$.

ω: Hour angle. It is the angular displacement of the sun east or west of the local meridian due to rotation of the earth on its axis at 15° per hour. It takes morning negative and afternoon positive values. At the solar noon it is zero, $\omega=0$.

Then the zenith angle, θ_z, can be calculated by:

$$\cos\theta_z = \sin\phi \sin\delta + \cos\phi \cos\delta \cos\omega \quad (6.34)$$

Solar altitude angle, h is calculated by $\theta_z + h = 90^0$ and also, the solar altitude angle of reflected beam, h' is equal to the solar altitude angle, h.

And then, the solar azimuth angle can be determined by the following equation:

$$\cos\gamma_s = (-\cos\phi \sin\delta + \sin\phi \cos\delta \cos\omega) / \sin\theta_z \quad (6.35)$$

The shade of the reflector on the tilted surface can be calculated using the fictive sun method.

The length of the shaded area on a horizontal surface is:

$$GU_{horizontal} = \frac{H_{reflector}}{tgh'} \quad (6.36)$$

where $H_{reflector}$ is the height of the reflector. And according to the law of sines, the length of the shaded area on the tilted surface is:

$$GU_{\beta} = \frac{GU_{horizontal}}{\cos\beta} \quad (6.37)$$

The shaded area on the tilted surface can be calculated as follows:

$$A_{sh} = GU_{\beta}\, W_{reflector} \quad (6.38)$$

where $W_{reflector}$ is the width of the reflector, but this shaded area is not yet the area on the solar still. The effective shaded area, A_{she}, on the solar still can be calculated with geometrical method. This area is the intersection of the shaded area on tilted surface, A_{sh}, and glass cover of the solar still.

The extra solar energy gain through reflected beams could be calculated as follows: First of all the energy of the beams falling on to the reflector must be calculated. And then, taking into account the reflectance of the reflector, $r_{reflector}$, the amount of the reflected solar energy is calculated.

The reflected solar energy per unit time and area is:

$$I^*_{oR}' = I^*_{o.}\, r_R.\, cos\theta' \quad [W/m^2] \tag{6.39}$$

And the total energy per unit time is:

$$Q^*_{oR}' = A_{she}.\, I^*_{oR}' d_g \quad [W] \tag{6.40}$$

where d_g is the transmittance of glass, the calculation of transmittance of glass will be shown in Appendix A, A_{she}. is the effective shaded area on the solar still. I^*_{oR}'is the solar radiation reflected energy per unit time and area and Q^*_{oR}' is the total solar radiation, reflected energy per unit time [25].

6.3. Calculation of Solar Radiation on Inclined Surface

At any point in time, the solar radiation incident on a horizontal plane outside of the atmosphere is the normal incident solar radiation as given by as follows:

$$I^*_{oz} = I^*_0(1+0.033\cos\frac{360n}{365})\cos\theta_z \quad [W/m^2] \tag{6.41}$$

where I^*_0 is the solar constant and equals 1353 (W/m^2), n is the day of the year and θ_z is the zenith angle.

Extraterrestrial solar radiation on inclined surface at any point in time is:

$$I^*_{o\beta} = I^*_0(1+0.033\cos\frac{360n}{365})\cos\theta \quad [W/m^2] \tag{6.42}$$

where θ is angle of incidence.

Hourly extraterrestrial solar radiation on inclined surface :

$$I_{oh\beta} = \frac{24.3600}{2\pi} I_0^* (1 + 0.033 \cos \frac{360n}{365})(\sin\delta \sin\phi \cos\beta \frac{2\pi}{360}(\omega_2 - \omega_1) - \sin\delta \cos\phi$$
$$\sin\beta \cos\gamma \frac{2\pi}{360}(\omega_2 - \omega_1) + \cos\delta \cos\phi \cos\beta (\sin\omega_2 - \sin\omega_1) + \cos\delta \sin\phi \sin\beta \cos\gamma$$
$$(\sin\omega_2 - \sin\omega_1) - \cos\delta \sin\beta \sin\gamma (\cos\omega_2 - \cos\omega_1))$$

(6.43)

and the hourly extraterrestrial solar radiation on horizontal surface calculated by the following formula:

$$I_{oh\beta} = \frac{24.3600}{2\pi} I_0^* (1 + 0.033 \cos \frac{360n}{365})(\sin\delta \sin\phi \frac{2\pi}{360}(\omega_2 - \omega_1) + \cos\delta \cos\phi (\sin\omega_2 - \sin\omega_1))$$

(6.44)

and the daily extraterrestrial solar radiation on tilted surface,

$$I_{oh\beta} = \frac{24.3600}{2\pi} I_0^* (1 + 0.033 \cos \frac{360n}{365})(\sin\delta \sin\phi \cos\beta \frac{2\pi}{360}(\omega_{\beta,s} - \omega_{\beta,r}) - \sin\delta \cos\phi$$
$$\sin\beta \cos\gamma \frac{2\pi}{360}(\omega_{\beta,s} - \omega_{\beta,r}) + \cos\delta \cos\phi \cos\beta (\sin\omega_{\beta,s} - \sin\omega_{\beta,r}) + \cos\delta \sin\phi \sin\beta \cos\gamma$$
$$(\sin\omega_{\beta,s} - \sin\omega_{\beta,r}) - \cos\delta \sin\beta \sin\gamma (\cos\omega_{\beta,s} - \cos\omega_{\beta,r}))$$

(6.45)

and on horizontal surface,

$$I_{oh\beta} = \frac{24.3600}{2\pi} I_0^* (1 + 0.033 \cos \frac{360n}{365})(\sin\delta \sin\phi \frac{2\pi}{360} \omega_{\beta,s} + \cos\delta \cos\phi \sin\omega_{\beta,s})$$

(6.46)

Taking all the atmospheric factors into account, the terresterial direct normal solar radiation on inclined surface is given :

$$I_{c\iota\beta}^* = I_{on}^* \tau_b \cos\theta \qquad (6.47)$$

And the direct solar radiation on horizontal surface is:

$$I_{cn}^{*} = I_{on}^{*}\tau_b \cos\theta_z \tag{6.48}$$

where τ_b is the atmospheric transmittance for direct radiation [26].

Calculation of the atmospheric transmittance for direct radiation, τ_b:

Hottel has presented a method for estimating the beam radiation transmitted through clear atmospheres, which takes into account zenith angle and altitude for a standard atmosphere and four climate types. The atmospheric transmittance for beam radiation τ_b is given in the form:

$$\tau_b = a_0 + a_1 \exp(-k/\cos\theta_z) \tag{6.49}$$

The constants a_0, a_1 and k for the standard atmosphere with 23 km visibility are found from a_0^{*}, a_1^{*} and k^{*}, which are given for altitudes less than 2.5 km by:

$$a_0^{*} = 0.4237 - 0.00821(6 - A)^2 \tag{6.50}$$

$$a_1^{*} = 0.5055 + 0.00595(6.5 - A)^2 \tag{6.51}$$

$$k^{*} = 0.2711 + 0.01858(2.5 - A)^2 \tag{6.52}$$

where A is the altitude of the observer in kilometers.

Correction factors are applied to a_0^{*}, a_1^{*} and k^{*} to allow for changes in climate types. The correction factors $r_0 = a_0 / a_0^{*}$, $r_1 = a_1 / a_1^{*}$, and $r_k = k / k^{*}$ are given in Table 6.1.

Table.6.1. Correction Factors For Climate Types [26]

Climate Type	r_0	r_1	r_k
Tropical	0.95	0.98	1.02
Midlatitude summer	0.97	0.99	1.02
Subarctic summer	0.99	0.99	1.01
Midlatitude winter	1.03	1.01	1.02

It is also necessary to estimate the clear sky diffuse radiation on a horizontal and inclined surface to get the total radiation. Liu and Jordan (1960) developed an empirical relationship between the transmission coefficient for direct and diffuse radiation for clear days:

$$\tau_d = 0.2710 - 0.2939\tau_b \tag{6.53}$$

Thus, the diffuse solar radiation on inclined and horizontal surface is:

$$I^*_{cd\beta} = I^*_{on}\tau_d \cos\theta \tag{6.54}$$

and

$$I^*_{cdz} = I^*_{on}\tau_d \cos\theta \tag{6.55}$$

And the total solar radiation on inclined and horizontal surface is [26]:

$$I^*_{ct\beta} = I^*_{c\imath\beta} + I^*_{cd\beta} \tag{6.56}$$

and

$$I^*_{ctz} = I^*_{c\imath\imath} + I^*_{cdz} \tag{6.57}$$

6.4. Experimental Study of Solar Still

6.4.1. The Solar Still Used in Experimental Study

A basin type solar still was investigated in this study, in IZTECH Gülbahçe Campus Area. The construction of the still was made in the workshop of the Mechanical Engineering Department.

The basin type solar still was constructed with chrome sheet and galvanized iron. The bottom and sides of the chrome box were well insulated by polystyrene insulation material. The thickness of polystyrene insulation is 5 cm in east and west sides, 10 cm in other parts of the still and it was covered by galvanized sheet. The

dimensions of chrome sheet that used for inside box is shown in Figure 6.5. Thickness of the glass is 4 mm which is used as a cover. A chrome channel was fitted under the lower side of the glass cover to collect the condensed water. The channel was ended with a small plastic pipe in order to drain the fresh water into external vessel. The glass was mounted at an angle of 38^0 to the solar still to ensure that the condensate will run down the glass in the condensate-collecting channel. And also two aluminum collecting channels were stick to the glass cover to collect condensate flowing down. The absorbing plate is also made of chrome which has dimensions 2 m x 0.5 m and the effective area of the solar still is 1 m^2. The absorbing plate of the solar still has 1-meter square area and it was painted with black dye. The plates were connected by welding. Afterwards, three holes were drilled to the solar still, one of them for seawater inlet, second for condensed water outlet and the third for discharging of remaining seawater.

After construction of solar still it was painted by cellulose based black paint. After painting process was finished, the insulation material was fixed between the chrome sheet and galvanized sheet. The aluminum collecting channels were stick to the glass cover and then glass cover was settled on to the construction. Thermocouples were located in different places of the still before fixing the glass cover. They record the different temperatures, such as outside glass cover, solar basin water, inside moist air temperature and seawater interface. A data logger was used to record temperature values. Rubber band was used to be no air will escape through small spaces between cover and still.

A metallic reflector 2100mm x 500mm in dimension (made of aluminum, having the reflectivity of about 90%) was attached to the still in the second part of the experiment. The reflector was designed to concentrate the incident solar radiation.

The long side of the solar still is aligned in north-south direction. Technical specifications of solar still are given in Table 6.2. and schematic view of the solar still is shown in Figure 6.6 and 6.7. And also schematic view of the solar still with scale is given in Appendix G.

Table 6.2. Technical Specifications of Solar Still

Specifications of the Solar Still	
Length, m	2
Width, m	0.5
Base area, m^2	1
Cover inclination,^{0}	38
Glass area, m^2	1.4
Glass depth, mm	4

Sea water was taken with a galvanized pipe into the still. During the experiment the solar still was fed by Gülbahçe- Urla seawater and the water depth was kept 1 cm in the solar still. Experiments was carried on sunny, particularly sunny and cloudy days. The temperatures of glass cover, ambient temperature, temperature of seawater (in the still), seawater interface temperature, moist air temperature, bottom temperature and humidity of ambient air was recorded. Thermocouples (Ni-Cr, K type) were used to measure temperatures, the ambient air temperature and humidity of ambient air was measured with electronic thermo-hygrometer which was donated by Alexander von Humbolt Foundation and Elimko data logger recorded temperatures. The distilled water was collected each hour in a storage bottle.

This study had been performed in two main parts. One of them was carried out without reflector, and the second was carried out with reflector at İzmir Institute of Technology Campus Area with using Gülbahçe - Urla Seawater.

Experiments were carried out during the period of March 31 to May 12, 2003. The amount of distilled water was weighed starting from 9 am until 5 pm.

In the second part of the experiment, a reflector was added to the system and under the same condition experiments were repeated.

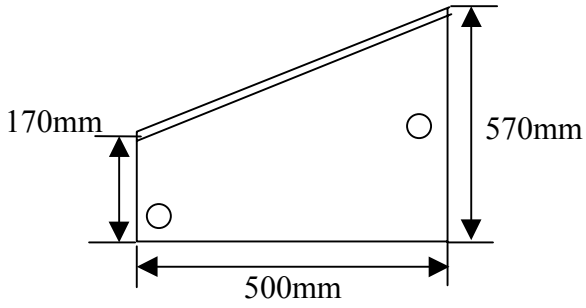
170mm
570mm
500mm

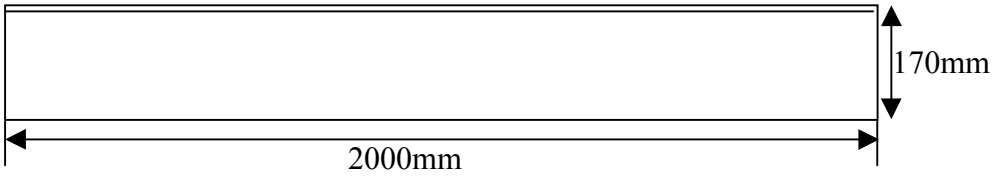
170mm
2000mm

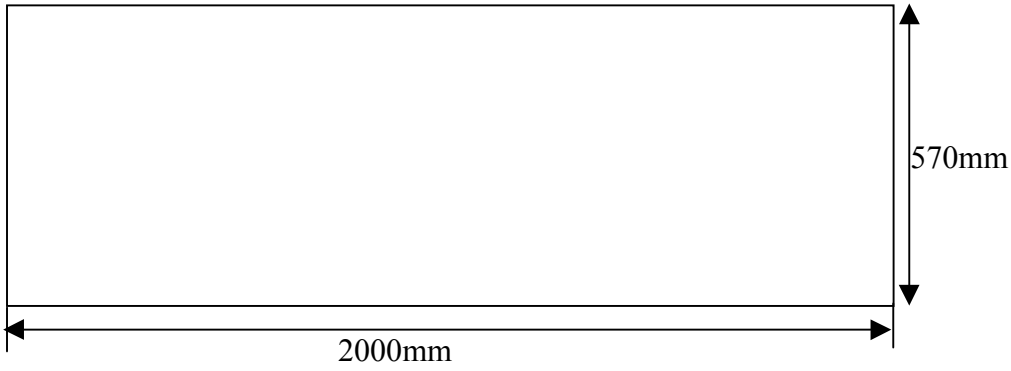
570mm
2000mm

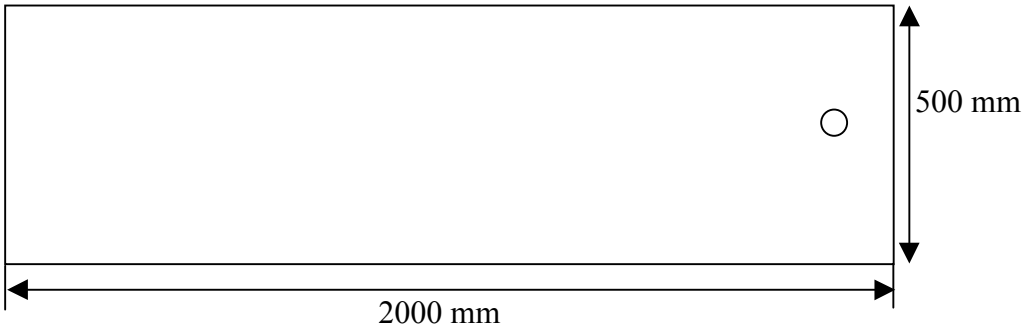
500 mm
2000 mm

Figure 6.5. Side, Front , Back and Bottom Chrome Plates of Solar Still

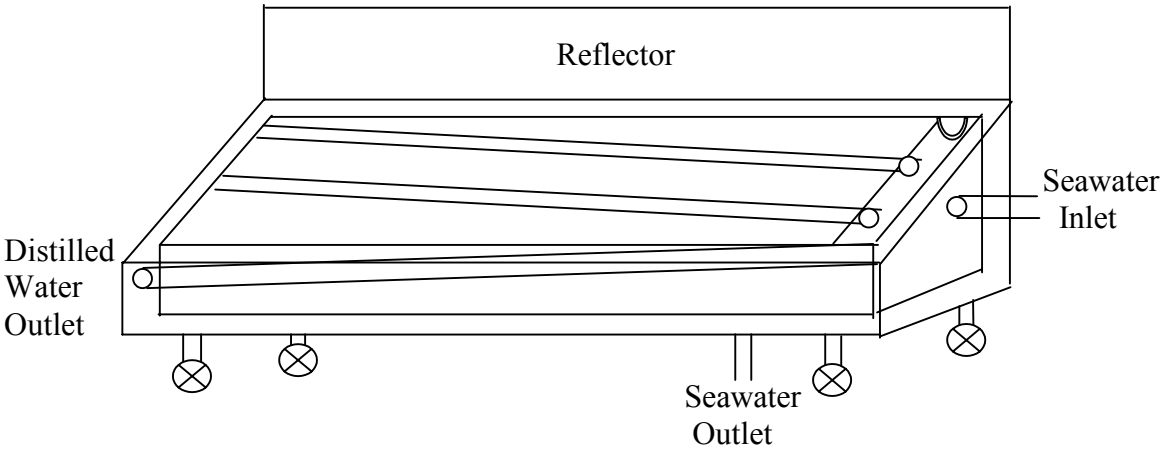

Figure 6.6. Schematic view of Solar Still

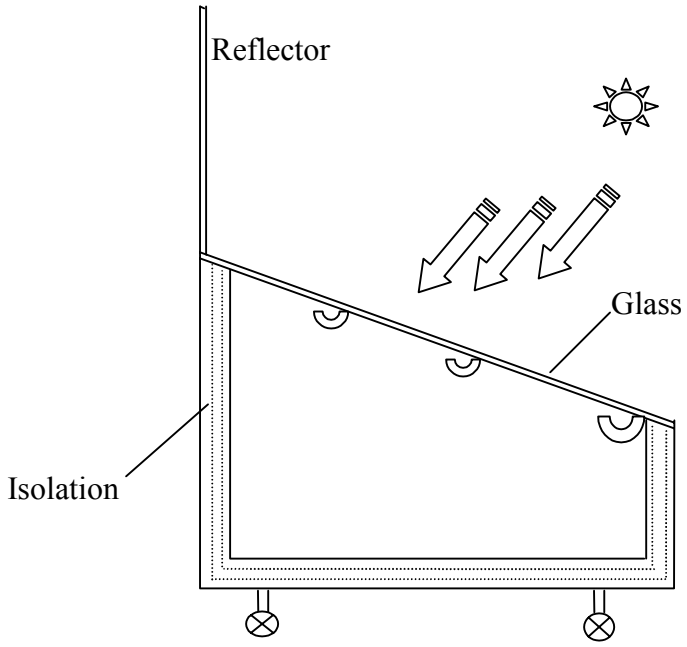

Figure 6.7. Cross-section of Solar Still

The amount of distilled water was measured every hour during the experiment. The data logger was available to read the recordings of thermocouples. These measured temperature values help in theoretical solution of the solar still. Figure 6.8

shows photograph of the data logger thermocouples and hygrometer used in the experiment and also Figure 6.9 shows the photograph of the solar still.

Figure 6.8. Photograph of the data logger, thermocouples and hygrometer used in the experiment

Figure 6.9. Photographs of the solar still

6.4.2. Properties of Gülbahçe – Urla Seawater

This experimental study is aimed on the distillation of seawater. During the experiment Gülbahçe – Urla seawater was used for the system. In each experiment, ten liter seawater was put into solar still. Table 6.3 shows the characteristics of Gülbahçe – Urla seawater in Spring 1997. Urla seawater has high salinity if it is compared with the other seawater's salinities.

Table 6.3. Properties of Gülbahçe- Urla Seawater [27]

	Surface	**Bottom**
pH	7.19	7.32
T(^{0}C)	21.0	19.0
Ca(mg/l)	456.9	440.9
Mg(mg/l)	1498.1	1556.4
HCO_3(mg/l)	134.2	137.2
NO_3(µgat/l)	4.74	0.40
Silica(µgat/l)	0.034	0.165
PO_4^{3-}(µgat/l)	0.41	0.47

Salinity (g/l)	36.85	38.61

6.4.3. Calculation of Solar Radiation on Tilted Surface

The terrestrial solar radiation coming from the sun is measured by meteorological station in İzmir. They measure solar radiation on horizontal surface. But in this experiment, the solar still has a slope 38^0 and the solar intensity on tilted surface should be calculated from the meteorological measured value.

It can be assumed (as suggested by Hottel and Woertz(1942)) that the combination of diffuse and ground–reflected radiation is isotropic. With this assumption, the sum of the diffuse from the sky and the ground-reflected radiation on the tilted surface is the same regardless of orientation, and the total radiation on the tilted surface is the sum of the beam contribution calculated as $I_{ihz}R_b$ and the diffuse on a horizontal surface, I_{dhz}. This represents an improvement over the assumption that all radiation can be treated as beam, but better methods are available.

An improvement on these models the isotropic diffuse model, was derives by Liu and Jordan (1963). The radiation on the tilted surface was considered to include three components: beam, isotropic diffuse, and solar radiation diffusely reflected from the ground. A surface tilted at slope β from the horizontal has a view factor to the sky F_{c-s} which is given by (1+cos β)/2. (If the diffuse radiation is isotropic, this is also R_d, the ratio of diffuse on the tilted surface to that on the horizontal surface.) The surface has a view factor to the ground F_{c-g} of (1-cos β)/2, and if the surroundings have a diffuse reflectance of ρ_g for the total solar radiation, the reflected radiation from the surroundings on the surface will be $I_{thz}\rho_g(1-\cos\beta)/2$. Thus the total solar radiation on the tilted surface for an hour as the sum of the three terms:

$$I_{th\beta} = I_{ihz}R_b + I_{dhz}\left(\frac{1+\cos\beta}{2}\right) + I_{thz}\rho_g\left(\frac{1-\cos\beta}{2}\right) \qquad (6.58)$$

where I_{dhz} is the hourly diffuse solar radiation on horizontal surface and it can be calculated by The Orgill and Hollands correlation. This correlation produces results that

are for practical purposes the same as those of Erbs et al., and is represented by the following equations:

$$\frac{I_{dhz}}{I_{thz}} = 1.0 - 0.249k_{th} \qquad \text{for} \qquad k_{th} < 0.35 \tag{6.59}$$

$$\frac{I_{dhz}}{I_{thz}} = 1.557 - 1.84k_{th} \qquad \text{for} \qquad 0.35 < k_{th} < 0.75 \tag{6.60}$$

$$\frac{I_{dhz}}{I_{thz}} = 0.177 \qquad \text{for} \qquad k_{th} > 0.75 \tag{6.61}$$

where k_{th} is the hourly clearness index and I_{thz} is the hourly total solar radiation on horizontal surface. [23,26]

The solar radiation values on tilted surface were calculated by this method with a computer program. The computer program and its results was given in Appendix B.

Chapter 7

RESULTS AND DISCUSSION

In this work, a solar distillation in a single basin is studied theoretically and experimentally. The aluminum reflector was assembled to the still and effect of the reflector on the still productivity was examined. The numerical solution of the basic heat and mass transfer equations was also established. The theoretical results were compared with the experimental results obtained as part of this work.

The effect of the predicted solar radiation on the yield of the solar still will be examined. A computer program was developed to find theoretical values of daily and

hourly solar extraterrestrial radiation and also to calculate effect of reflector. The program and the results of the program are shown in Appendix B. In this program, sunrise and sun set hour angles and extraterrestrial solar radiation values were calculated and the effect of the reflector was examined with calculation of effective shaded area, A_{she}. Afterwards, the reflected total solar energy, which can be obtained by reflector, was calculated with using this program. Calculations were carried out for İzmir where latitude is 38.46 and slope of the inclined surface is 38. And also, the solar radiation values on tilted surface were calculated with using hourly horizontal solar radiation values. The radiation values which was taken from Güzelyalı Meteorology Station was used for some days(31.04.2003, 04.04.2003) and for the other days, the measured values in IZTECH Campus was used for calculations. The program which is used to find solar radiation on tilted surface and the results of the program is also shown in Appendix B.

Another computer program was developed (Appendix C) based on energy balance equations to reach temperature of glass cover, inside moist air, bottom and interface. Temperature values also help us to evaluate theoretically the amount of evaporated water for known solar radiation and ambient temperature. In this program, gradient-based optimization method was used to solve four non-linear equations [28]. According to this method, in order to be able to find a solution set for our energy balance equations, first a function E is obtained as follows:

$f_1(T_b,T_i,T_r,T_g)=0$

$f_2(T_b,T_i,T_r,T_g)=0$

$f_3(T_b,T_i,T_r,T_g)=0$

$f_4(T_b,T_i,T_r,T_g)=0$

$E= f_1^2+ f_2^2+ f_3^2+ f_4^2$

Then, a solution set that minimizes the function E is searched using steepest descent method iteratively as follows:

$$T_b = T_b - \frac{\partial E}{\partial T_b}\eta$$

$$T_i = T_i - \frac{\partial E}{\partial T_i}\eta$$

$$T_r = T_r - \frac{\partial E}{\partial T_r}\eta$$

$$T_g = T_g - \frac{\partial E}{\partial T_g}\eta$$

The flowchart of the program is given in Appendix F.

To find the unknown temperature values (glass cover temperature, inside moist air temperature, bottom temperature and interface temperature) equations 6.2(f_1), 6.10(f_2), 6.24(f_3) and 6.28(f_4) solved with using known constant values. The used constant values are given in Appendix D.

From solution of these equations simultaneously, yields temperature of bottom, interface, glass cover and moist air.

Using the calculated temperature values, the amount of evaporated water in unit time can be calculated theoretically with using Reynolds analogy.

Reynolds analogy holds mass transfer coefficient is:

$$h_M = \frac{h}{\rho c_p} \quad [\text{ m/s}]$$

and then mass flow rate of evaporated water mass will be calculated according to the semi-permeable plane theory. For this purpose first of all the mass flux for a non permeable plane according to the Reynolds analogy, is calculated. Using this value, the mass transfer coefficient for semi permeable plane will be as follows,

$$h_{M,h} = h_M \frac{P}{p_i - p_r} \ell n \frac{P - p_r}{P - p_i} \text{ [m/s]}$$

and then mass flow rate of evaporated water mass is,

$$m^*_{vapour} = h_{M,h} \frac{1}{RT}(p_{v,w} - p_{v,air})A_b \quad [\text{ kg/s}]$$

According to Reynolds analogy, the following product fresh water values were calculated. Figure 7.1 presents the theoretical hourly variation of temperatures (seawater interface, bottom, inside moist air, glass) on the 31st day of March and theoretical productivity of the still in each hour is shown in Figure 7.2. These calculations were made with known solar radiation and ambient air.

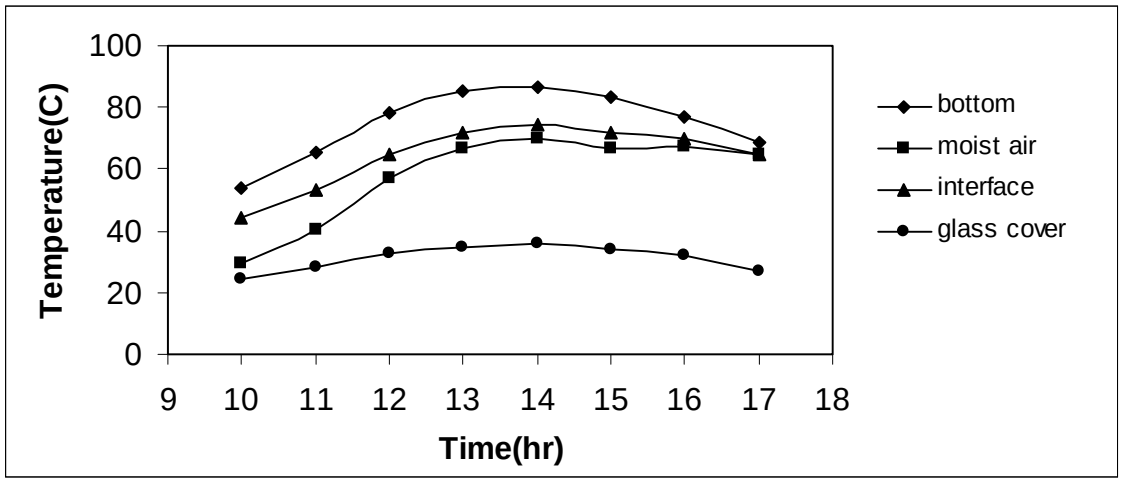

Figure 7.1. Hourly Variation of Theoretical Temperatures for 31/03/2003

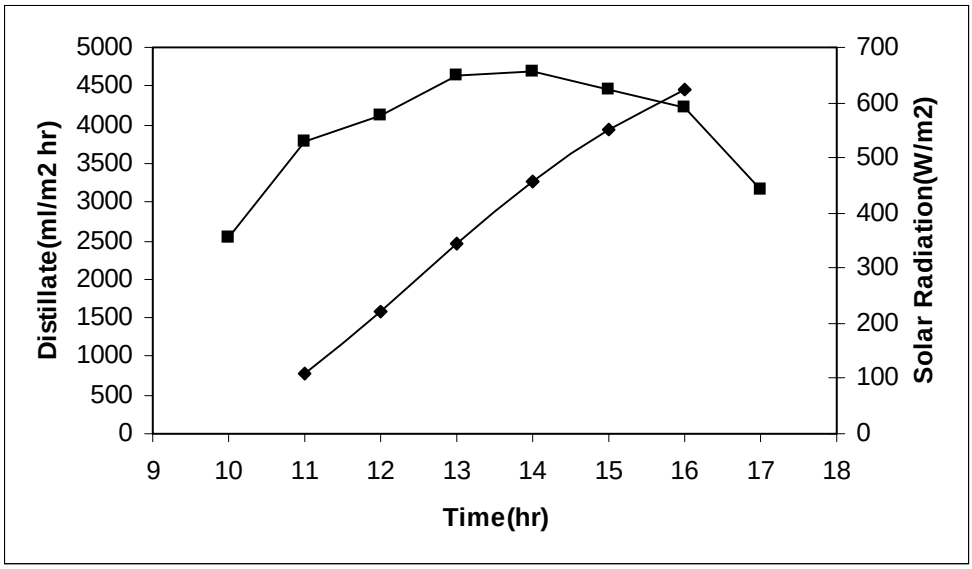

Figure 7.2. Hourly Variation of Theoretical Cumulative Evaporated Water for 31/03/2003

Theoretical hourly variation of temperatures (seawater interface, bottom, inside moist air, glass) on the 28th and 29th day of April and theoretical productivity of the still are shown in Appendix E.

In experimental part of this study, the solar still mentioned was tested. The amount of distilled water and some temperature values was measured. The quantity of fresh water obtained from the still was 1.430 l/m^{2}day on the 31st day of March using the still with a tilt angle of 38^0. Figure 7.3 shows meteorological data was given by Meteorology station of Güzelyalı-İzmir. The solar radiation measurements made with

the help of actinograph but it is not as same value as measured with pyronometer. Because of this, two correlations were used to obtain real solar intensity values. The following correlations were used:

$$Y=-1.83+0.96\ X \quad \text{for } 0\text{-}40(cal/cm^2min)$$
$$Y=-3.65+1.18X \quad \text{for } 40\text{-}80(cal/cm^2min)$$

where X is the hourly measurement values with actinograph and Y is the hourly measurement values with pyronometer[29]. According to this, the total daily radiation on horizontal surface was 22.94 MJ/m^2day. The solar still used in this experiment has a slope 38^0. For this, the solar radiation values on inclined surface were calculated. The calculated values were given in Figure 7.4 and the total solar radiation on tilted surface is 21.45 MJ/m^2 between 9.00 to 17.00. Figure 7.5 presents the hourly variation of temperatures for the experiment. As shown by the figure, the maximum water temperature occurred between the hours of 13.00 and 14.00. It ranged between 70-80 ^0C where the ambient air temperature was nearly 20^0C.

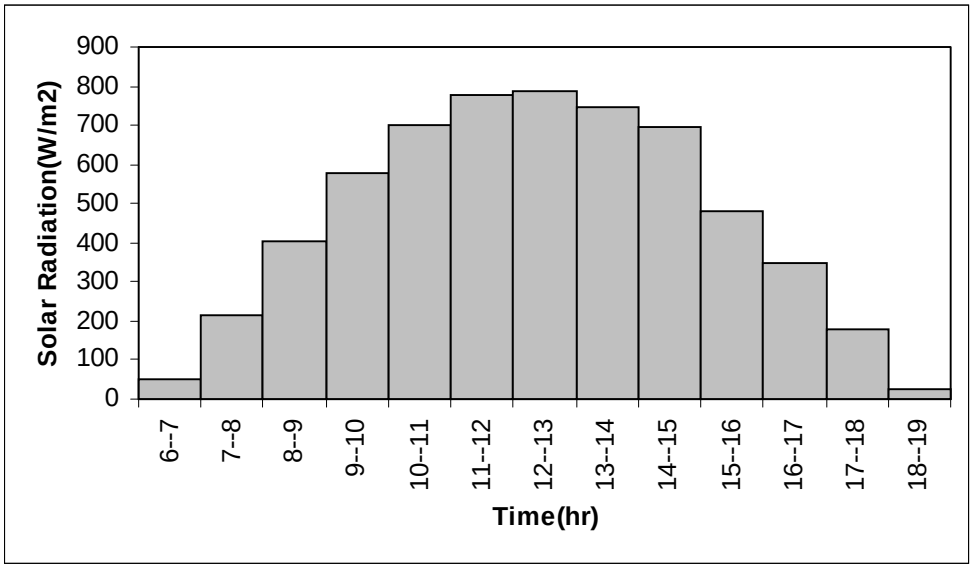

Figure 7.3.Hourly Solar Radiation values on horizontal surface for 31/03/2003

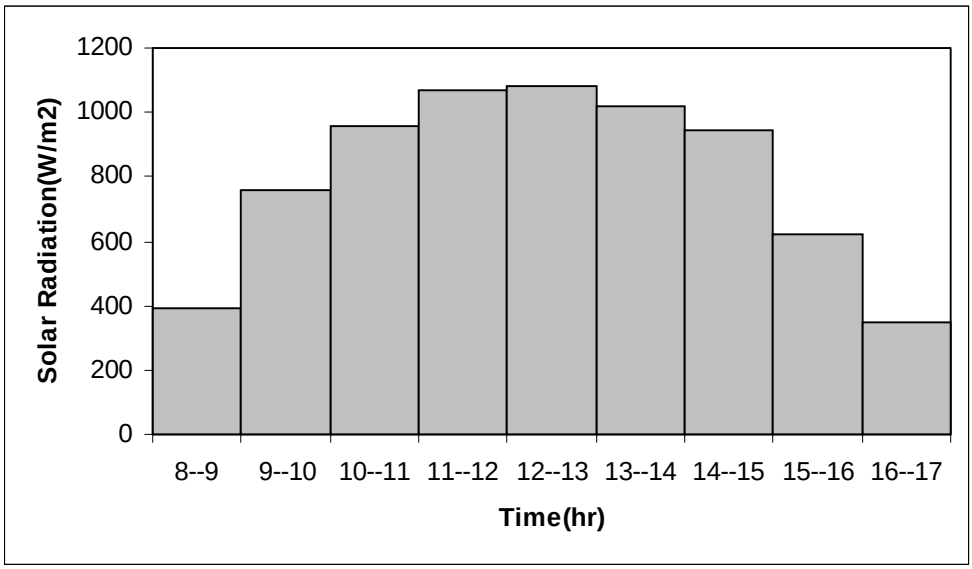

Figure 7.4. Hourly solar Radiation values on tilted surface($\beta=38^0$) for 31/03/2003

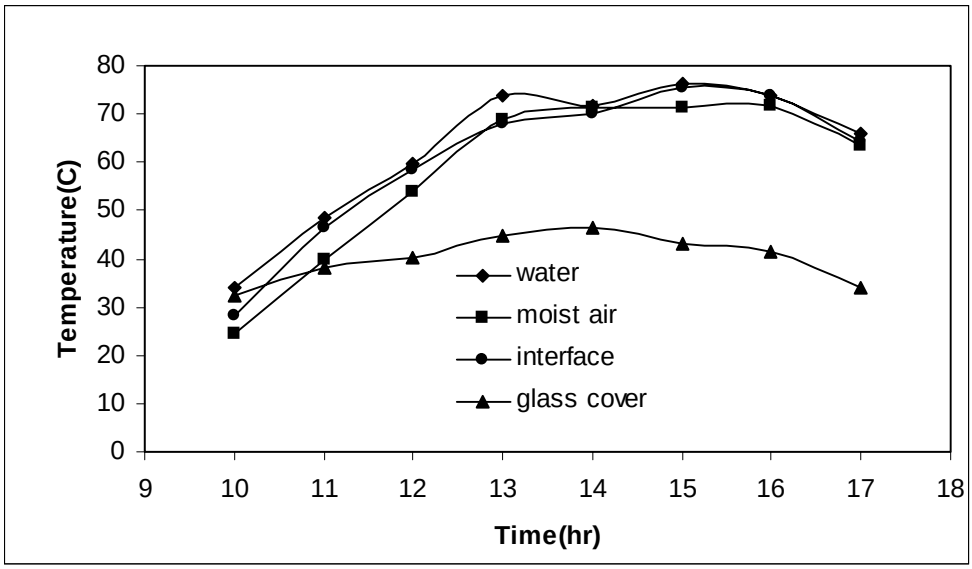

Figure 7.5. Hourly Variation of Experimental Temperatures for 31/03/2003

Figure 7.6 shows the output of fresh water of the still. As shown by Figure 7.4, the production rate starts very slowly due to warming of the still and the somewhat low solar energy during the morning hours. A peak production rate is obtained at about 16.00. And then it starts to decrease. The total daily yield of the still was 1.430 l/m^2day.

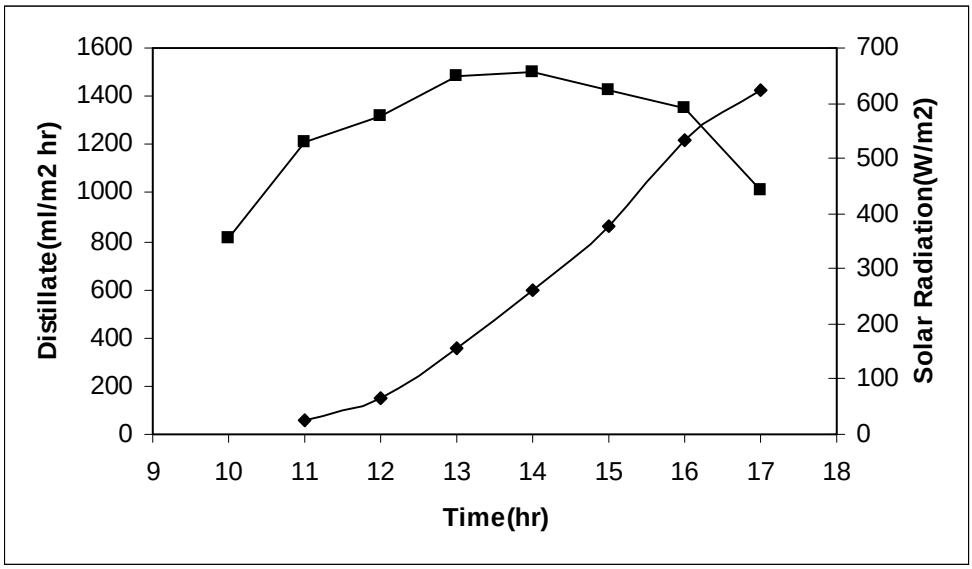

Figure 7.6. Hourly Variation of Experimental Distilled Water Yield and Solar Radiation for 31/03/2003

During the experiment, ambient air temperature and relative humidity was also measured. Figure 7.7 shows hourly variation of Ambient Air Temperature and Relative Humidity.

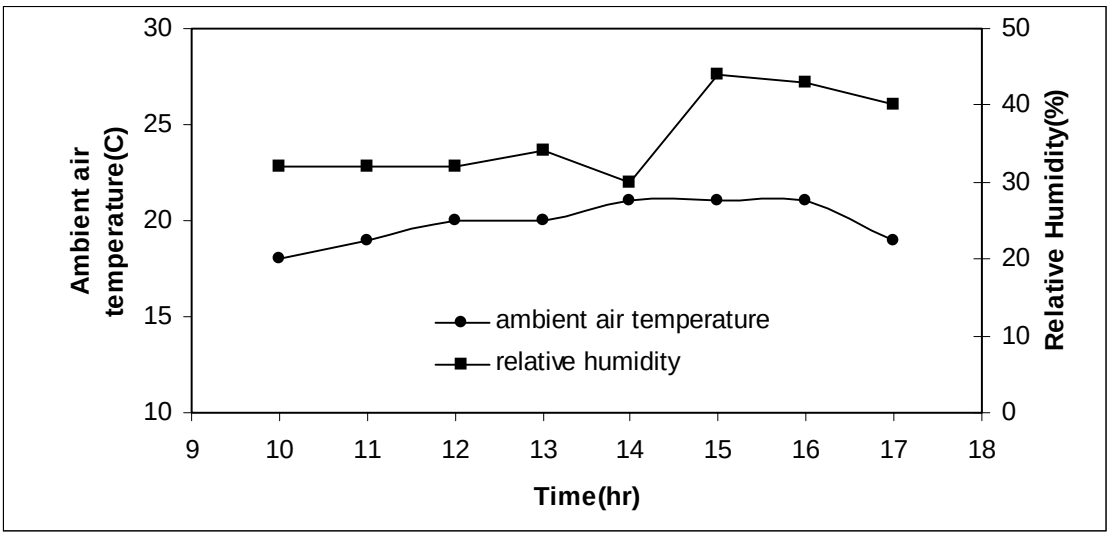

Figure 7.7. Hourly Variation of Ambient Air Temperature and Relative Humidity

Afterwards, theoretical and experimental values on 31st of March were compared. Figure 7.8 shows comparison of theoretical and experimental interface

temperature values hourly. As shown, the temperatures have the same trend, as they increase in the morning hours to maximum values before they start to decrease late in the afternoon. Figure 7.9 shows comparison of theoretical and experimental moist air temperature values. Measured and calculated values are rather close together.

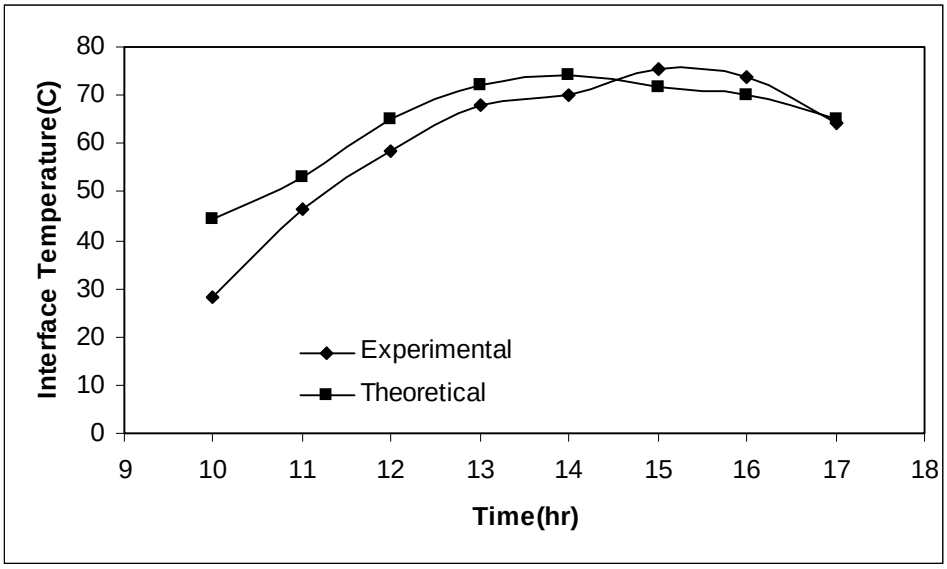

Figure 7.8.Comparison of theoretical and experimental "interface temperature" values

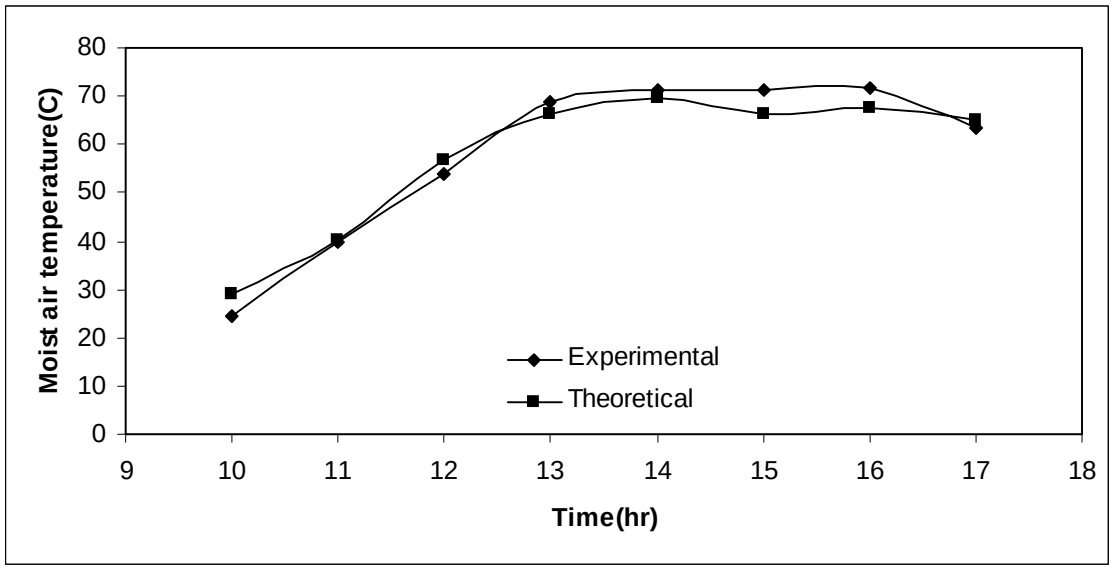

Figure7.9. Comparison of theoretical and experimental "moist air temperature" values

Theoretical and experimental glass cover temperature values are shown in Figure 7.10. As shown from the figure, theoretical and experimental glass cover temperatures have same the trend. On the other hand, there are differences where experimental glass cover temperature values are higher than theoretical values. It can be result from thermocouple which was used to measure glass cover temperature. It was stick on the cover. It can be heated by the sun over its real temperature value. Because of this reason, the glass cover temperatures can be different for experimentally and theoretically.

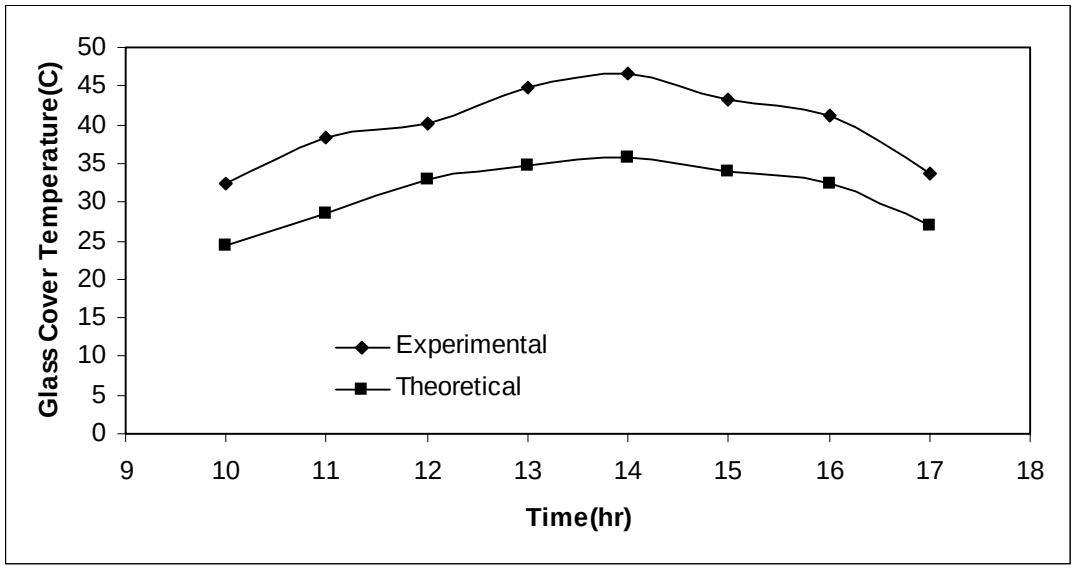

Figure 7.10. Comparison of theoretical and experimental "glass cover temperature" values

In the second part of the experimental study, the experiment was repeated with reflector. The reflector was added to the still, temperature values and amount of distilled water was measured. The experiment was made on the 4th day of April. Figure 7.11 presents the variation of hourly temperatures for the experiment. The water temperature in the base of the solar still was always the highest between all the temperatures since solar energy is absorbed there. The maximum water temperature occurred between the hours 13.00 to 14.00.

Figure 7.12 shows hourly variation of distilled water yield. The quantity of fresh water obtained from the still was 1.410 l/m^{2}day. The maximum amount of distilled water was obtained between the hours 14.00 to 15.00. The total solar radiation on inclined surface was 16.93 MJ/m^2 between the hours 9.00 to 17.00. If the reflector did not use, the total solar radiation on tilted surface would be 13.77 MJ/m^2 between the

hours 9.00 to 17.00 so 23% extra solar energy was obtained by reflector. Figure 7.13 shows the hourly variation of solar radiation on horizontal surface for 04.04.2003 and the calculated values of solar radiation on tilted surface for 04.04.2003 was given in Figure 7.14.

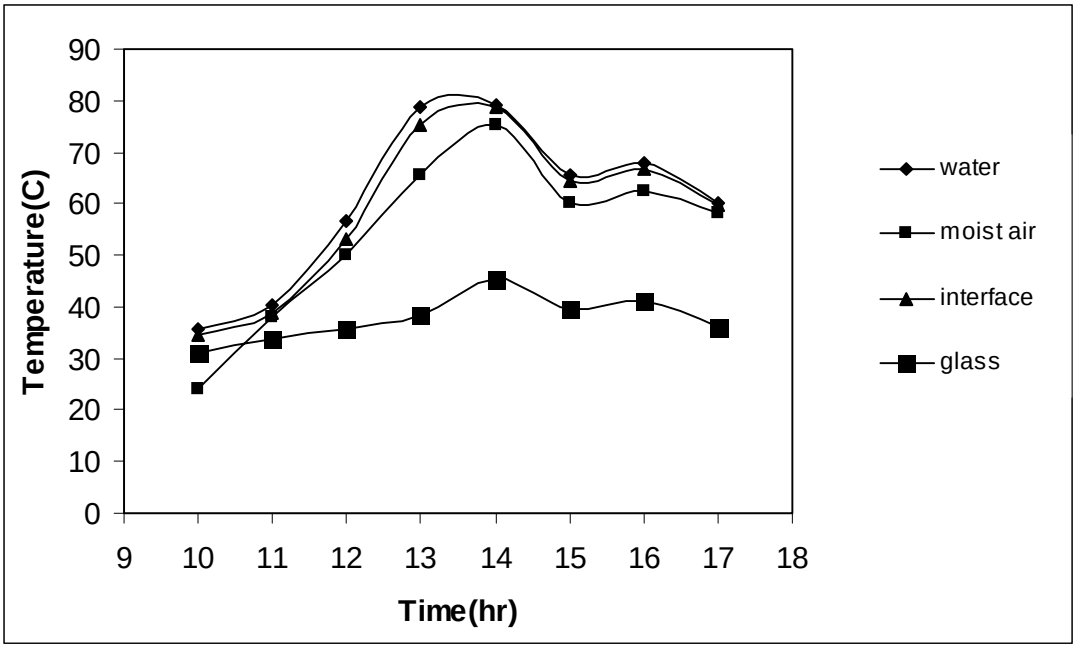

Figure 7.11.Hourly variation of temperature values for 04/04/2003

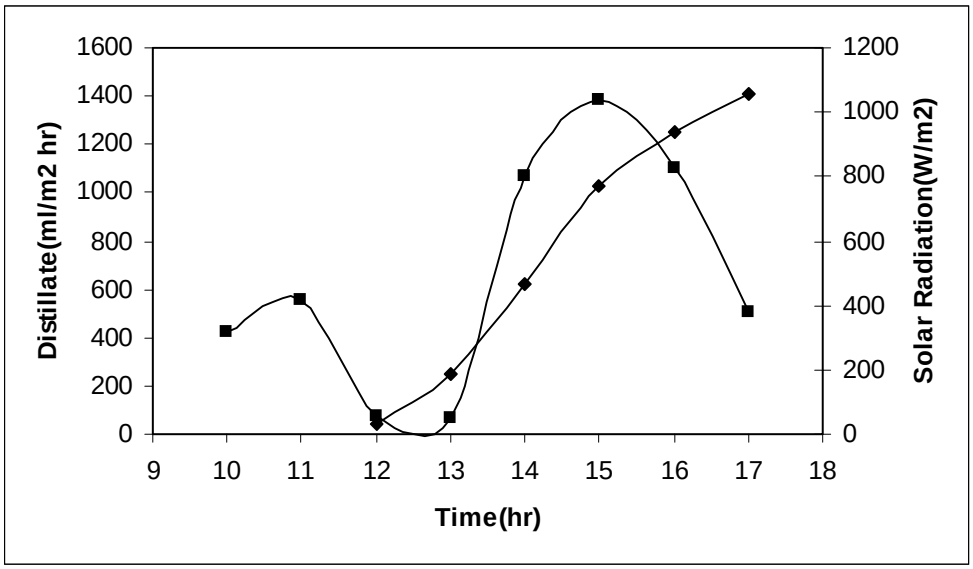

Figure 7.12.Hourly variation of Experimental Distilled Water Yield and Solar Radiation values for 04/04/2003

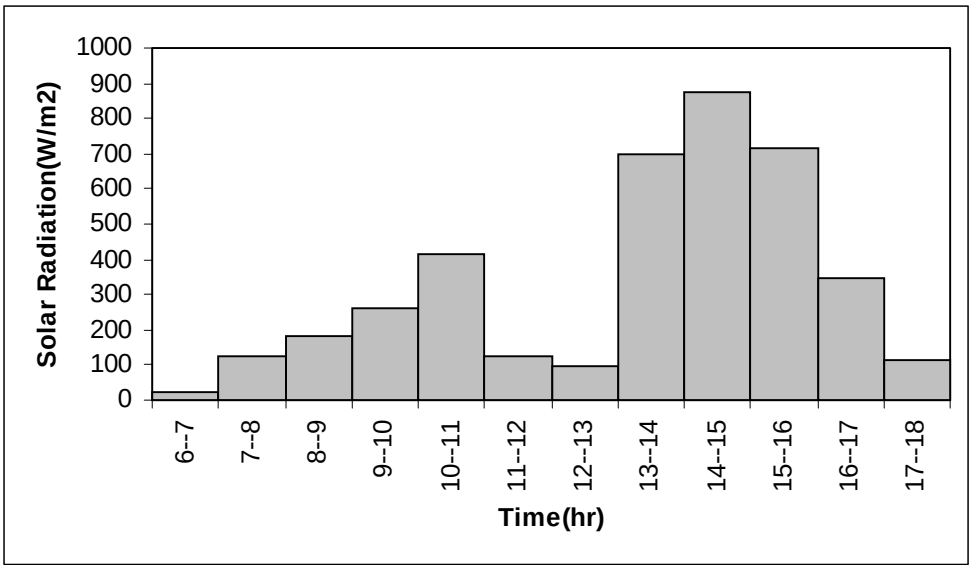

Figure 7.13.Hourly Solar Radiation values on horizontal surface for 04/04/2003

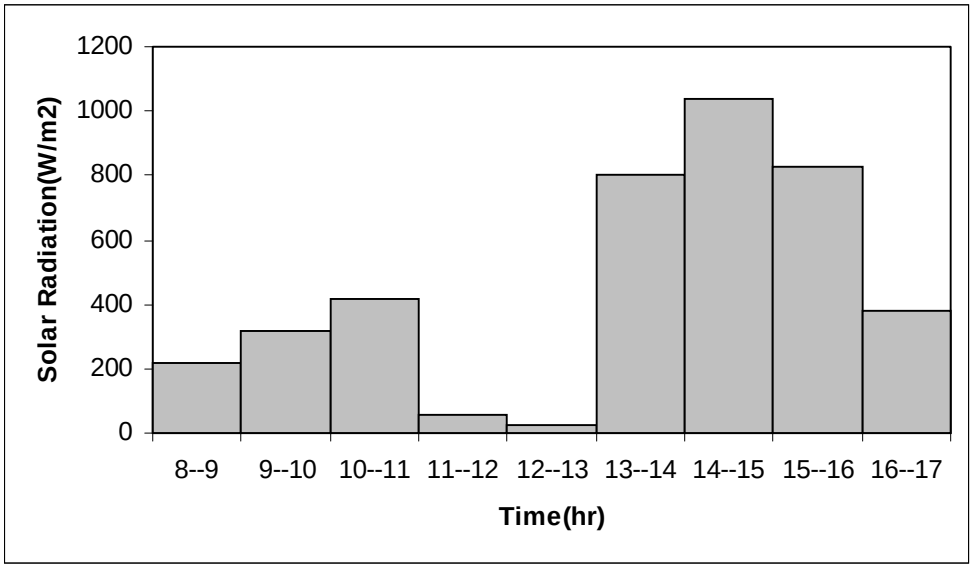

Figure 7.14. Hourly solar Radiation values on tilted surface($\beta=38^0$) for 04/04/2003

Other experimental results (with reflector and without reflector) were shown in Appendix E and solar radiation values were shown which was measured in IZTECH Campus.

The efficiency of a still can be calculated by the following equation:

$$\frac{\text{Water output} * \text{Latent heat of evaporation of water} *}{\text{Daily solar radiation}} 100\ \%$$

for the system without reflector:

$$\eta = \frac{m^* x 2500.7}{I_{s.t} x A_g} x100\%$$

and efficiency can be found by using the following formula for the system with reflector:

$$(\eta)_R = \frac{m^* x 2500.7}{I_{s.t} x A_g + I_{s,b} x A_{she}} x100$$

where m^* is the daily output (kg/m^2 s), 2500.7 is the latent heat of evaporation of water(kJ/kg) and $I_{s.t}$ is the daily total solar radiation(kJ/m^2s), $I_{s.b}$ is the beam radiation reflected from the reflector (kJ/m^2s) and A_{she} is the effective shaded area on the glass cover.

Table 7.1 shows daily efficiency values for 31st of March, 4th of April and 29th of April. The hourly variation of still efficiency without reflector for 31st of March is shown in Figure 7.15 which indicates that the efficiency of the still increases to a maximum value late in the afternoon. Figure 7.16 shows hourly variation of efficiency for the 29th day of April and Figure 7.17 shows variation of hourly efficiency values with reflector.

Table 7.1. Daily Efficiency Values for31st of March , 4th of April and 29th of April

Date	Efficiency (%)
31.03.2003	16.67
04.04.2003	20.82
29.04.2003	28.25

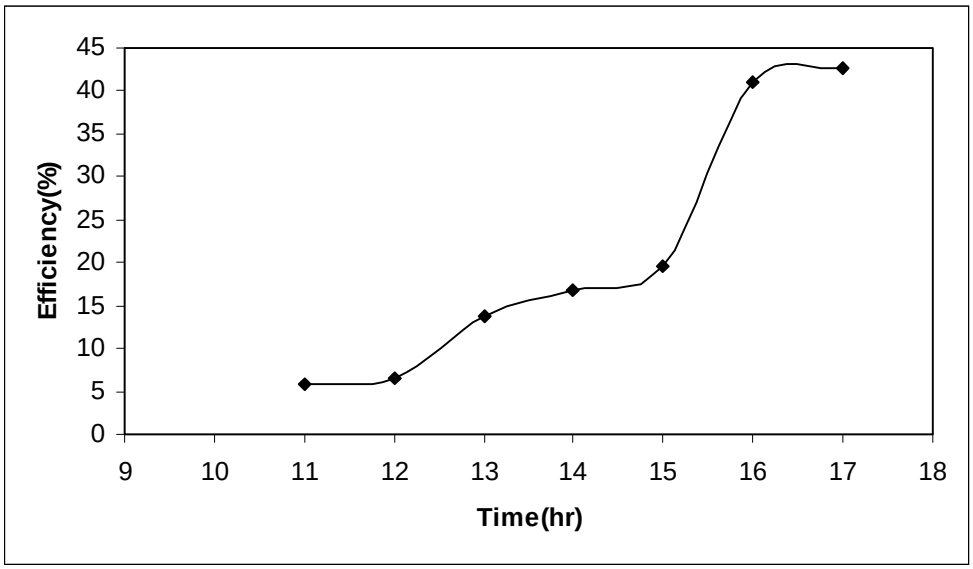

Figure 7.15. Experimental hourly efficiency of still for 31/03/2003

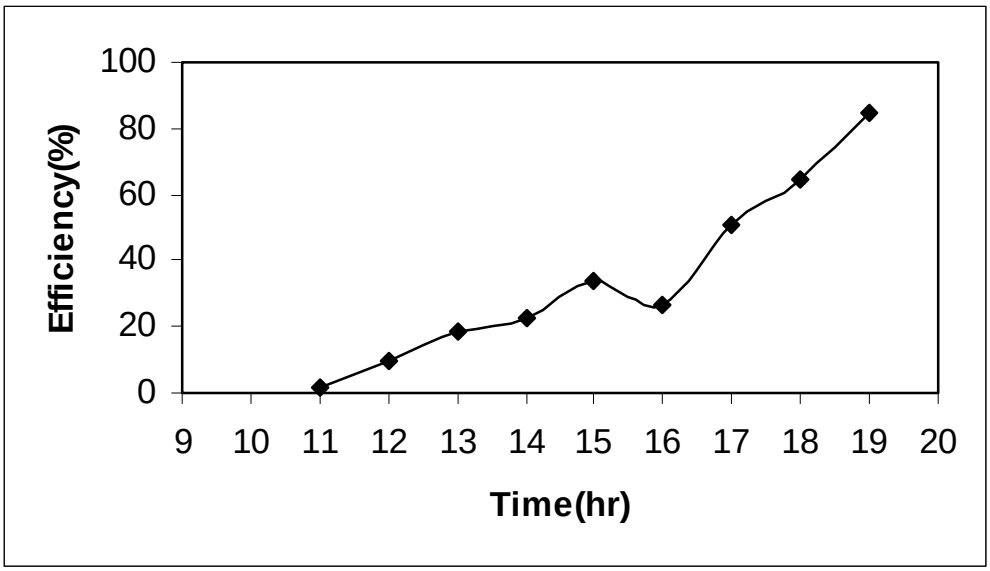

Figure 7.16. Experimental hourly efficiency of still for 29/04/2003

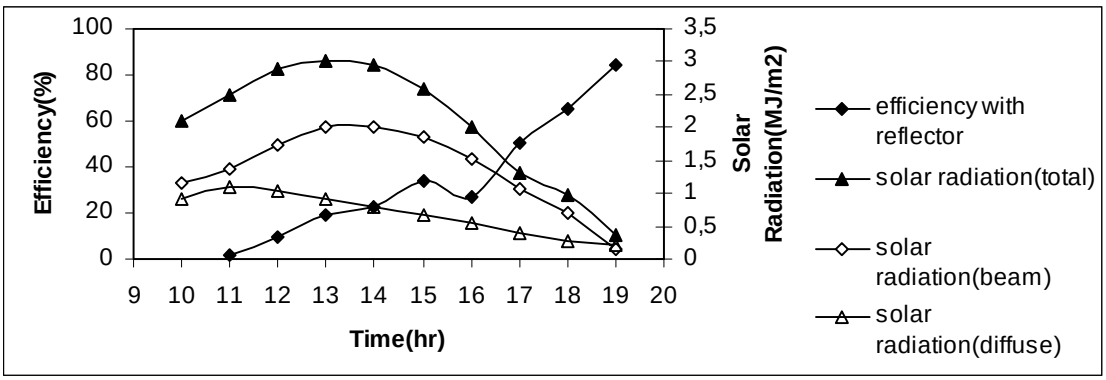

Figure 7.17. Experimental hourly efficiency of still and variation of solar radiation for 29/04/2003

A sample of the distilled water was tested in the laboratory at the Faculty of Fisheries of Ege University. The testing parameters were pH, salinity, amount of Ca, amount of Mg, hardness of Ca, total hardness, SBV(temporary hardness), carbonate, bicarbonate, nitrate(NO3), nitrite(NO2), ammonium(NH4), orthophosphate(PO4) and dissolved organic matter(DOM). pH measure was made with Orion pHmeter. Mohr-Knudsen method was used to find salinity value of distilled water. Nutrient analysis was made with the help of Hach DR 2000 model UV visible spectrophotometer. Permanganate method was used to find organic materials values. Hardness, Ca, Mg, carbonate and bicarbonate indications were measured with titration method.

The value of pH gives an indication of whether the water is acidic or basic. The water is acidic if pH is less than 7.0 and basic if pH is greater than 7.0. Table 7.2 shows the result of the tests. pH, salinity, amount of Ca, amount of Mg, hardness of Ca, total hardness, SBV(temporary hardness) and bicarbonate values analyzed in tests were suitable for water standards. But nitrate, nitrite and ammonium values were higher than the standard values. There are different reasons for this. For example, storage condition of seawater and evaporation of water under low temperature can cause increase in biological activation in water so it can affect compound with nitrogen values in water. In addition to this another important factor is types of construction materials and equipment (such as dye, silicone, adhesive and PVC). The distilled water can not use for drinking but it can use for watering or irrigation. Ion decomposition or reverse osmosis methods may use to obtain drinking water from distilled water.

Table 7.2. Analysis of Distilled Water

	Distilled water	Drinking Water Standards
pH	6.74	6.5-9.2
Salinity(gr/l)	0.15	<0,25
Calcium (mg/l)	32.06	<200
Magnesium(mg/l)	24.32	<150
Hardness of calcium(mg/l)	80	-
French Hardness	4.1	-
Total Hardness(mg/l)	180	<500
SBV(temporary hardness)	0.82	-
Carbonate	----	-
Bicarbonate(mg/l)	50.02	-
Nitrite(microgram/l)	142.18	<50
Nitrate(microgram/l)	90.77	<45
Ammonium(NH4) (microgram/l)	5419.50	<50
Orthophosphate(PO4) (microgram/l)	169.23	-
Dissolved Organic Matter(DOM)(mgKMnO4/l)	6.32	-

Chapter 8

CONCLUSION

In this work, the numerical solution of the basic heat and mass transfer equations was established. The theoretical solutions were compared with experimental results obtained as part of this work and the effect of reflector had been studied.

According to experiments, following points may be concluded:

- The important factor which affects productivity of the solar still is solar radiation. When higher solar insolation is received the productivity of the solar still increase.
- Efficiency of the solar still has a little alteration with increasing of ambient air temperature.
- When the temperature difference between the interface temperature and glass cover temperature increase, amount of distilled water from the still raise.
- The reflector which is used to concentrate solar radiation into the still increased solar radiation value 13.77 to 16.93 MJ/m^2 on 04.04.2003.
- The maximum amount of distillate obtained from the still on 09.05.2003 is 3615 ml/m^2hr.

The deviation between the theoretical and experimental yields for the solar still is due to the following reason. The governing equations used in the calculations do not consider the heat loss due to the leakage of the saturated water from the still. Although rubber band was used for leakage, it could not prevent. As the vapor pressure inside the still is higher than the atmospheric pressure, the saturated air escape to the outside. The coming air from the outside to the still is no more saturated and it takes some time to be heated and saturated. This causes to reduce the productivity of solar still. This is not taken into account in the theoretical solution which predicts higher production rates.

For future work, it is advised to use a thin glass cover to allow more solar energy to pass to saline water in the still. A good quality glass will be suitable for solar desalination application. It has low iron contents, hence low absorptivity of radiation and consequently high transmissivity.

Another suggestion is that solar still can be coupled with a device such as solar collector to increase initial inside seawater temperature. Thus, early in the morning the evaporation can start and the productivity of the solar still increase.

On the other hand, the cost of the solar distillation unit is important. For design of solar still cheaper but long lasting materials should be preferred. Cost of the solar still depends on productivity and the productivity also depends on solar radiation intensity, it changes due to the location of the solar still. In this respect, the choosing of the location is an important factor on cost.

The important variables on solar desalination are solar radiation, ambient air, inclination of glass cover and wind velocity. The important factor to increase efficiency is the prevention of the leakage of the moist air from the still.

REFERENCES

[1] D. Jamieson, Experimental Methods for the Determination of the Properties of Saline Water, *Measurements and Control in Water Desalination*, edited by N. Lior (Elsevier, Netherlands, 1986) p:219-240

[2] Solar Radiation Resource Information - http://rredc.nrel.gov/solar/

[3]Solar Radiation for Energy - http://www.eren.doe.gov/consumerinfo/refbriefs/v138.html

[4] Introduction to Meteorology and Climatology-http://www.geog.ouc.bc.ca/physgeog/contents/chapter7.html

[5] The American Solar Energy Society - http://www.ases.org/

[6] O.K. Buros, The ABC's of Desalting, (Topfield, Massachusetts, USA,2000)

[7] S. Kalogirou "Survey of Solar Desalination Systems and System Selection," *Energy*. **22**, (1997), 69-81

[8] Solar Radiation - http:// nsidc.org/arcticmet/factors/radiation.html

[9] G.Atagündüz, "Solar Desalination, " Ege University

[10] A.N. Minasian, A.A. Al-Karaghouli and S.K. Habeeb, "Utilization of a Cylindrical Parabolic Reflector For Desalination of Saline Water," *Energy Conversion and Management*. **38**,(1997), 701-704 .

[11] M.F.A. Goosen, S. S. Sablani, W.H.Shayya and C. Paton, "Thermodynamic and Economic Considerations in Solar Desalination," *Desalination.* **129**, (2000), 63-89.

[12] M.T. Chabi, "An Overview of Solar Desalination for Domestic and agriculture water needs in Remote Arid Areas ," *Desalination.* **127**, (2000), 119-133.

[13] A.Ghoneyem, "Experimental Study on the Effects of the Cover and Numerical Prediction of a Solar Still Output," M.S. Thesis, METU, Ankara, (1995).

[14] M.ABD Elkader, "An Investigation of the Parameters Involved in Simple Solar Still with Inclined Yute, "*Renewable Energy*. **14**, (1998), 333-338

[15] G.M. Capelletti, "An Experiment with a Plastic Solar Still," *Desalination*. **142**, (2002), 221-227

[16] Ç.Tırıs, "Experimental Studies on Selective Coated Flat Plate Collectors Integrated Solar Stills," Ph.D. Thesis, Ege University, İzmir,(1996).

[17] S. Kumar, G.N. Tiwari and H.N. Singh, "Annual Performance of an Active Solar Distillation System," *Desalination.* **127**, (2000), 79-88.

[18]M. Boukar and A. Harmim, "Effect of Climatic Conditions on Performance of a Simple Basin Solar Still," *Desalination.* **137**, (2001), 15-22.

[19] B. Bouchekima, B. Gros, R. Ouahes and M. Diboun, "The Performance of the Capillary Film Solar Still Installed in South Algeria," *Desalination.* **137**, (2001), 31-38.

[20] P. Valsaraj, "An Experimental Study on Solar Distillation in a Single Basin Still by Surface Heating the Water Mass," *Renewable Energy.* **25**, (2002), 607-612.

[21]A.S. Nafey, M.Abdelkader, A.Abdelmotalip and A.A. Mabrouk, "Parameters Affecting Solar Still Productivity ," *Energy Conversion and Management.* **41**, (2000), 1797-1809.

[22] J.P. Molly, "Windenergie Theorie, Anwendung, Messung," Verlag CF Müller Karlsruhe (1986) p:51

[23] G. Atagündüz, "Güneş Enerjisi Temelleri ve Uygulamaları,"p: 112-119.

[24] VDI-Warmeatlas (Springer-Heilderberg, Berlin, 2002) p. Fa1-Fa4.

[25] G.Atagündüz, "Omega Type Solar Charge Station, " Strojarstvo,**44**,(2002),p:5-16

[26] J.A. Duffie and W.A. Beckman, "Solar Engineering of Thermal Processes," Wiley & Sons(1991) p:73 -77.

[27] A. Kaymakçı, U. Sunlu, Ö. Egemen, "Assessment of Nutrient Pollution Caused by Land Based Activities in İzmir/Türkiye," *Options Mediterranenes Serie A*, **44**, (2001), p:47-53

[28] S.Chapra and R.P. Canale, "Numerical Methods For Engineers," Mc Graw Hill(2002) p: 154

[29] F.Ayaz, "Türkiye'de aktinograf gereci ile ölçülen, yatay yüzey üzerine gelen toplam güneş radyasyonu değerlerinin pironometre ölçüm değerleri ile karşılaştırılması," Yüksek Lisans Tezi, Ege University, İzmir,(1989).

APPENDIX A

Calculation of Transmittance, Reflectance and Absorptance of Glass

The transmittance, reflectance, and absorptance are functions of the incoming radiation, thickness, refractive index, and extinction coefficient of the material. Generally, the refractive index n and the extinction coefficient K of the cover material are functions of the wavelength of the radiation. All properties initially will be assumed to be independent of wavelength for calculations.

For smooth surfaces Fresnel has derived expressions for the reflection of unpolarized radiation on passing from medium 1 with a refractive index n_1 to medium 2 with a refractive index n_2:

$$r_{\perp} = \frac{\sin^2(\theta_2 - \theta_1)}{\sin^2(\theta_2 + \theta_1)}$$

$$r_{\text{II}} = \frac{\tan^2(\theta_2 - \theta_1)}{\tan^2(\theta_2 + \theta_1)}$$

The reflection of unpolarized radiation as the average of two components is;

$$r = \frac{1}{2}(r_{\perp} + r_{\text{II}})$$

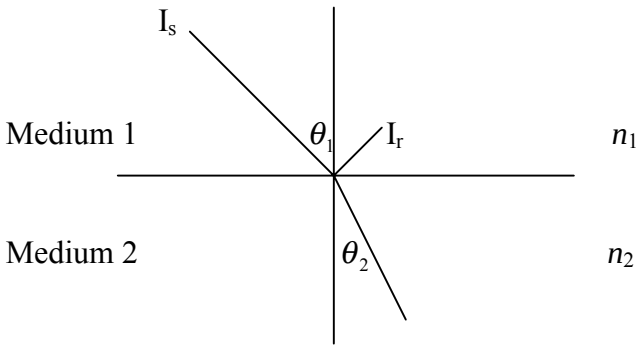

Figure.A.1. Angles of incidence and reflection in media with refractive indices n_1 and n_2

where θ_1 and θ_2 are the angles of incidence and refraction, as shown in Figure A.1 and

$r_\perp$ is the perpendicular component of unpolarized radiation and r_{II} is the parallel component of unpolarized radiation.

The angles θ_1 and θ_2 are related to the indices of refraction by Snell's law,

$$\frac{n_1}{n_2} = \frac{\sin\theta_2}{\sin\theta_1}$$

where n_1 is the refractive index of air, and n_2 is the average refractive index of glass. (n_1=1 and n_2=1.526)

Exactly the same expansion results when the parallel component of polarization is considered. The components $r_\perp$ and r_{II} are not equal (except at normal incidence), and the transmittance of initially unpolarized radiation is the average transmittance of the two components,

$$\tau_r = \frac{1}{2}\left(\frac{1-r_{II}}{1+r_{II}} + \frac{1-r_\perp}{1+r_\perp}\right)$$

According to Bouguer's law, the absorbed radiation is proportional to the local intensity in the medium and the thickness δ_g the radiation has traveled in the medium,

$$\tau_a = e^{-K\delta_g/\cos\theta_2}$$

where the value of K is 32 m^{-1} for poor glass.

The transmittance of a single cover becomes,

$$d_g = \tau_a \tau_r$$

The absorptance of a glass will be,

$$a_g = 1 - \tau_a$$

The reflectance of a single cover is then found from $r = 1 - a - d$, so that

$$r_g = \tau_a(1-\tau_r) = \tau_a - d_g \quad [26]$$

Calculations of d_g, a_g and r_g values for glass are given in Appendix B.

APPENDIX B

COMPUTER PROGRAM 1 AND RESULTS

```
#include<stdio.h>
#include<math.h>
#include<classlib\date.h>
#define max(a,b) (a>b)?a:b
#define min(a,b) (a<b)?a:b
int i, j;
double rad=M_PI/180.0;
double irad=180.0/M_PI;
double beta=38, fi=38.46;
double gama=0, dec, a,b,c,d,e,k,kk,l,m,p,n;
double wbeta1, wbeta2, ws, wr, wbeta_r, wbeta_s;
double Ion, Io=1353.0, Iobeta, Ionbeta, costeta, costeta_2;
double w, ww, wnext, gu_beta, gu_hori, h_reflector=0.50, w_reflector=2.1;
double h, A_sh, A_she, r_reflector=0.9, tetaz, gama_s, I_or;
double sigma_g=0.004, teta1, teta2, r1, r2, r, to_a, to_r, a_g, d_g, r_g;
double q_or, I_ohbeta1, I_ohbeta2;
double I_thz, I_dhz, kth, I_ihz, ro_g, I_thbeta, I_ohz, r_b;
// ------------------------------------------------------------------------------------------
// 31.03.2003
// double
I_thz_values[11]={1317600,2300400,2833200,3157200,3186000,3009600,2800800,1886400,1123200,0,
0};
// ------------------------------------------------------------------------------------------
// 01.04.2003
// double
I_thz_values[11]={856800,918000,1072800,1238400,1062000,658800,698400,925200,633600,0,0};
// ------------------------------------------------------------------------------------------
// 04.04.2003
// double
I_thz_values[11]={644400,932400,1486800,450000,356400,2505600,3157200,2566800,1245600,0,0};
// ------------------------------------------------------------------------------------------
// 10.04.2003
// double
I_thz_values[11]={1315800,1861200,2296800,2888400,2700000,2592000,2264400,1796400,1209600,5
50800,0};
// ------------------------------------------------------------------------------------------
// 22.04.2003
// double
I_thz_values[11]={882600,597600,1018800,1026000,1436400,1620000,957600,201600,133200,0,0};
// ------------------------------------------------------------------------------------------
// 25.04.2003
// double
I_thzvalues[11]={246300,1119600,1432800,1749600,1573200,1749600,806400,1177200,1393200,0,0};
// ------------------------------------------------------------------------------------------
// 28.04.2003
// double
I_thz_values[11]={1519200,2077200,2498400,2732400,2833200,2714400,2394000,1940400,1346400,7
09200,158400};
// ------------------------------------------------------------------------------------------
// 29.04.2003
```

```
// double
I_thz_values[11]={1558800,2156400,2484000,2786400,2934000,2822400,2534400,2077200,1479600,8
31600,129600};
// ------------------------------------------------------------------------------------------
// 30.04.2003
// double
I_thz_values[11]={1551600,2120400,2584800,2876400,2966400,2865600,2541600,2044800,1407600,9
75600,0};
// ------------------------------------------------------------------------------------------
// 02.05.2003
// double
I_thz_values[11]={1585200,2142000,2592000,2869200,2973600,2887200,2541600,2023200,1407600,8
13600,0};
FILE *dat, *sat, *kat;
unsigned gun, ay, yil;
TDate *sta, *sto;
void calculate1(int N)
{ // EXTRATERRESTRIAL SOLAR INTENSITY ON INCLINED SURFACE ////////////////////////////////////
        dec=23.45*sin(360.0*(284.0+(double)N)/365.0*rad);
        a=sin(dec*rad)*sin(fi*rad)*cos(beta*rad);
        b=sin(dec*rad)*cos(fi*rad)*sin(beta*rad)*cos(gama*rad);
        c=cos(dec*rad)*cos(fi*rad)*cos(beta*rad);
        d=cos(dec*rad)*sin(fi*rad)*sin(beta*rad)*cos(gama*rad);
        e=cos(dec*rad)*sin(beta*rad)*sin(gama*rad);
        k=a-b;
        l=c+d;
        n=2*k*l;
        m=l*l+e*e;
        p=k*k-e*e;
        wbeta1=acos((-n-sqrt(fabs(n*n-4*m*p)))/(2*m))*irad;
        wbeta2=acos((-n+sqrt(fabs(n*n-4*m*p)))/(2*m))*irad;
        ws=acos(-tan(fi*rad)*tan(dec*rad))*irad;
                if(gama==0){
                        wbeta_r=max(-wbeta1, -ws);
                        wbeta_s=min(wbeta1,ws);
                }
                else if(gama>-180 && gama<0){
                        wbeta_r=max(-max(wbeta1,wbeta2),-ws);
                        wbeta_s=min(min(wbeta1,wbeta2),ws);
                }
                else if(gama<180 && gama>0){
                        wbeta_r=max(-min(wbeta1,wbeta2),-ws);
                        wbeta_s=min(max(wbeta1,wbeta2),ws);
                }
                else if(gama==180 || gama==-180){
                        wbeta_r=max(-wbeta1, -ws);
                        wbeta_s=min(wbeta1,ws);
                }
         Ion=Io*(1+0.033*cos(360*(double)N/365*rad));

Ionbeta=24.0*3600.0/(2*M_PI)*Io*(1+0.033*cos(360.0*(double)N/365.0))*(sin(dec*rad)*sin(fi*rad)*co
s(beta*rad)*rad*(wbeta_s-wbeta_r)-
sin(dec*rad)*cos(fi*rad)*sin(beta*rad)*cos(gama*rad)*rad*(wbeta_s-
wbeta_r)+cos(dec*rad)*cos(fi*rad)*cos(beta*rad)*(sin(wbeta_s*rad)-
sin(wbeta_r*rad))+cos(dec*rad)*sin(fi*rad)*sin(beta*rad)*cos(gama*rad)*(sin(wbeta_s*rad)-
sin(wbeta_r*rad))-cos(dec*rad)*sin(beta*rad)*sin(gama*rad)*(cos(wbeta_s*rad)-wbeta_r));
```

```
 printf("\nN\tdec\twbeta1\twbeta2\tws\twbeta_r\twbeta_s\tIonbeta(J/m2)\n");
                printf("%d\t%.2f\t%.2f\t%.2f\t%.2f\t%.2f\t%.2f\t%.2f\n
",N,dec,wbeta1,wbeta2,ws,wbeta_r,wbeta_s,Ionbeta);
                fprintf(dat,"\nN\tdec\twbeta1\twbeta2\tws\twbeta_r\twbeta_s\tIonbeta(J/m2)\n");
                fprintf(dat,"%d\t%.3f\t%.3f\t%.3f\t%.3f\t%.3f\t%.3f\t%.3f\t%.3f\n
",N,dec,wbeta1,wbeta2,ws,wbeta_r,wbeta_s,Ionbeta);

printf("w\tcosteta\tIobeta\tIonbeta\ttetaz\tgama_s\tgu_beta\tA_sh\tA_she\tI_or\tq_or\td_g\ta_g\tr_g\n");

fprintf(dat,"w\tcosteta\tIobeta\tIonbeta\ttetaz\tgama_s\tgu_beta\tA_sh\tA_she\tI_or\tq_or\td_g\ta_g\tr_g\n
");
               for(w=-60; w<=75; w+=15){
                I_thz=I_thz_values[i];
                costeta=sin(dec*rad)*sin(fi*rad)*cos(beta*rad)-
sin(dec*rad)*cos(fi*rad)*sin(beta*rad)*cos(gama*rad)+cos(dec*rad)*cos(fi*rad)*cos(beta*rad)*cos(w*r
ad)+cos(dec*rad)*sin(fi*rad)*sin(beta*rad)*cos(gama*rad)*cos(w*rad)+cos(dec*rad)*sin(beta*rad)*sin(
gama*rad)*sin(w*rad);
                Iobeta=Ion*costeta;

I_ohbeta1=12.0*3600.0/M_PI*Io*(1.0+0.033*cos(360.0*(double)N/365.0))*(sin(dec*rad)*sin(fi*rad)*c
os(beta*rad)*rad*(wnext-w)-sin(dec*rad)*cos(fi*rad)*sin(beta*rad)*cos(gama*rad)*rad*(wnext-
w)+cos(dec*rad)*cos(fi*rad)*cos(beta*rad)*(sin(wnext*rad)-
sin(w*rad))+cos(dec*rad)*sin(fi*rad)*sin(beta*rad)*cos(gama*rad)*(sin(wnext*rad)-sin(w*rad))-
cos(dec*rad)*sin(beta*rad)*sin(gama*rad)*(cos(wnext*rad)-cos(w*rad)));

printf("%.2f\t%.2f\t%.2f\t%.2f\t%.2f\t%.2f\t%.2f\t%.2f\t%.2f\t%.2f\t%.2f\t%.2f\t%.2f\t%.2f\n",w,costeta,
Iobeta,Ionbeta,tetaz,gama_s,gu_beta,A_sh,A_she,I_or,q_or,d_g,a_g,r_g);

fprintf(dat,"%.3f\t%.3f\t%.3f\t%.3f\t%.3f\t%.3f\t%.3f\t%.3f\t%.3f\t%.3f\t%.3f\t%.3f\t%.3f\t%.3f\t%.3f\n",w,co
steta,Iobeta,Ionbeta,tetaz,gama_s,gu_beta,A_sh,A_she,I_or,q_or,d_g,a_g,r_g);
                }
}
void calculate2(int N, double W1, double W2)
{               // HOURLY SOLAR INTENSITY ON INCLINED SURFACE ////////////////////
                dec=23.45*sin(360.0*(284.0+(double)N)/365.0*rad);
                Ion=Io*(1+0.033*cos(360*(double)N/365*rad));
                printf("w\tcosteta\tIobeta\tI_ohbeta1\tI_ihz\tIonbeta\ttetaz\tgama_s\tgu_beta\tA_sh\tA_she\tI_
or\tq_or\n");
                fprintf(sat,"w\tcosteta\tIobeta\tI_ohbeta1\tI_ihz\tIonbeta\ttetaz\tgama_s\tgu_beta\tA_sh\tA_sh
e\tI_or\tq_or\td_g\ta_g\tr_g\n");
                fprintf(kat,"w\tI_ohz\tk_th\tI_dhz\tI_ihz\tr_b\tI_thbeta\n");
  for(w=W1,i=0; w<W2; w+=15.0, i++){
                wnext=w+15.0;
                I_thz=I_thz_values[i];
                costeta=sin(dec*rad)*sin(fi*rad)*cos(beta*rad)-
sin(dec*rad)*cos(fi*rad)*sin(beta*rad)*cos(gama*rad)+cos(dec*rad)*cos(fi*rad)*cos(beta*rad)*cos(w*r
ad)+cos(dec*rad)*sin(fi*rad)*sin(beta*rad)*cos(gama*rad)*cos(w*rad)+cos(dec*rad)*sin(beta*rad)*sin(
gama*rad)*sin(w*rad);
                I_ohbeta1=12.0*3600.0/M_PI*Io*(1.0+0.033*cos(360.0*(double)N/365.0))*(sin(dec*rad)*si
n(fi*rad)*cos(beta*rad)*rad*(wnext-w)-
sin(dec*rad)*cos(fi*rad)*sin(beta*rad)*cos(gama*rad)*rad*(wnext-
w)+cos(dec*rad)*cos(fi*rad)*cos(beta*rad)*(sin(wnext*rad)-
sin(w*rad))+cos(dec*rad)*sin(fi*rad)*sin(beta*rad)*cos(gama*rad)*(sin(wnext*rad)-sin(w*rad))-
cos(dec*rad)*sin(beta*rad)*sin(gama*rad)*(cos(wnext*rad)-cos(w*rad)));
                ro_g=0.4;
                I_ohz=12.0*3600.0/M_PI*Io*(1.0+0.033*cos(360.0*(double)N/365.0))*(sin(dec*rad)*sin(fi*
rad)*rad*(wnext-w)+cos(dec*rad)*cos(fi*rad)*(sin(wnext*rad)-sin(w*rad)));
```

```
// calculation of hourly clearness index
		kth=I_thz/I_ohz;
		if(kth<0.35){
		  I_dhz=I_thz*(1.0-0.249*kth);
		} else if(kth>0.35 && kth<0.75){
		  I_dhz=I_thz*(1.557-1.84*kth);
		} else if(kth>0.75){
		  I_dhz=I_thz*0.177;
		}I_ihz=I_thz-I_dhz;
		r_b=(cos((fi-beta)*rad)*cos(dec*rad)*cos((wnext+w)*0.5*rad)+sin((fi-
beta)*rad)*sin(dec*rad))/(cos(fi*rad)*cos(dec*rad)*cos((wnext+w)*0.5*rad)+sin(fi*rad)*sin(dec*rad));
		// total solar radiation on tilted surface for an hour
		I_thbeta=I_ihz*r_b+I_dhz*(1.0+cos(beta*rad))/2.0+I_thz*ro_g*(1.0-cos(beta*rad))/2.0;
		fprintf(kat,"%.3f -
%.3f\t%.3f\t%.3f\t%.3f\t%.3f\t%.3f\t%.3f\n",w,wnext,I_ohz,kth,I_dhz,I_ihz,r_b,I_thbeta);
// CALCULATION OF SHADED AREA BETWEEN ////////////////////////////////
		tetaz=acos(sin(fi*rad)*sin(dec*rad)+cos(fi*rad)*cos(dec*rad)*cos(w*rad))*irad;
		h=90-tetaz;
		gama_s=acos((-
cos(fi*rad)*sin(dec*rad)+sin(fi*rad)*cos(dec*rad)*cos(w*rad))/sin(tetaz*rad))*irad;
		if(h!=0) gu_hori=h_reflector/tan(h*rad); else gu_hori=h_reflector/tan((h+0.00001)*rad);
		gu_beta=gu_hori/cos(beta*rad);
		A_sh=gu_beta*w_reflector;
		if(fabs(gama-gama_s)==0)
			A_she= gu_beta*2.1;
		else if(fabs(gama-gama_s)<66.8){
			kk=0.9/cos(fabs(gama-gama_s)*rad);
			if(gu_beta>kk)
				A_she= (2.1+2.1-tan(fabs(gama-gama_s)*rad)*0.9)*0.9/2.0;
			else
				A_she= (2.1+2.1-sin(fabs(gama-
gama_s)*rad)*gu_beta)*cos(fabs(gama-gama_s)*rad)*gu_beta/2.0;
		}
		else if(fabs(gama-gama_s)>=66.8){
			kk=2.1/cos((90.0-fabs(gama-gama_s))*rad);
			if(gu_beta>kk)
				A_she=2.1*2.1*tan((90.0-fabs(gama-gama_s))*rad)/2.0;
			else
				A_she= (2.1+2.1-sin(fabs(gama-
gama_s)*rad)*gu_beta)*cos(fabs(gama-gama_s)*rad)*gu_beta/2.0;
		}
		I_or=I_ihz*r_reflector*costeta;
		teta1=acos(costeta)*irad;
		teta2=asin(sin(teta1*rad)/1.526)*irad;
		r1=pow(sin((teta2-teta1)*rad),2.0)/pow(sin((teta2+teta1)*rad),2.0);
		r2=pow(tan((teta2-teta1)*rad),2.0)/pow(tan((teta2+teta1)*rad),2.0);
		r=0.5*(r1+r2);
		to_r=0.5*((1-r2)/(1+r2)+(1-r1)/(1+r1));
		to_a=exp(-32.0*sigma_g/cos(teta2*rad));
		d_g=to_r*to_a;
		a_g=1-to_a;
		r_g=to_a-d_g;
		q_or=I_or*d_g*A_she;
```

```
printf("%.2f -
%.2f\t%.2f\t%.2f\t%.2f\t%.2f\t%.2f\t%.2f\t%.2f\t%.2f\t%.2f\t%.2f\t%.2f\t%.2f\n",w,wnext,costeta,Iobeta,
I_ohbeta1,I_ihz,Ionbeta,tetaz,gama_s,gu_beta,A_sh,A_she,I_or,q_or);
                fprintf(sat,"%.3f -
%.3f\t%.3f\t%.3f\t%.3f\t%.3f\t%.3f\t%.3f\t%.3f\t%.3f\t%.3f\t%.3f\t%.3f\t%.3f\t%.3f\t%.3f\t%.3f\n",w,w
next,costeta,Iobeta,I_ohbeta1,I_ihz,Ionbeta,tetaz,gama_s,gu_beta,A_sh,A_she,I_or,q_or,d_g,a_g,r_g);
                }
}
void main()
{
 int i;
 char s[10];
 dat=fopen("result.xls","w");
 sat=fopen("sonuc.xls","w");
 kat=fopen("radiation.xls","w");
  printf("Baslangic gununu giriniz (gun.ay.yil)="); scanf("%u.%u.%u",&gun,&ay,&yil);
  sta=new TDate(gun,ay,yil);
  printf("Bitis gununu giriniz (gun.ay.yil)="); scanf("%u.%u.%u",&gun,&ay,&yil);
  sto=new TDate(gun,ay,yil);
  for(i=sta->Day(); i<=sto->Day(); i++) calculate1(i);
  for(i=sta->Day(); i<=sto->Day(); i++) calculate2(i,-60.0,105.0);
 fcloseall();
}
```

Table B1. Computer program results

04.04.2003

n	declination	w_{beta_r}	w_{beta_s}	I_{onbeta}	
94	5.204	-90.042	90.042	37141431	
Time	**cosθ**	**I_{ohbeta}(J/m2)**	**I_{onbeta}(J/m2)**	**θz**	**$Gama_s$**
8--9	0,499	2951397	37141431	63,492	74,531
9--10	0,705	3845258	37141431	52,567	62,476
10-11	0,863	4477314	37141431	42,966	46,935
11-12	0,963	4804490	37141431	35,937	26,051
12-13	0,997	4804490	37141431	33,256	0
13-14	0,963	4477314	37141431	35,937	26,051
14-15	0,863	3845258	37141431	42,966	46,935
15-16	0,705	2951397	37141431	52,567	62,476
16-17	0,499	1856644	37141431	63,492	74,531

Time	d_g	a_g	r_g	GU_{beta}	Ashe(m)	I_{or}(J/m2)	q_{or}(J/m2)
8--9	0,72	0,144	0,136	1,272	0,505	17961,67	6527,157
9--10	0,78	0,135	0,086	0,829	0,664	41825,95	21637,68
10-11	0,798	0,127	0,075	0,591	0,76	192940,1	117126
11-12	0,805	0,122	0,073	0,46	0,826	10827,66	7199,062
12-13	0,807	0,12	0,073	0,416	0,874	7031,211	4955,465
13-14	0,805	0,122	0,073	0,46	0,826	1439639	957182,8
14-15	0,798	0,127	0,075	0,591	0,76	2018523	1225362
15-16	0,78	0,135	0,086	0,829	0,664	1340172	693306,4
16-17	0,72	0,144	0,136	1,272	0,505	430835,8	156563

Time	I_{ohz}(J/m2)	k_{th}	I_{dhz}(J/m2)	I_{bhz}(J/m2)	r_b	I_{thbeta}(J/m2)
8--9	2583467	0.249	604377,2	40022,8	1,143	613374,1
9--10	3283421	0.284	866470,9	65929,12	1,171	891390,1
10-11	3778363	0.394	1238435	248365,1	1,185	1464575
11-12	4034564	0.112	437502,4	12497,63	1,191	425094
12-13	4034564	0.088	348560,7	7839,314	1,191	336062,8
13-14	3778363	0.663	843922,8	1661677	1,185	2830175
14-15	3283421	0.962	558824,4	2598376	1,171	3677162
15-16	2583467	0.994	454323,6	2112476	1,143	2929049
16-17	1726201	0.722	285597,3	960002,7	1,076	1341147

10.04.2003

n	declination	w_{beta_r}	w_{beta_s}	I_{onbeta}	
100	7,534	-90,061	90,061	36554169	
Time	**cosθ**	**I_{ohbeta}**	**I_{onbeta}**	**θz**	**$Gama_s$**
8--9	0,497	2904803	36554169	61,986	76,531
9--10	0,702	3784075	36554169	50,916	64,568
10--11	0,86	4405815	36554169	41,077	48,971
11--12	0,959	4727650	36554169	33,759	27,499
12--13	0,992	4727650	36554169	30,926	0
13--14	0,959	4405815	36554169	33,759	27,499
14--15	0,86	3784075	36554169	41,077	48,971
15--16	0,702	2904803	36554169	50,916	64,568
16--17	0,497	1827919	36554169	61,986	76,531
17--18	0,258	626811,4	36554169	73,593	86,598

Time	d_g	a_g	r_g	GU_{beta}	Ashe(m)	I_{or}(J/m2)	q_{or}(J/m2)
8--9	0,719	0,144	0,137	1,193	0,422	207017,6	62885,29
9--10	0,779	0,135	0,086	0,781	0,586	546364,3	249490,792
10--11	0,798	0,127	0,075	0,553	0,687	966298,1	529579,487
11--12	0,805	0,122	0,073	0,424	0,753	1849270	1120837,741
12--13	0,806	0,121	0,073	0,38	0,798	1585223	1020451,359
13--14	0,805	0,122	0,073	0,424	0,753	1532530	928862,064
14--15	0,798	0,127	0,075	0,553	0,687	1201592	658532,305
15--16	0,779	0,135	0,086	0,781	0,586	776269,4	354474,262
16--17	0,719	0,144	0,137	1,193	0,422	359949,5	109341,11
17--18	0,519	0,152	0,329	2,155	0,131	75978,01	5165,569

Time	I_{ohz}(J/m2)	k_{th}	I_{dhz}(J/m2)	I_{bhz}(J/m2)	r_b	I_{thbeta}(J/m2)
8--9	2663635	0,494	852723,7	463076,3	1,091	1323340
9--10	3352165	0,555	996466,4	864733,6	1,129	1946230
10--11	3839029	0,598	1047735	1249065	1,148	2467948
11--12	4091048	0,706	744935,9	2143464	1,156	3266116
12--13	4091048	0,66	925131,6	1774868	1,156	2993156
13--14	3839029	0,675	815665,7	1776334	1,148	2878282
14--15	3352165	0,676	711187,2	1553213	1,129	2485728
15--16	2663635	0,674	567794,3	1228606	1,091	1924177
16--17	1820362	0,664	404431,1	805168,9	1,005	1221851
17--18	879813,4	0,626	223119,7	327680,3	0,713	456566,9

22.04.2003

n	declination	w_{beta_r}	w_{beta_s}	I_{onbeta}	
111	11,579	-90,094	90,094	35474172	
Time	**cosθ**	**I_{ohbeta}**	**I_{onbeta}**	**θz**	**$Gama_s$**
8--9	0,491	2819104	36554169	59,443	80,138
9--10	0,694	3671617	36554169	48,143	68,442
10--11	0,85	4274435	36554169	37,892	52,896
11--12	0,948	4586477	36554169	30,025	30,446
12--13	0,981	4586477	36554169	26,881	0
13--14	0,948	4274435	36554169	30,025	30,446
14--15	0,85	3671617	36554169	37,892	52,896
15--16	0,694	2819104	36554169	48,143	68,442
16--17	0,491	1774992	36554169	59,443	80,138
17--18	0,255	610437	36554169	71,132	89,968

Time	d_g	a_g	r_g	GU_{beta}	Ashe(m)	I_{or}(J/m2)	q_{or}(J/m2)
8--9	0,717	0,144	0,139	1,075	0,289	30727,99	6368,509
9--10	0,778	0,135	0,087	0,708	0,461	16062,48	5756,02
10--11	0,797	0,127	0,075	0,494	0,567	50289,6	22731,38
11--12	0,804	0,123	0,073	0,367	0,635	53547,12	27321,26
12--13	0,806	0,121	0,073	0,322	0,675	108648,4	59138,29
13--14	0,804	0,123	0,073	0,367	0,635	278042,3	141865,1
14--15	0,797	0,127	0,075	0,494	0,567	50491,73	22822,74
15--16	0,778	0,135	0,087	0,708	0,461	2265,088	811,699
16--17	0,717	0,144	0,139	1,075	0,289	989,711	205,122
17--18	0,515	0,152	0,332	1,857	0,001	0	0

Time	I_{ohz}(J/m2)	k_{th}	I_{dhz}(J/m2)	I_{bhz}(J/m2)	r_b	I_{thbeta}(J/m2)
8--9	2791826	0,316	813123,4	69476,64	1,01	834554,3
9--10	3459402	0,173	571894,9	25705,11	1,062	563909,2
10--11	3931450	0,259	953060,8	65739,22	1,088	966741,1
11--12	4175799	0,246	963229,7	62770,34	1,099	973603,8
12--13	4175799	0,344	1313370	123029,9	1,099	1370244
13--14	3931450	0,412	1294066	325933,7	1,088	1580105
14--15	3459402	0,277	891596,6	66003,44	1,062	907778,4
15--16	2791826	0,072	197975,1	3624,867	1,01	189200,7
16--17	1974216	0,067	130962,2	2237,758	0,9	124742

25.04.2003

n	declination	w_{beta_r}	w_{beta_s}	I_{onbeta}	
114	12,616	-90,103	90,103	37363146	
Time	**cosθ**	**I_{ohbeta}**	**I_{onbeta}**	**θz**	**$Gama_s$**
8--9	0,49	2969252	37363146	58,807	81,093
9--10	0,692	3866948	37363146	47,454	69,489
10--11	0,847	4501714	37363146	37,097	53,992
11--12	0,944	4830293	37363146	29,079	31,31
12--13	0,978	4830293	37363146	25,844	0
13--14	0,944	4501714	37363146	29,079	31,31
14--15	0,847	3866948	37363146	37,097	53,992
15--16	0,692	2969252	37363146	47,454	69,489
16--17	0,49	1869805	37363146	58,807	81,093
17--18	0,254	643530,5	37363146	70,511	90,847

Time	d_g	a_g	r_g	GU_{beta}	Ashe(m)	I_{or}(J/m2)	q_{or}(J/m2)
8--9	0,716	0,144	0,14	1,048	0,257	2221,011	408,336
9--10	0,777	0,135	0,088	0,691	0,43	52517,4	17563,14
10--11	0,797	0,128	0,075	0,48	0,538	92821,95	39776,4
11--12	0,804	0,123	0,073	0,353	0,605	246379,5	119923,2
12--13	0,806	0,121	0,073	0,307	0,645	128485,9	66810,35
13--14	0,804	0,123	0,073	0,353	0,605	312256,2	151988,1
14--15	0,797	0,128	0,075	0,48	0,538	33352,01	14292,13
15--16	0,777	0,135	0,088	0,691	0,43	121432	40609,9
16--17	0,716	0,144	0,14	1,048	0,257	394775,3	72580,06
17--18	0,514	0,153	0,333	1,793	0	0	0

Time	I_{ohz}(J/m2)	k_{th}	I_{dhz}(J/m2)	I_{bhz}(J/m2)	r_b	I_{thbeta}(J/m2)
8--9	2997225	0,082	241260,3	5039,748	0,991	231126,5
9--10	3700181	0,303	1035247	84353,31	1,046	1061185
10--11	4197246	0,341	1311012	121788,4	1,073	1363482
11--12	4454546	0,393	1459706	289894,3	1,085	1693646
12--13	4454546	0,353	1427163	146036,7	1,085	1501015
13--14	4197246	0,417	1382194	367406	1,073	1704105
14--15	3700181	0,218	762640	43760,01	1,046	761749,8
15--16	2997225	0,393	982156,3	195043,7	0,991	1121310
16--17	2136283	0,652	497406,2	895793,8	0,876	1288507

28.04.2003

n	declination	w_{beta_r}	w_{beta_s}	I_{onbeta}	
118	13,946	-90,114	90,114	35042337	
Time	**cosθ**	**I_{ohbeta}**	**I_{onbeta}**	**θz**	**$Gama_s$**
8--9	0,487	2784858	35042337	58,002	82,337
9--10	0,688	3626533	35042337	46,585	70,865
10--11	0,842	4221688	35042337	36,094	55,458
11--12	0,939	4529762	35042337	27,875	32,496
12--13	0,972	4529762	35042337	24,514	0
13--14	0,939	4221688	35042337	27,875	32,496
14--15	0,842	3626533	35042337	36,094	55,458
15--16	0,688	2784858	35042337	46,585	70,865
16--17	0,487	1754021	35042337	58,002	82,337
17--18	0,253	604271,2	35042337	69,721	91,985

Time	dg	ag	rg	gubeta	Ashe	Ior	qor(J/m2)
8--9	0,715	0,145	0,141	1,016	0,216	275527,4	42594,33
9--10	0,777	0,135	0,088	0,671	0,392	672835,4	204825,4
10--11	0,797	0,128	0,075	0,463	0,501	1119131	446539,7
11--12	0,804	0,123	0,073	0,336	0,569	1448404	662205,4
12--13	0,805	0,121	0,073	0,289	0,608	1663010	813868,9
13--14	0,804	0,123	0,073	0,336	0,569	1583548	723992,9
14--15	0,797	0,128	0,075	0,463	0,501	1248199	498038,9
15--16	0,777	0,135	0,088	0,671	0,392	820524,4	249785,1
16--17	0,715	0,145	0,141	1,016	0,216	376789,6	58248,67

Time	I_{ohz}(J/m2)	k_{th}	I_{dhz}(J/m2)	I_{bhz}(J/m2)	r_b	I_{thbeta}(J/m2)
8--9	2879895	0,528	890805,3	628394,7	0,968	1468873
9--10	3538984	0,587	990856,5	1086343	1,025	2087744
10--11	4005030	0,624	1022294	1476106	1,055	2576595
11--12	4246273	0,643	1019167	1713233	1,067	2855458
12--13	4246273	0,667	933014	1900186	1,067	2982238
13--14	4005030	0,678	841312,6	1873087	1,055	2842619
14--15	3538984	0,676	747655,3	1646345	1,025	2457930
15--16	2879895	0,674	615601,5	1324799	0,968	1914585
16--17	2072680	0,65	487056,6	859343,4	0,847	1220439

29.04.2003

n	declination	w_{beta_r}	w_{beta_s}	I_{onbeta}	
119	14,269	-90,117	90,117	35668463	
Time	**cosθ**	I_{ohbeta}	I_{onbeta}	**θz**	$Gama_s$
8--9	0,487	2834627	35668463	57,809	82,641
9--10	0,687	3691277	35668463	46,377	71,204
10--11	0,841	4297020	35668463	35,854	55,824
11--12	0,938	4610575	35668463	27,585	32,798
12--13	0,971	4610575	35668463	24,191	0
13--14	0,938	4297020	35668463	27,585	32,798
14--15	0,841	3691277	35668463	35,854	55,824
15--16	0,687	2834627	35668463	46,377	71,204
16--17	0,487	1785450	35668463	57,809	82,641
17--18	0,253	615245,4	35668463	69,53	92,263

Time	dg	ag	rg	gubeta	Ashe	Ior	qor(J/m2)
8--9	0,715	0,145	0,141	1,008	0,207	283800,1	41895,42
9--10	0,776	0,135	0,088	0,666	0,383	719301,5	213818,1
10--11	0,797	0,128	0,076	0,459	0,492	1052287	412440,9
11--12	0,804	0,123	0,073	0,332	0,56	1469271	661358
12--13	0,805	0,122	0,073	0,285	0,599	1762058	849449,5
13--14	0,804	0,123	0,073	0,332	0,56	1695686	763273,6
14--15	0,797	0,128	0,076	0,459	0,492	1403594	550134,2
15--16	0,776	0,135	0,088	0,666	0,383	949838,9	282347,2
16--17	0,715	0,145	0,141	1,008	0,207	468446,8	69153,53

Time	I_{ohz}(J/m2)	k_{th}	I_{dhz}(J/m2)	I_{bhz}(J/m2)	r_b	I_{thbeta}(J/m2)
8--9	2948451	0,529	910683,5	648116,5	0,962	1503780
9--10	3619266	0,596	993468,6	1162931	1,02	2166343
10--11	4093604	0,607	1094171	1389829	1,05	2543142
11--12	4339139	0,642	1046111	1740289	1,063	2903404
12--13	4339139	0,676	917888,1	2016112	1,063	3088248
13--14	4093604	0,689	813931,6	2008468	1,05	2956664
14--15	3619266	0,7	680576,3	1853824	1,02	2607684
15--16	2948451	0,705	541546,9	1535653	0,962	2049623
16--17	2126875	0,696	409804,4	1069796	0,84	1328036

02.05.2003

n	declination	w_{beta_r}	w_{beta_s}	I_{onbeta}	
122	15,21	-90,125	90,125	36721994	
Time	**costeta**	**Iohbeta**	**Ionbeta**	**tetaz**	**gama_s**
8--9	0,485	2918384	36721994	57,249	83,538
9--10	0,684	3800141	36721994	45,775	72,21
10--11	0,838	4423637	36721994	35,159	56,917
11--12	0,934	4746383	36721994	26,741	33,714
12--13	0,967	4746383	36721994	23,25	0
13--14	0,934	4423637	36721994	26,741	33,714
14--15	0,838	3800141	36721994	35,159	56,917
15--16	0,684	2918384	36721994	45,775	72,21
16--17	0,485	1838456	36721994	57,249	83,538
17--18	0,252	633953,5	36721994	68,977	93,077

Time	dg	ag	rg	gubeta	Ashe	Ior	qor(J/m2)
8--9	0,714	0,145	0,142	0,986	0,179	268090	34192,75
9--10	0,776	0,136	0,089	0,652	0,356	641638,8	177461,6
10--11	0,796	0,128	0,076	0,447	0,467	1096368	407343,7
11--12	0,803	0,123	0,073	0,32	0,535	1474711	633649,4
12--13	0,805	0,122	0,073	0,273	0,572	1692186	779962,4
13--14	0,803	0,123	0,073	0,32	0,535	1670827	717915,7
14--15	0,796	0,128	0,076	0,447	0,467	1304903	484822,7
15--16	0,776	0,136	0,089	0,652	0,356	808611,1	223642
16--17	0,714	0,145	0,142	0,986	0,179	367366,4	46854,67

Time	I_{ohz}(J/m2)	k_{th}	I_{dhz}(J/m2)	I_{bhz}(J/m2)	r_b	I_{thbeta}(J/m2)
8--9	3087224,314	0,513	970480,8	614719,2	0,946	1516354
9--10	3777699,887	0,567	1100342	1041658	1,007	2123007
10--11	4265939,847	0,608	1137913	1454087	1,038	2635843
11--12	4518671,448	0,635	1115154	1754046	1,051	2961971
12--13	4518671,448	0,658	1029318	1944282	1,051	3089583
13--14	4265939,847	0,677	899890,8	1987309	1,038	2988795
14--15	3777699,887	0,673	810937,6	1730662	1,007	2574736
15--16	3087224,314	0,655	710473,8	1312726	0,946	1962797
16--17	2241567,896	0,628	565244,2	842355,8	0,821	1256583

APPENDIX C

COMPUTER PROGRAM 2

```
#include<math.h>
#include<stdio.h>
#include<stdlib.h>
#include<malloc.h>
#define MAX_ITER 100000000   // maximum iteration number
#define N 4

typedef double * vector;
typedef double ** matrix;
double learning_rate=0.00000005;
double error_tolerance=1e-25;
double x,y,yd;
double EE;
double l=0.2;
double vis=1.77625e-5;
double g=9.81;
double pr=0.7;
double fpr=0.401;
double k_air=0.02752;
double ro=1.09525;
double cp=1007.5;
double A=2892.3693;
double B=19.3011421;
double C=-2.892736;
double D=-4.9369728e-3;
double E=5.606905e-6;
double F=-4.645869e-9;
double G=3.7874e-12;
double P=101325.0; // N/m2
double R=287.0; // Nm/kgC
double Ag=1.4, Ab=1.0, Ak_air=2.8616, Ak_l=0.54;
double beta, gr, ra, hm, hm_h, m_vapor, nu, hr, p_i, p_r;
double Is=339.0, Rg=0.075, Cs=5.667, Tsky, Ta=20.0, V=2.0, Lgal=40.0;
double Lc=37.0, Liz=0.028, Dgal=0.002, Diz=0.05, Dc=0.002, hg=2418.0e3, hair_r=2400.75e3,
hi=2388.75e3;
double Ew=0.9, Dw=0.0, Dg=0.045, Kw=0.6, tw=0.01, Rw=0.04, Eg=0.88;
double dg=0.824, rg=0.049, ag=0.127, dw=0.999, rw=0.001, rb=0.05;

void calculate_hr(vector par)
{       // calculation of hr ////////////////////////////////////////////////////////
            beta=1.0/(par[4]+273.0);
            gr=g*pow(l,3.0)*beta*(fabs(par[3]-par[4]))/pow(vis,2.0);
            ra=gr*pr;
            if((ra*fpr)>=7e4) nu=0.15*pow(ra*fpr,1.0/3.0);
            else nu=0.766*pow(ra*fpr,1.0/5.0);
            hr=nu*k_air/l;
            hm=hr/(ro*cp);
            p_i=133.322*pow(10.0, -
A/(par[3]+273.0)+B+C*log10(par[3]+273.0)+D*(par[3]+273.0)+E*pow(par[3]+273.0,2.0)+F*pow(par[3
]+273.0,3.0)+G*pow(par[3]+273.0,4.0));
            p_r=133.322*pow(10.0, -
A/(par[4]+273.0)+B+C*log10(par[4]+273.0)+D*(par[4]+273.0)+E*pow(par[4]+273.0,2.0)+F*pow(par[4
]+273.0,3.0)+G*pow(par[4]+273.0,4.0));
            hm_h=hm*P/(p_i-p_r)*log((P-p_r)/(P-p_i));
            m_vapor=hm_h*(p_i-p_r)/(R*(par[4]+273.0));
```

```
}
vector define_vector(nh)
unsigned int nh;
{
        double *v;
        v=(double *)malloc((nh+2)*sizeof(double));
        if (!v) printf("allocation failure in vector()");
        else *v=nh;
        return v;
}
void free_vector(v,nh)
double *v;
long nh;
{
        free((char*) (v));
}
double system1(vector x)
{ double Tb, Tg, Ti, Tr;
 Tb=x[1]; Tg=x[2]; Ti=x[3]; Tr=x[4];
 return Is-Is*rg*Ag/Ab-Eg*Cs*(pow((Tg+273.0)/100.0,4.0)-pow((Tsky+273.0)/100.0,4.0))*Ag/Ab-
(5.7+3.8*V)*(Tg-Ta)*Ag/Ab-1.0/(1.0/hr+Dgal/Lgal+Diz/Liz+Dc/Lc+1.0/(5.7+3.8*V))*(Tr-
Ta)*Ak_air/Ab-1.0/(Dgal/Lgal+Diz/Liz+Dc/Lc+1.0/(5.7+3.8*V))*((Ti+Tb)/2.0-Ta)*Ak_l/Ab-
1.0/(Dgal/Lgal+Diz/Liz+Dc/Lc+1.0/(5.7+3.8*V))*(Tb-Ta)-m_vapor*hg/Ab;
}
double system2(vector x){
 double Tb, Tg, Ti, Tr;
 Tb=x[1]; Tg=x[2]; Ti=x[3]; Tr=x[4];
 return Is*Ag/Ab+(pow((Ti+273.0)/100.0,4.0)-
pow((Tg+273.0)/100.0,4.0)+Dg*pow((Ti+273.0)/100.0,4.0)*(1.0-
Eg)/Eg)*0.7778/(1.0/(Eg*Cs)+1.0/(Ew*Cs)-1.0/Cs+(1.0-Ew-Eg)*Dg/(Ew*Cs*Eg))*Ag/Ab+hr*(Tr-
Tg)*Ag/Ab+m_vapor*hair_r-Is*rg*Ag/Ab-Is*dg*Ag/Ab-Eg*Cs*(pow((Tg+273.0)/100.0,4.0)-
pow((Tsky+273.0)/100.0,4.0))*Ag/Ab-(5.7+3.8*V)*(Tg-Ta)*Ag/Ab-m_vapor*hg;
}

double system3(vector x)
{
 double Tb, Tg, Ti, Tr;
 Tb=x[1]; Tg=x[2]; Ti=x[3]; Tr=x[4];
 return Is*dg-Is*dg*rw+Kw/tw*(Tb-Ti)-(pow((Ti+273.0)/100.0,4.0)-
pow((Tg+273.0)/100.0,4.0)+Dg*pow((Ti+273.0)/100.0,4.0)*(1.0-
Eg)/Eg)*0.7778/(1.0/(Eg*Cs)+1.0/(Ew*Cs)-1.0/Cs+(1.0-Ew-Eg)*Dg/(Ew*Cs*Eg))-hr*(Ti-Tr)-
m_vapor*hi-Is*dg*dw;
}
double system4(vector x)
{
 double Tb, Tg, Ti, Tr;
 Tb=x[1]; Tg=x[2]; Ti=x[3]; Tr=x[4];
 return Is*dg*dw-Is*dg*dw*rw*rb-1.0/(Dgal/Lgal+Diz/Liz+Dc/Lc+1.0/(5.7+3.8*V))*(Tb-Ta)-
Kw/tw*(Tb-Ti);
}
double energy(vector p)
{
 return pow(system1(p),2.0)+pow(system2(p),2.0)+pow(system3(p),2.0)+pow(system4(p),2.0);
}
void gradient(double (*energy)(vector v), vector x,  vector gr)
{
 int i, j, n=x[0];
 double h=1e-6;
 vector d;
```

```
 d=define_vector(n);

 for(i=1; i<=n; i++){

                        for(j=0;j<=n;j++) d[j]=x[j];

                        d[i]+=h;
                        gr[i]=(double) ((double)energy(d)-(double)energy(x))/(double)h;
 }
 free_vector(d);
}

main()
{
 unsigned long k;
 unsigned kj;
 double e=0, olde;
 double tot=0;
 double most;
 char ch;
 FILE *dat;
 vector par, grad;

 grad=define_vector(N);
 par=define_vector(N);
 // Initial values //
 par[1]=65.0;       // Tb
 par[4]=76.0;       // Tr
 par[3]=67.0;       // Ti
 par[2]=58.0;       // Tg
 ////////////////////
 for(k=0; k<MAX_ITER; k++){

             calculate_hr(par);
             gradient(energy, par, grad);
             for(kj=1; kj<=par[0]; kj++)
                         par[kj]-=learning_rate*grad[kj];

             olde=e; e=energy(par);
             if(fabs(e-olde)<error_tolerance) break;

             printf("%u. E=%.5f - Tb=%.5f Tr=%.5f Ti=%.5f Tc=%.5f   \r",k,e,par[1],par[4],par[3],par[2]);
 }
}
```

APPENDIX D

Constants Used in Theoretical Calculations

For visible light:

d_g(Transmissivity of glass cover) : 0.824

r_g(reflectivity of glass cover): 0.049

a_g(absorbtivity of glass cover): 0.127

d_w(Transmissivity of water): 0.999

r_w(reflectivity of water): 0.001

For infrared radiation:

ε_g(Emmissivity of glass): 0.88

d_g(Transmissivity of glass cover) : 0.045

ε_w(Emmissivity of water): 0.9

d_w(Transmissivity of water): 0

C_s :5.667 W/m^2K^4

$r_{reflector}$(reflectivity of aluminium):0.90

APPENDIX E

EXPERIMENTAL RESULTS

Table E.1. Experimental Results for 31.03.2003

31.03.2003	**Without reflector**		**Total Production:1430 ml**			
Time(hr)	**Twater(C)**	**Tmoistair(C)**	**Tinterface(C)**	**Tglass**	**Tambient**	**Distillate(ml)**
10	33,8	24,3	28,3	32,5	18	x
11	48,7	39,8	46,5	38,3	19	60
12	59,5	53,8	58,4	40,1	20	90
13	73,6	68,9	67,8	44,8	20	210
14	71,9	71,4	70,1	46,6	21	240
15	76,1	71,1	75,5	43,3	21	260
16	73,8	71,8	73,6	41,3	21	360
17	65,9	63,3	64,3	33,8	19	210

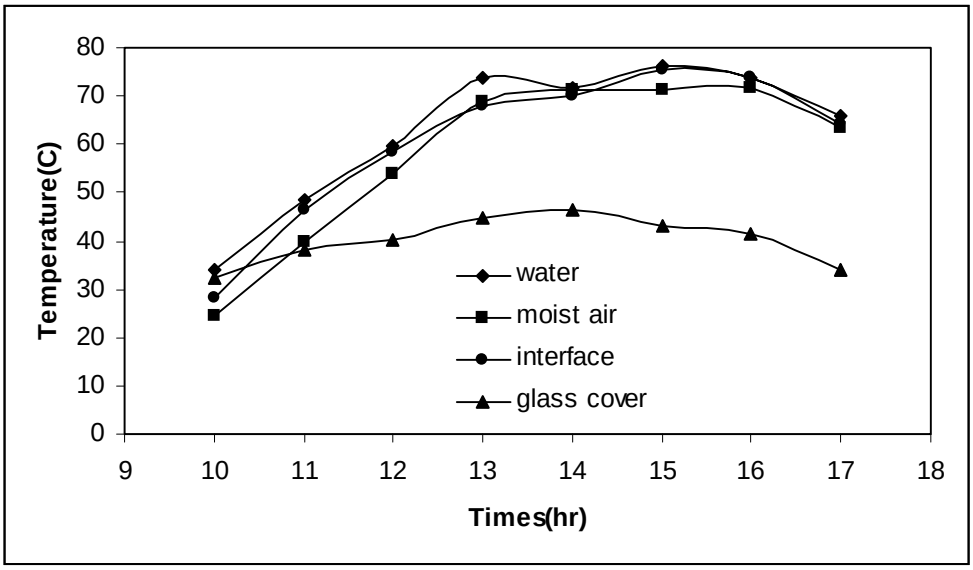

Figure E.1. Hourly variation of temperature values for 31.03.2003

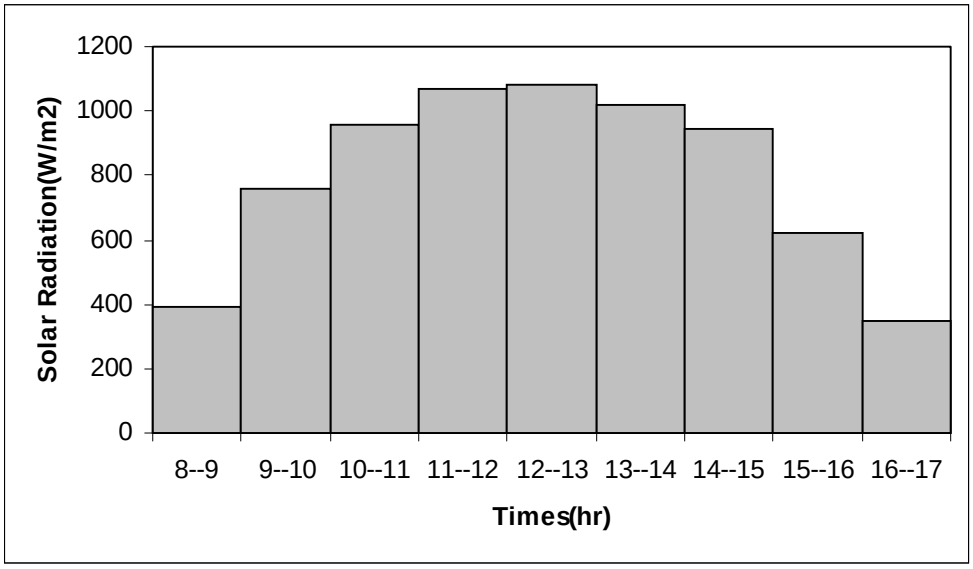

Figure E.2. Hourly variation of solar radiation for 31.03.2003

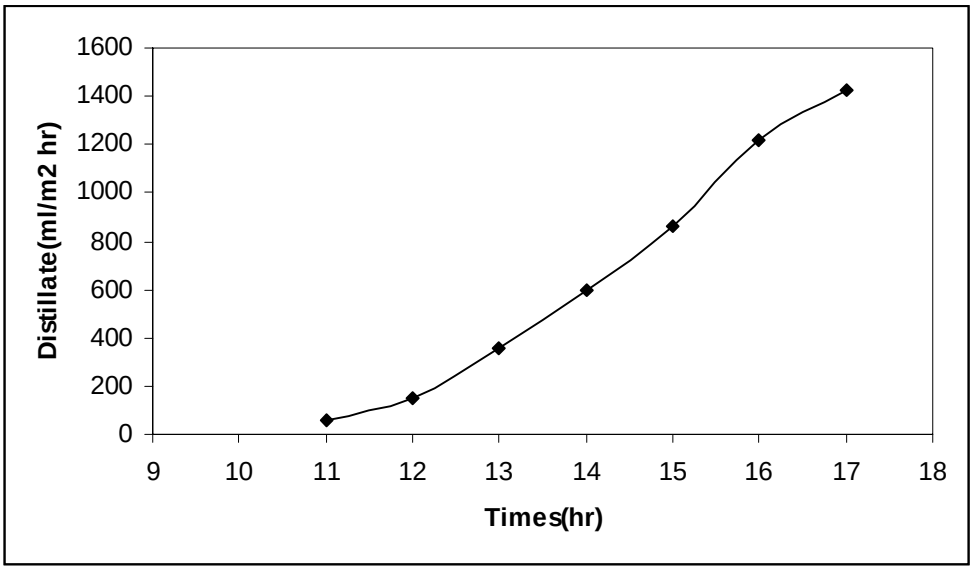

Figure E.3. Hourly variation of cumulative distillate output for 31.03.2003

Table E.2. Experimental Results for 01.04.2003

01.04.2003 **Without reflector**			**Total Production:629 ml**			
Time(hr)	**Twater(C)**	**Tmoistair(C)**	**Tinterface(C)**	**Tglass**	**Tambient**	**Distillate(ml)**
10	31,3	25,3	27,9	22,1	17	100
11	35,9	30,5	32,7	24,4	17	260
12	51,5	43,2	45,8	24,6	18	50
13	46,2	41,1	44,2	27,7	18	49
14	44,1	38	41	25,9	17	75
15	36,2	33,9	35,1	25	17	55
16	36,1	34,8	35,4	26,5	18	40

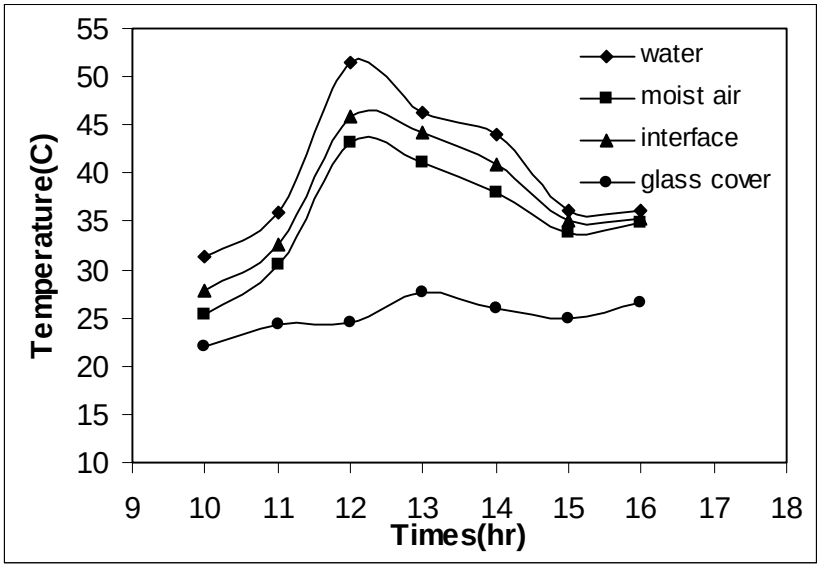

Figure E.4. Hourly variation of temperature values for 01.04.2003

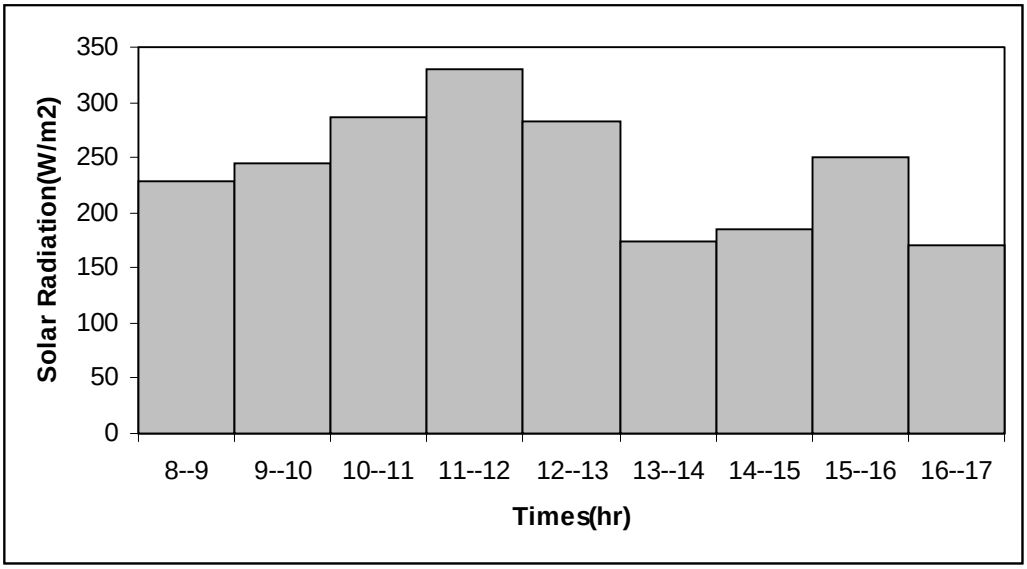

Figure E.5. Hourly variation of solar radiation for 01.04.2003

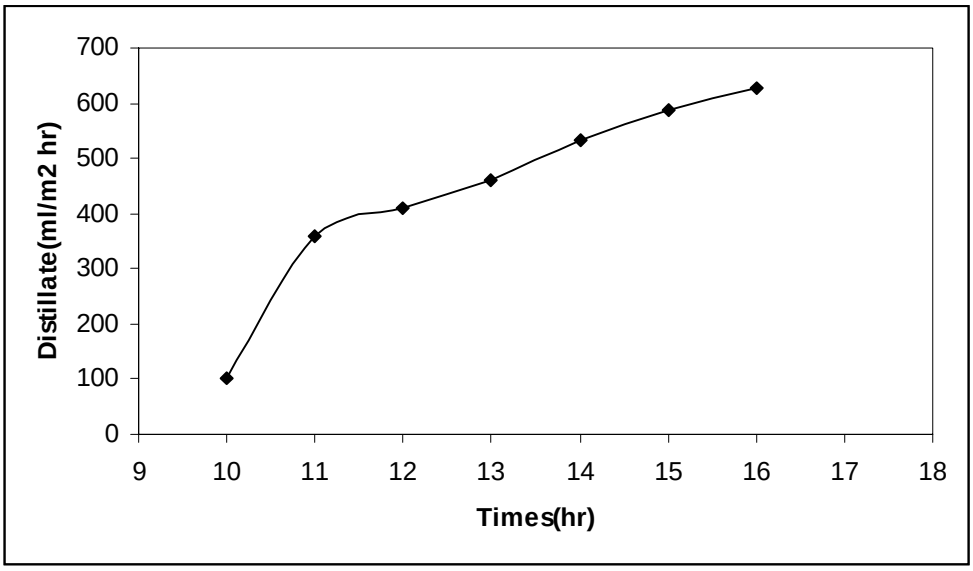

Figure E.6. Hourly variation of cumulative distillate output for 01.04.2003

Table E.3. Experimental Results for 04.04.2003

04.04.2003 (with reflector)			**Total Production:1410 ml**			
Time(hr)	**Twater(C)**	**Tmoistair(C)**	**Tinterface(C)**	**Tglass**	**Tambient**	**Distillate(ml)**
10	35,7	24	34,5	31,1	16	x
11	40,5	38,1	38,7	33,7	19	x
12	56,8	50,1	53,1	35,8	20	40
13	78,9	65,4	75,3	38,4	23	210
14	79,1	75,1	78,8	45,3	21	370
15	65,7	60	64,5	39,7	20	410
16	67,9	62,6	66,8	41,3	23	220
17	60,2	58,2	59,8	36,1	21	160

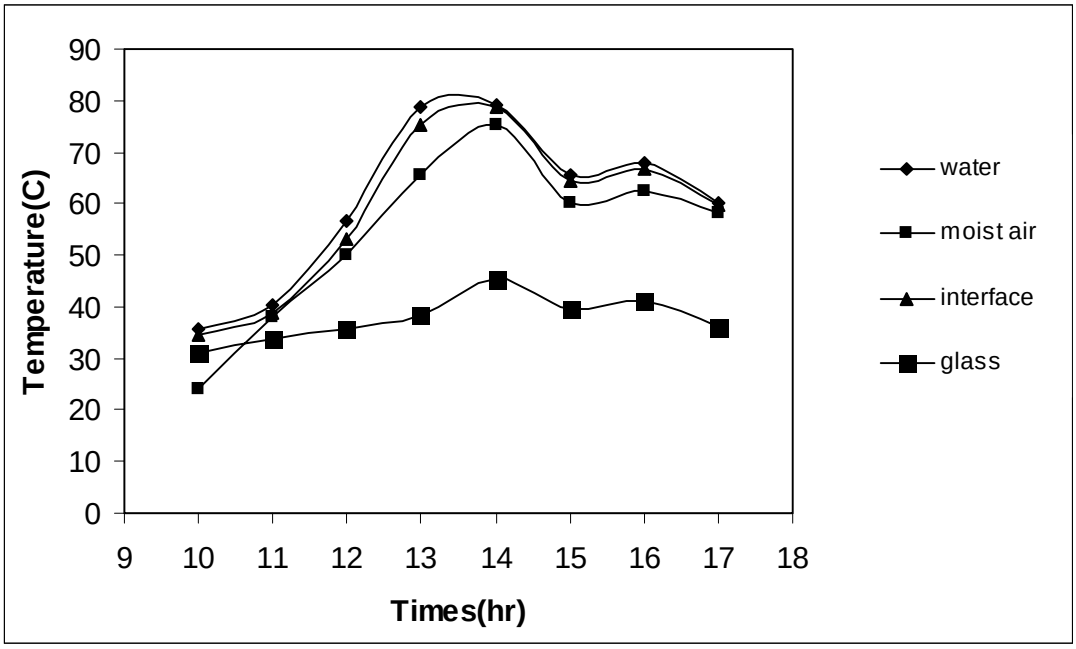

Figure E.7. Hourly variation of temperature values for 04.04.2003

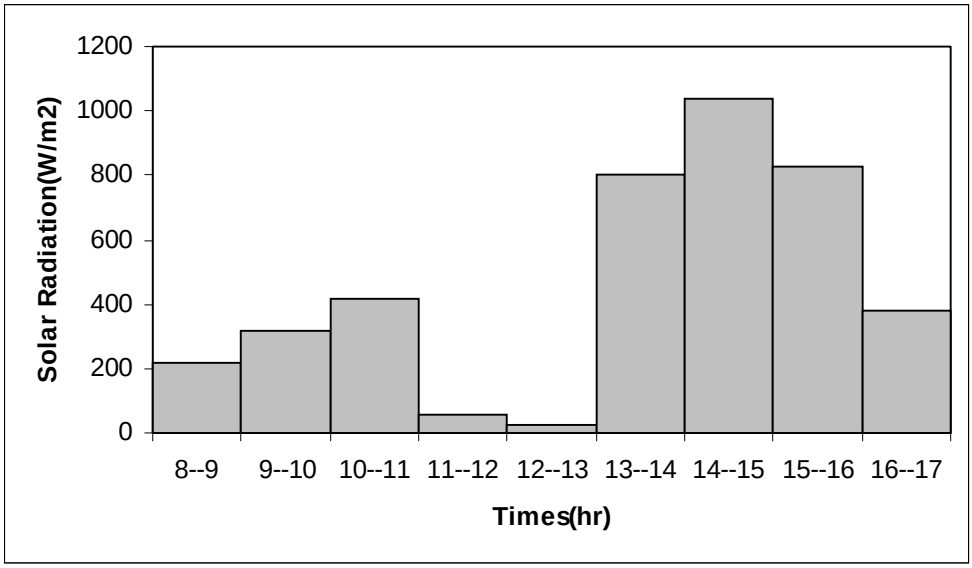

Figure E.8. Hourly variation of solar radiation for 04.04.2003

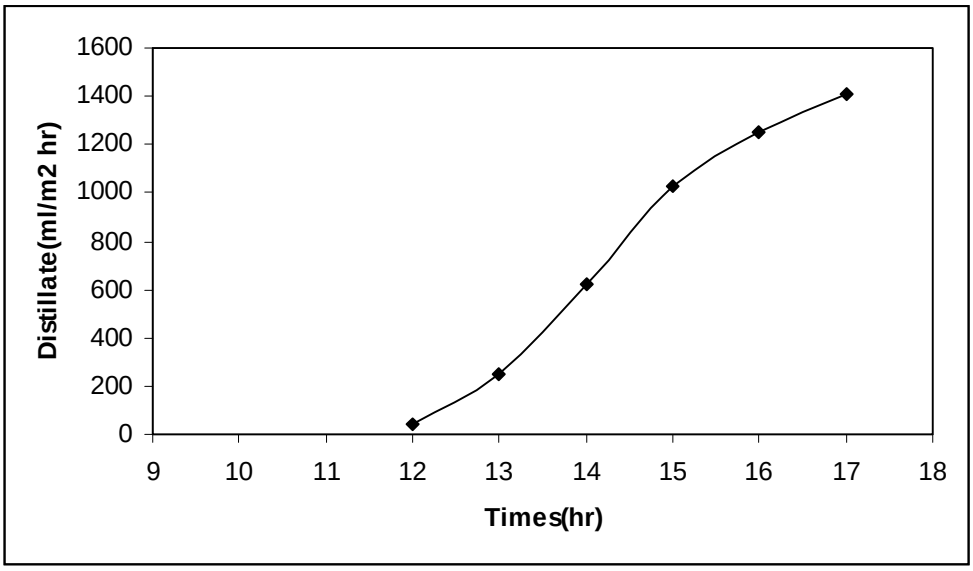

Figure E.9. Hourly variation of cumulative distillate output for 04.04.2003

Table E.4. Experimental Results for 10.04.2003

10.04.2003 (with reflector) **Total Production:1900 ml**

Time(hr)	Twater(C)	Tmoistair(C)	Tinterface(C)	Tglass	Tambient	Distillate(ml)
10	35,4	22,7	33,1	24,3	14	x
11	43,7	40,9	41,3	36,1	14	x
12	63,8	58,8	60,4	42,6	17	100
13	83,1	79,8	81,7	45,5	20	290
14	86,9	81,4	85,3	51,7	20	400
15	88,3	84,2	83,9	55,9	22	420
16	81,7	78,2	79,8	55	22	400
17	75,8	71,7	72,9	42,7	21	290

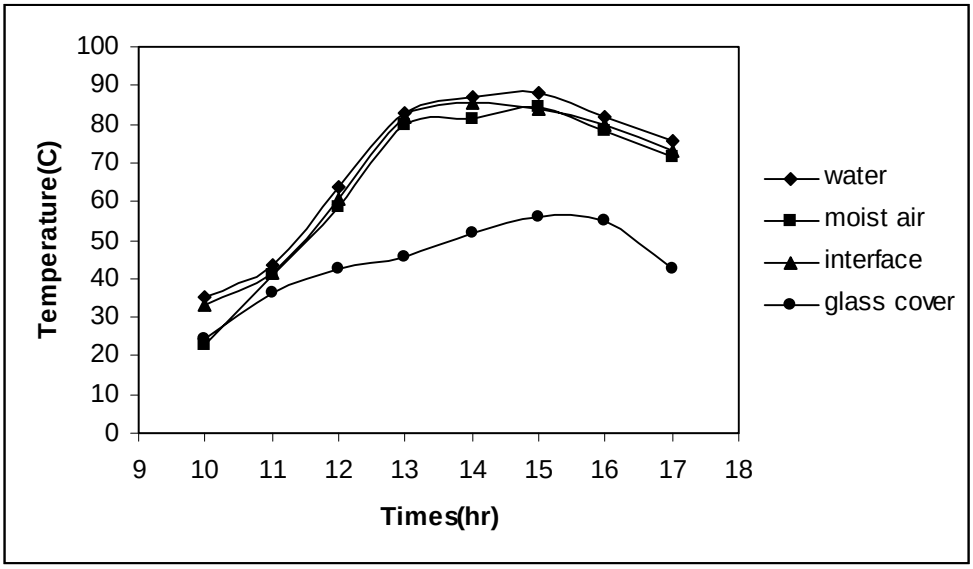

Figure E.10. Hourly variation of temperature values for 10.04.2003

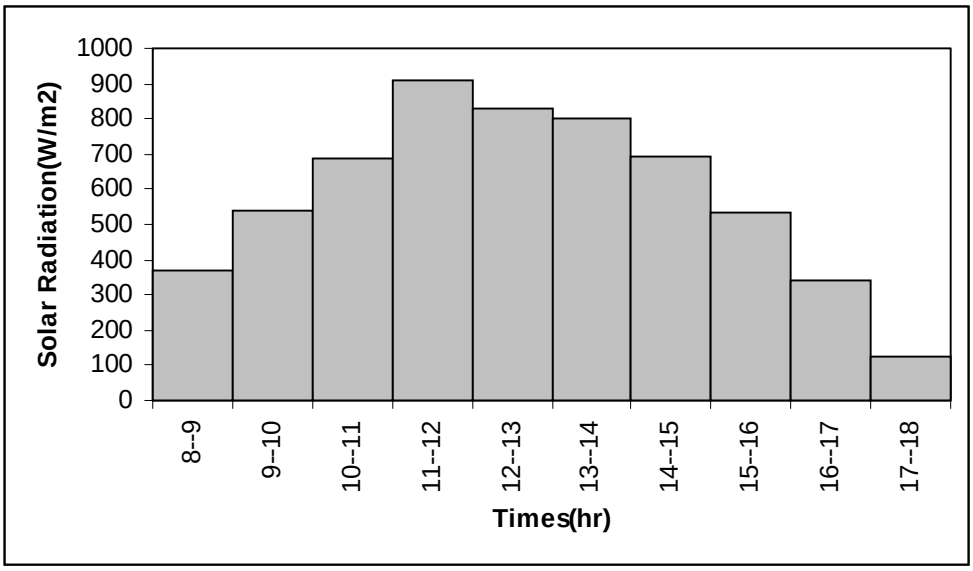

Figure E.11. Hourly variation of solar radiation for 10.04.2003

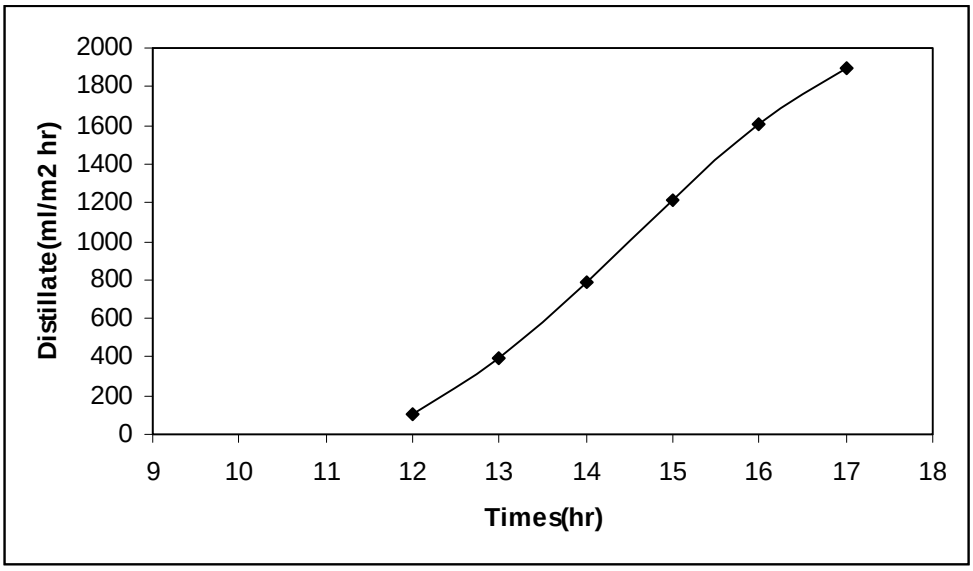

Figure E.12. Hourly variation of cumulative distillate output for 10.04.2003

Table E.5. Experimental Results for 22.04.2003

22.04.2003	**(with reflector)**		**Total Production:440 ml**			
Time(hr)	**Tbottom**	**Tmoistair**	**Tinterface**	**Tglass**	**Tambient**	**Distillate(ml)**
10	32,3	23,1	27,4	24,8	15	x
11	35,3	27,2	29,7	25,5	16	x
12	40,1	32,9	34,8	28,8	16	x
13	46,7	36,4	39,7	31,3	17	40
14	53,2	44,1	47,1	36,5	17	80
15	54,8	49,9	52,7	40,8	18	160
16	45,1	42,1	44,1	31,3	16	160

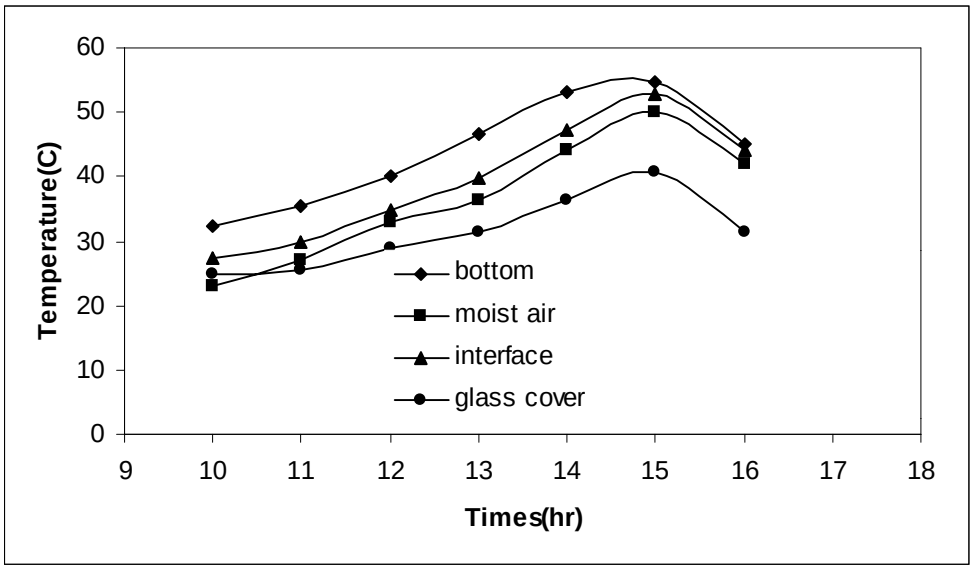

Figure E.13. Hourly variation of temperature values for 10.04.2003

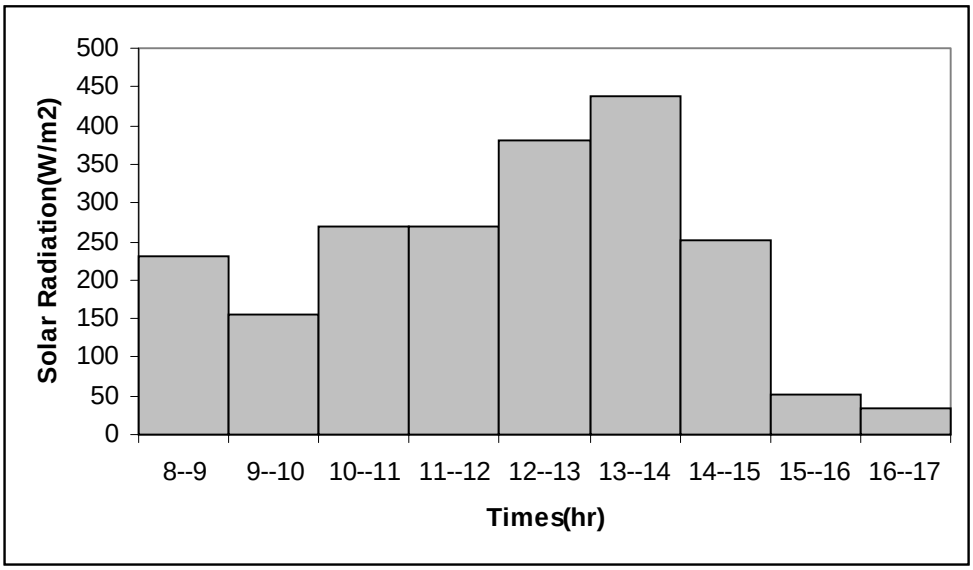

Figure E.14. Hourly variation of solar radiation for 10.04.2003

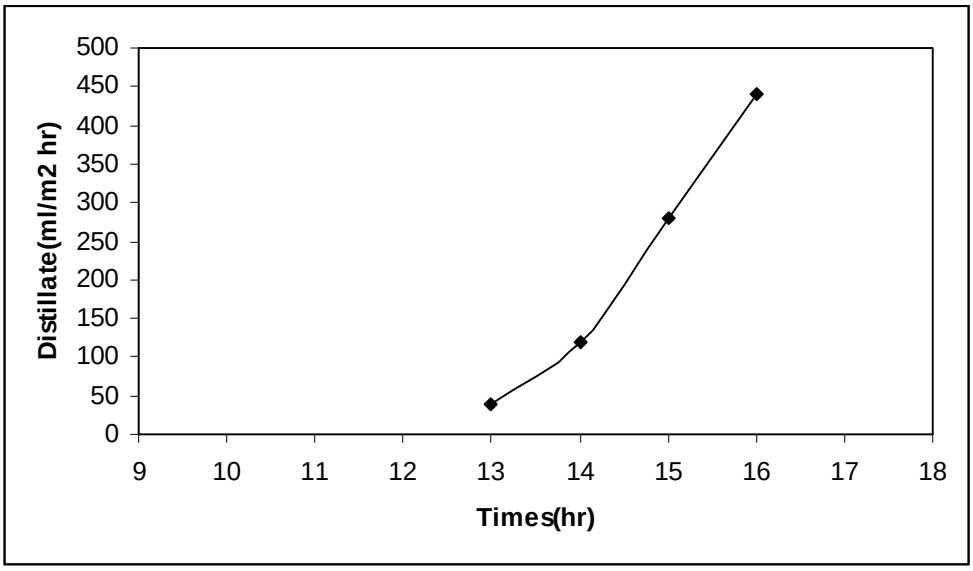

Figure E.15. Hourly variation of cumulative distillate output for 10.04.2003

Table E.6. Experimental Results for 25.04.2003

25.04.2003 (with reflector) **Total Production:895 ml**

Time(hr)	Tbottom	Tmoistair	Tinterface	Tglass	Tambient	RH(%)	Distillate(ml)
10	33,2	22,3	32,1	23,1	16	55	x
11	39,5	31	35,3	27,9	16	56	x
12	x	x	x	x	x	x	60
13	50,3	48	48,7	38,3	16	49	210
14	59,6	50,1	57,3	39,9	17	45	195
15	67,3	51,3	65,8	40,2	16	48	220
16	39,6	41,8	40,1	32,1	16	47	210

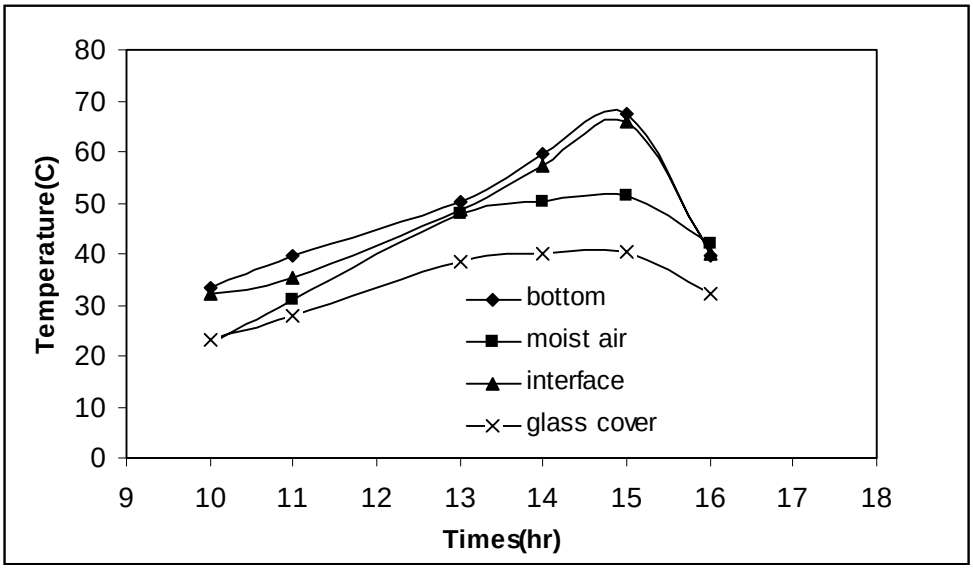

Figure E.16. Hourly variation of temperature values for 25.04.2003

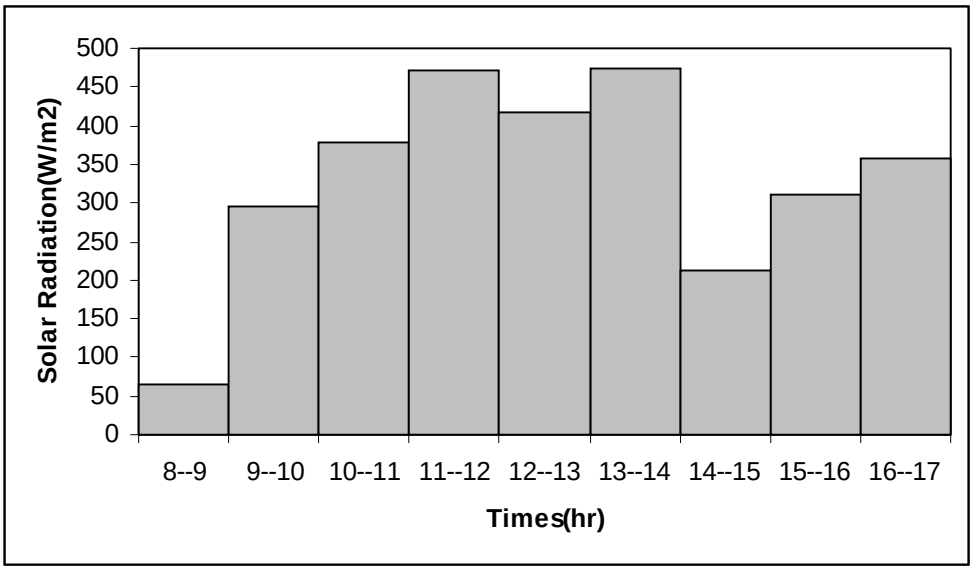

Figure E.17. Hourly variation of solar radiation for 25.04.2003

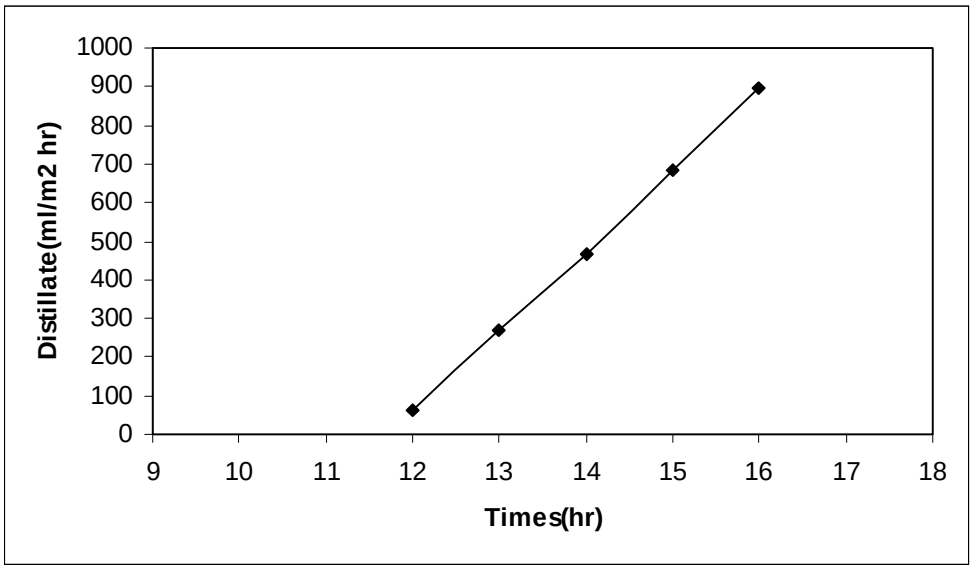

Figure E.18. Hourly variation of cumulative distillate output for 25.04.2003

Table E.7. Experimental and Theoretical Results for 28.04.2003

a-Experimental Results

28.04.2003 (with reflector) **Total Production:3130 ml**

Time(hr)	Tbottom	Tmoistair	Tinterface	Tglass	Tambient	RH(%)	Distillate(ml)
10	35,8	27,6	34	28,8	17	69	x
11	54,5	47,2	52,1	43,9	18	67	x
12	65,4	61,1	64,6	54,4	18	67	160
13	77,5	77,2	77,3	66,1	24	61	450
14	80,2	84,1	80	67,3	25	31	540
15	86,8	82,8	82,9	66,1	24	22	730
16	67,4	77,3	71,3	60	24	35	390
17	64,9	76,4	67,2	58,5	20	42	390
18	x	x	x	x	x	x	360
19	x	x	x	x	x	x	110

b-Theoretical Results

Time(hr)	Tbottom	Tmoistair	Tinterface	Tglass
10	47,14	25,85	39,67	21,1
11	62,26	45,01	53,47	25,97
12	73,91	58,19	64,12	28,65
13	89,06	76,38	79,12	35,98
14	94	83,3	84,88	37,87
15	89,84	80,24	81,81	35,62
16	82,72	77,2	77,38	34,28
17	76,98	74,78	73,66	29,76

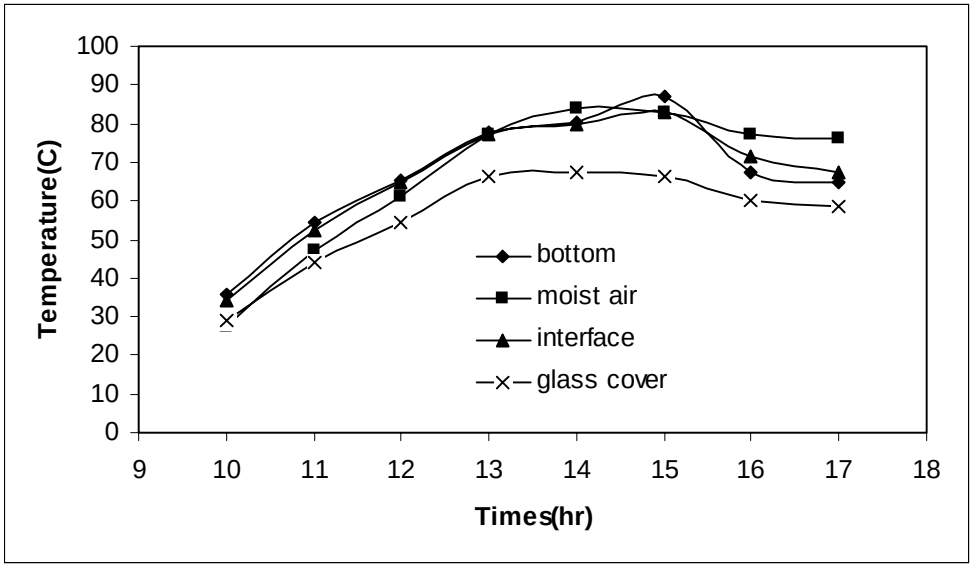

Figure E.19. Hourly variation of experimental temperature values for 28.04.2003

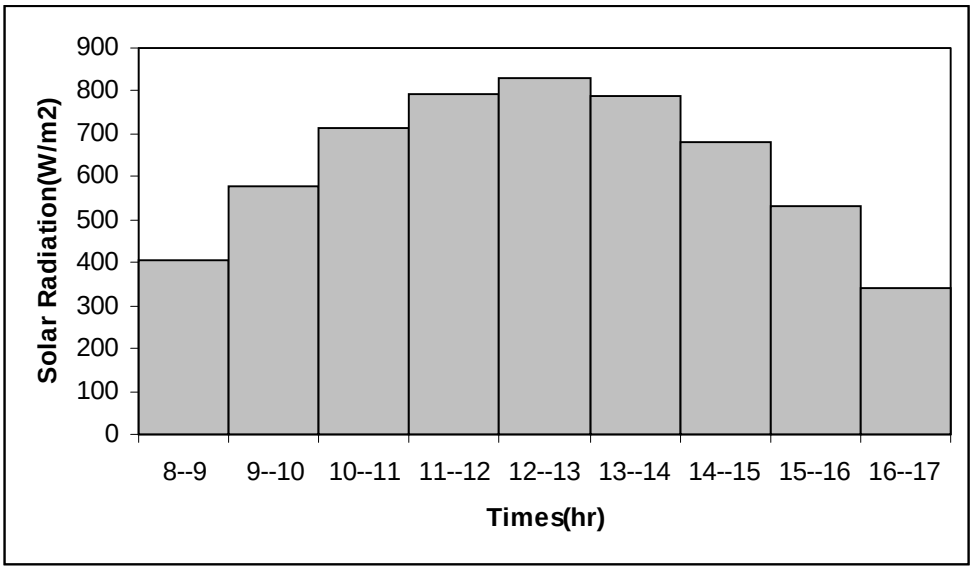

Figure E.20. Hourly variation of solar radiation for 28.04.2003

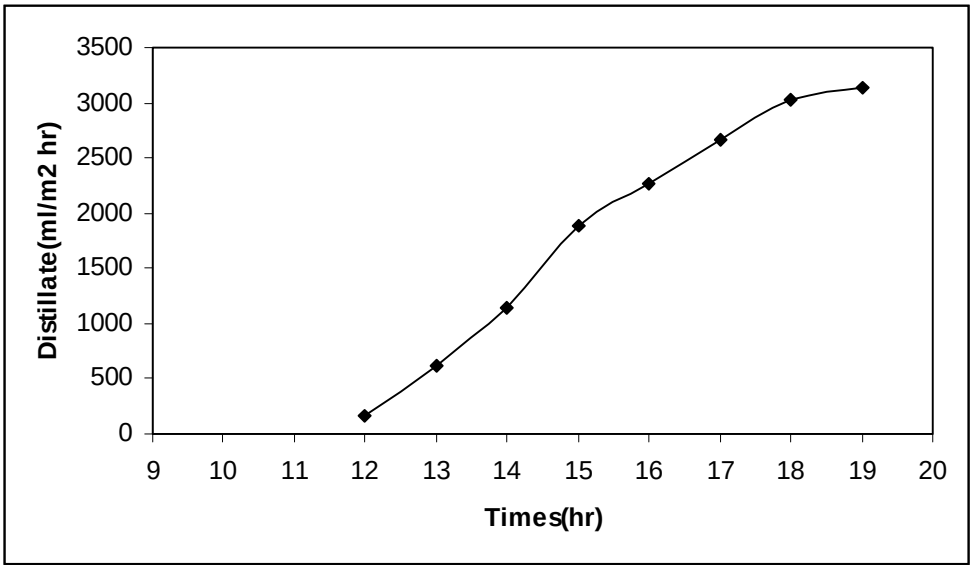

Figure E.21. Hourly variation of experimental cumulative distillate output for 28.04.2003

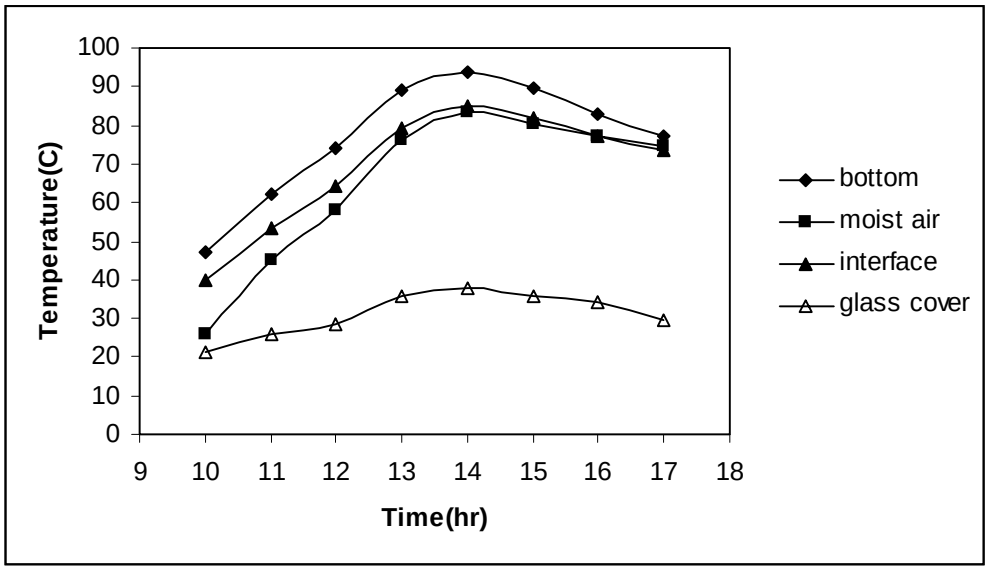

Figure E.22. Hourly variation of theoretical temperature values for 28.04.2003

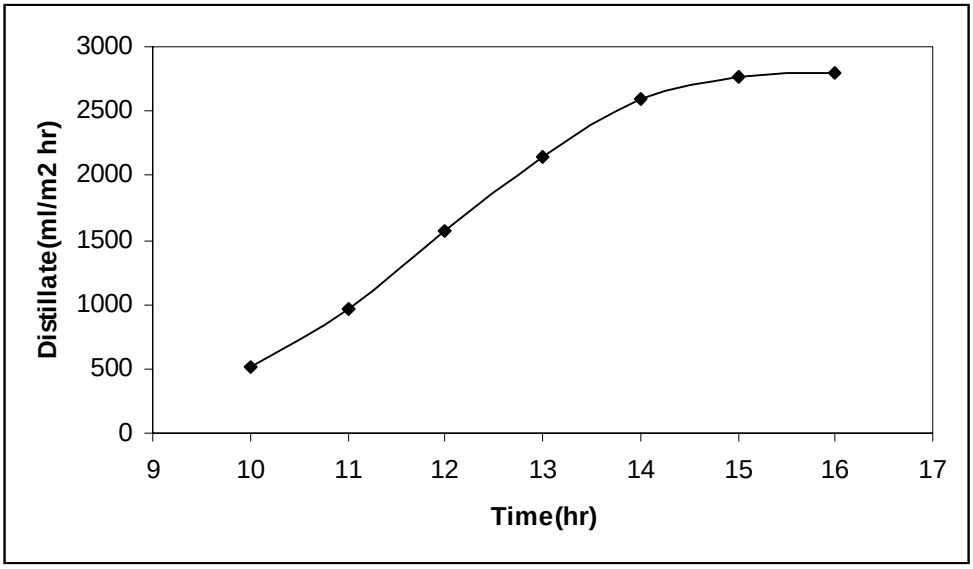

Figure E.23. Hourly variation of theoretical cumulative distillate output for 28.04.2003

Table E.8. Experimental and Theoretical Results for 29.04.2003

a-Experimental Results

29.04.2003 (with reflector) **Total Production:3040 ml**

Time(hr)	Tbottom	Tmoistair	Tinterface	Tglass	Tambient	Distillate(ml)
10	43	25,1	39,8	26,2	19	x
11	53,9	43,5	49,8	41,1	21	30
12	70	59,6	68,4	51,4	21	195
13	74,2	70	72,9	58,4	23	410
14	75,5	81,3	79,6	66,1	27	470
15	77,5	89,4	81,7	68,7	28	620
16	82,9	86,7	82,5	65,7	28	360
17	86,2	83,2	83,7	63,2	22	420
18	53,7	71,1	59,6	56	22	365
19	46,9	49,5	49,2	38,7	22	170

b-Theoretical Results

Time(hr)	Tbottom	Tmoistair	Tinterface	Tglass
11	59,5	41,47	50,93	27
12	74,73	58,65	64,72	30,65
13	84,2	71,18	74,49	34,92
14	92,25	80,89	82,82	39,01
15	90,13	80,56	82,04	38,93
16	87,89	81,8	82,12	37,86
17	84,89	80,61	80,48	30,97
18	71,25	70,65	68,92	29,75

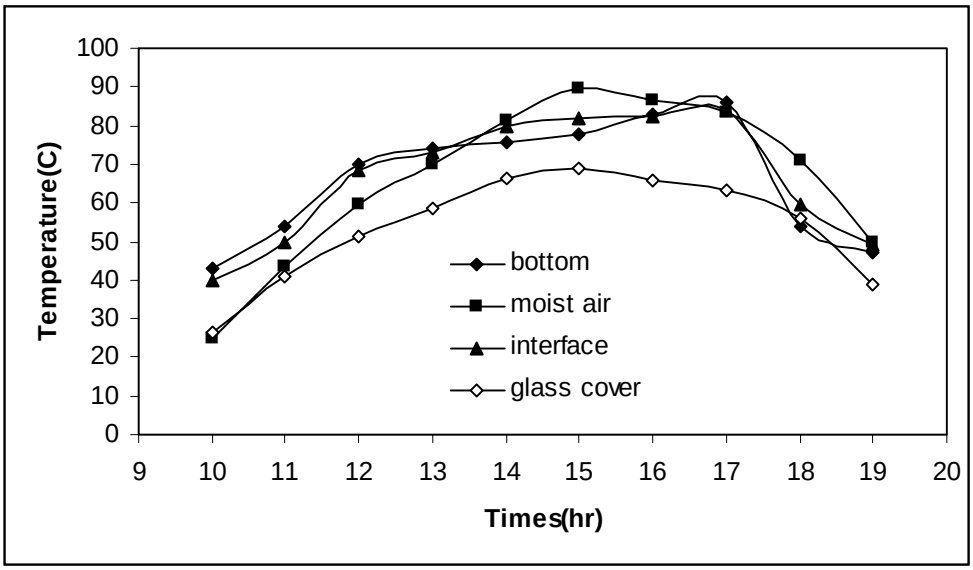

Figure E.24. Hourly variation of experimental temperature values for 29.04.2003

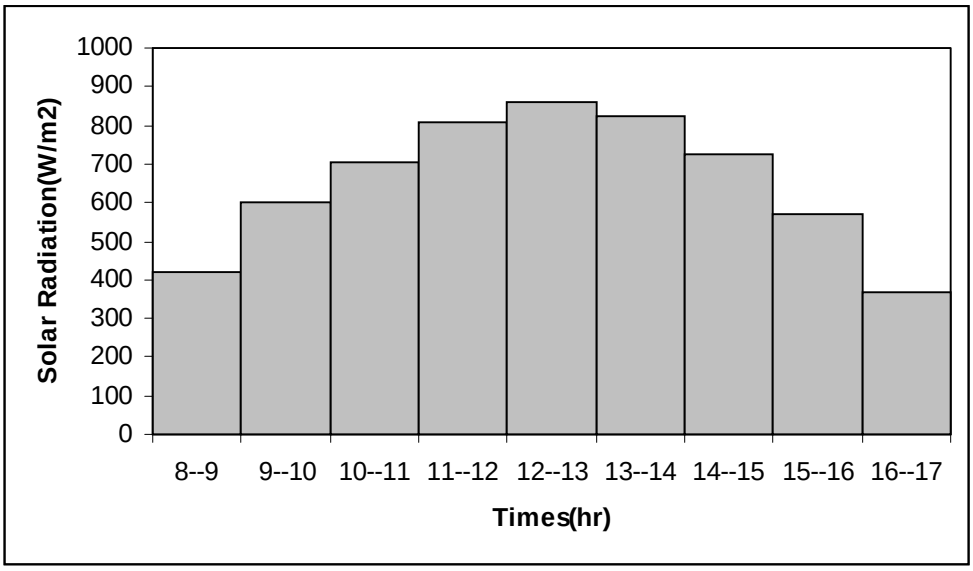

Figure E.25. Hourly variation of solar radiation for 29.04.2003

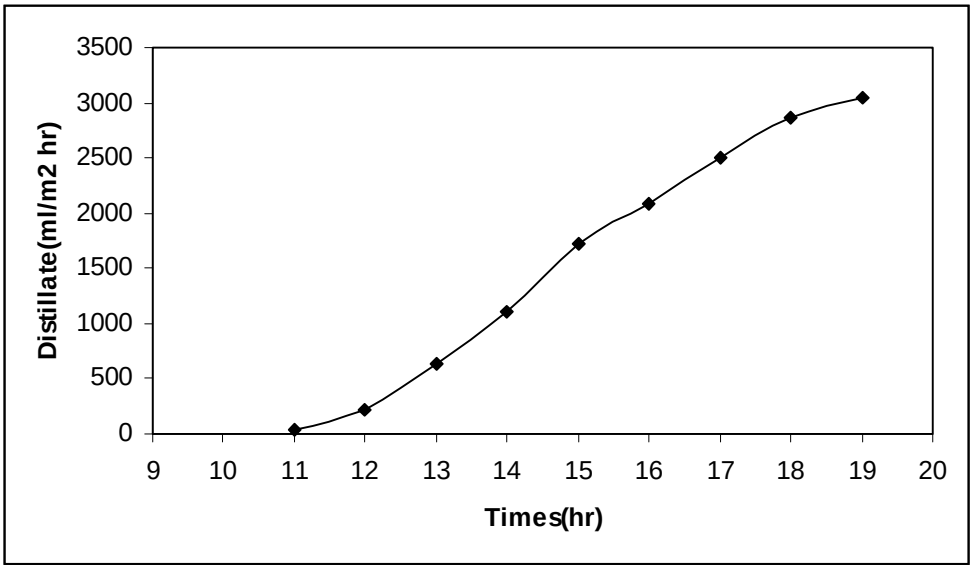

Figure E.26. Hourly variation of experimental cumulative distillate output for 29.04.2003

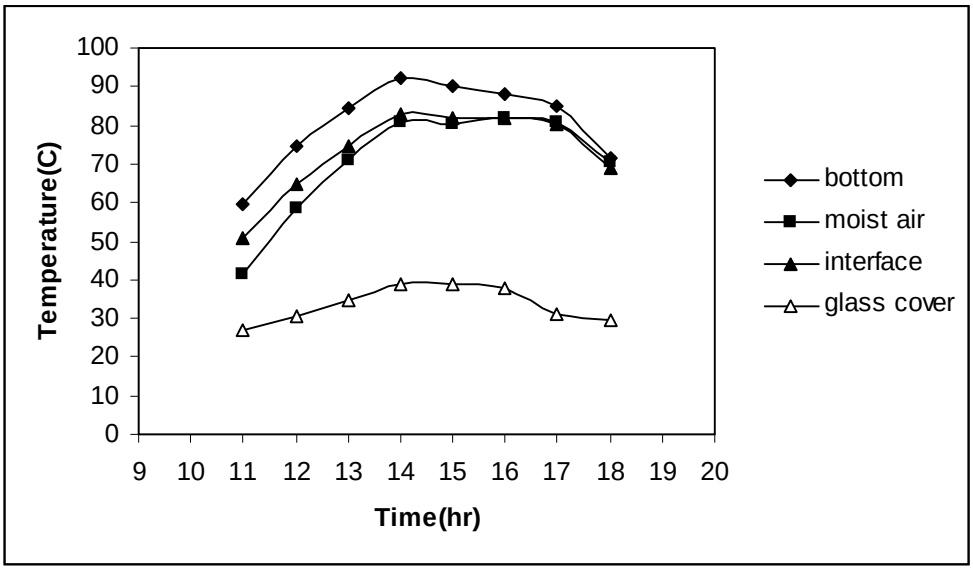

Figure E.27. Hourly variation of theoretical temperature values for 29.04.2003

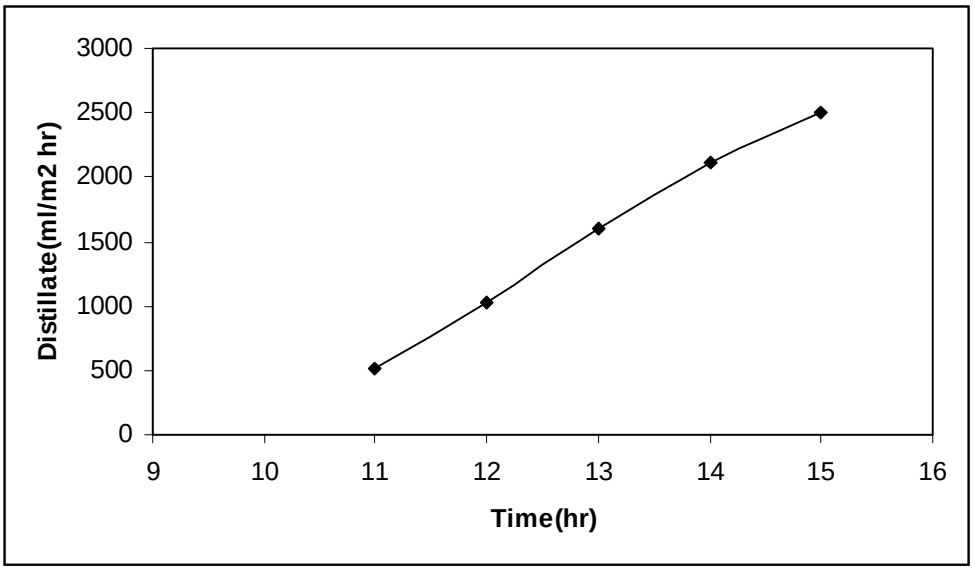

Figure E.28. Hourly variation of theoretical cumulative distillate output for 29.04.2003

Table E.9. Experimental Results for 30.04.2003

30.04.2003 (with reflector) **Total Production:2600 ml**

Time(hr)	Tbottom	Tmoistair	Tinterface	Tglass	Tambient	Distillate(ml)
10	44	24,9	40,6	27	21	x
11	56,8	44,7	55,7	45,2	22	40
12	74,5	63,2	73,3	57,5	21	160
13	82,1	83,5	82,7	69,7	30	490
14	85,1	91,6	84,1	73,4	25	425
15	78,9	90,6	78,9	69,7	29	550
16	73,8	86,9	73,9	65,3	30	495
17	70,4	83,2	71	61,2	22	440

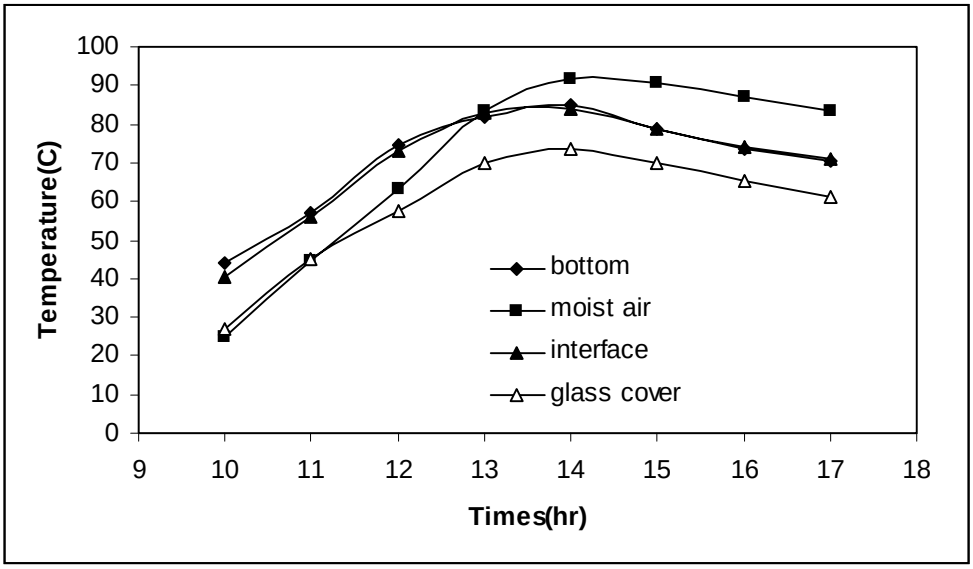

Figure E.29. Hourly variation of temperature values for 30.04.2003

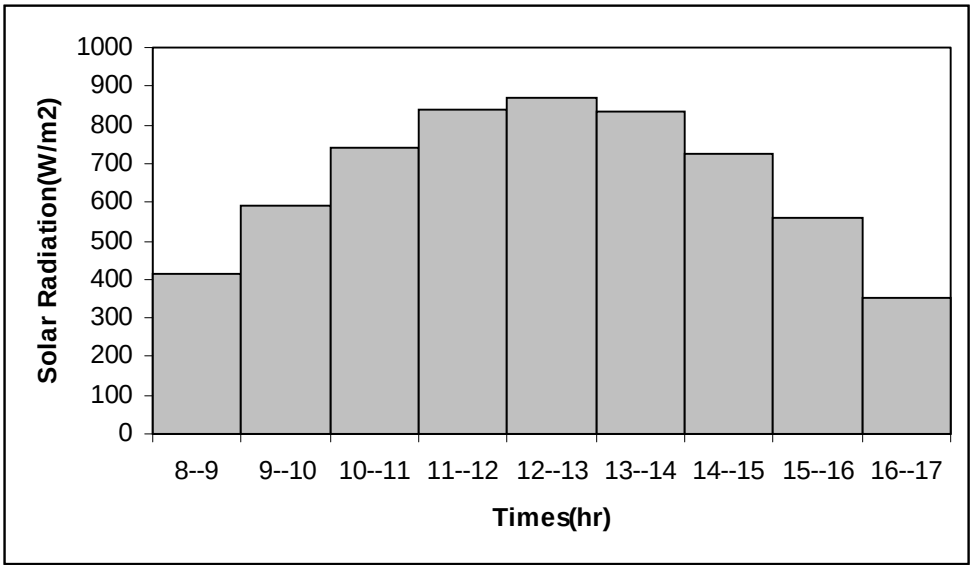

Figure E.30. Hourly variation of solar radiation for 30.04.2003

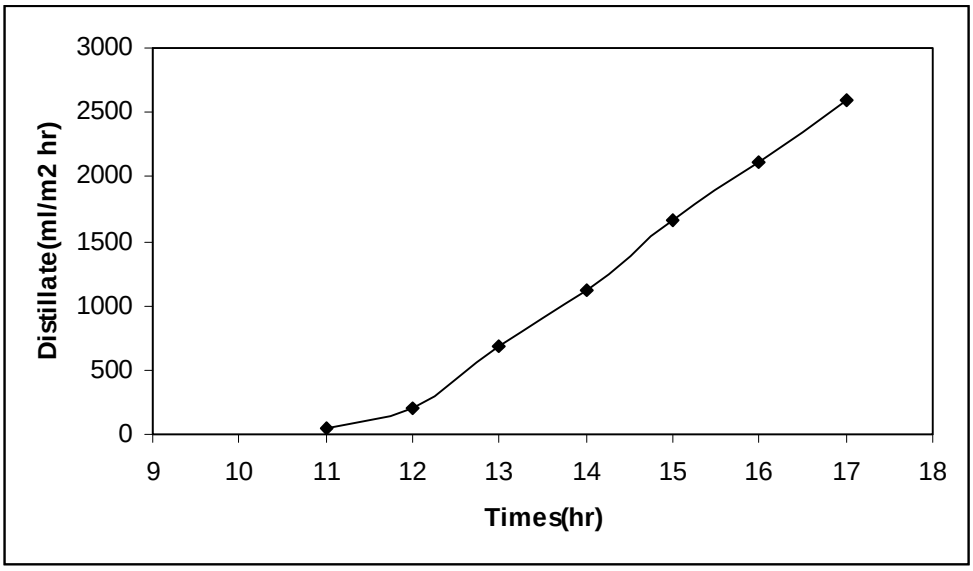

Figure E.31. Hourly variation of cumulative distillate output for 30.04.2003

Table E.10. Experimental Results for 02.05.2003

02.05.2003 (with reflector) **Total Production:2695 ml**

Time(hr)	Tbottom	Tmoistair	Tinterface	Tglass	Tambient	RH(%)	Distillate(ml)
9	17,6	18,1	17,4	18,3	20	71	x
10	37,7	30,3	37,5	31,5	20	72	x
11	59,7	48,5	59,6	45,3	22	66	20
12	74,6	63,2	71,7	55,3	24	63	240
13	81,2	80,9	77	65,5	24	61	395
14	84	91	84,6	74,2	24	52	600
15	82,4	94,1	85,4	75,1	24	24	520
16	76,6	90,4	78,8	71,1	28	26	500
17	69,3	83,1	70,6	63,3	26	44	420

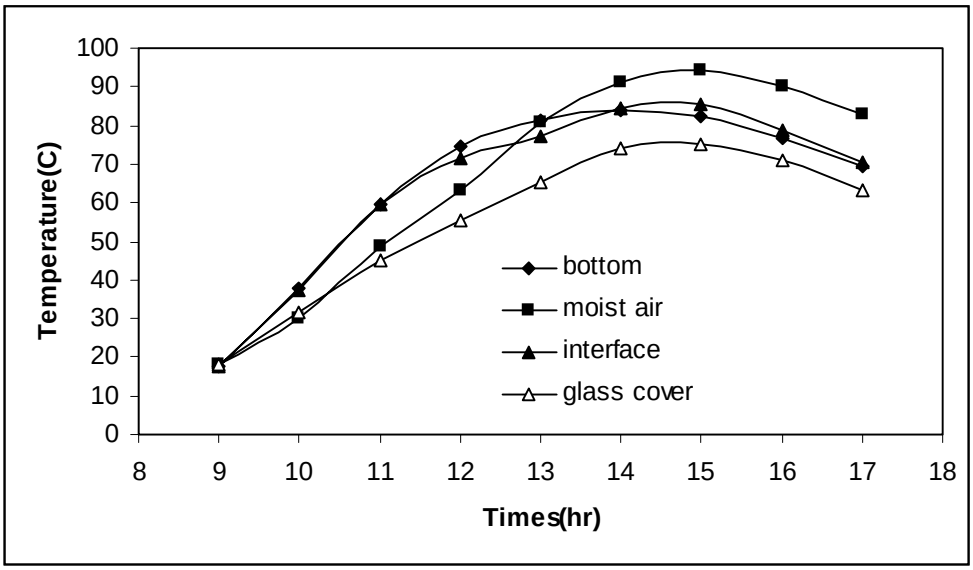

Figure E.32. Hourly variation of temperature values for 02.05.2003

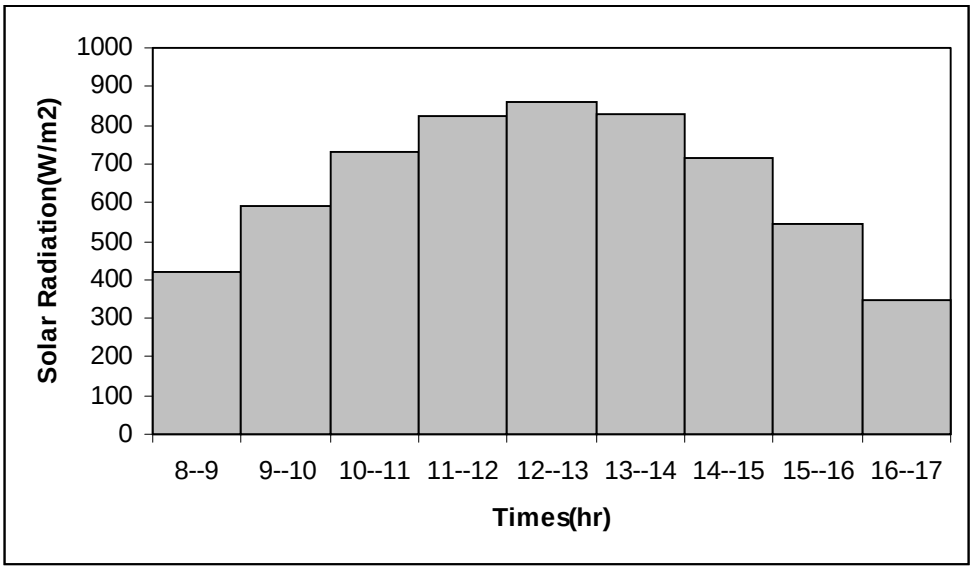

Figure E.33. Hourly variation of solar radiation for 02.05.2003

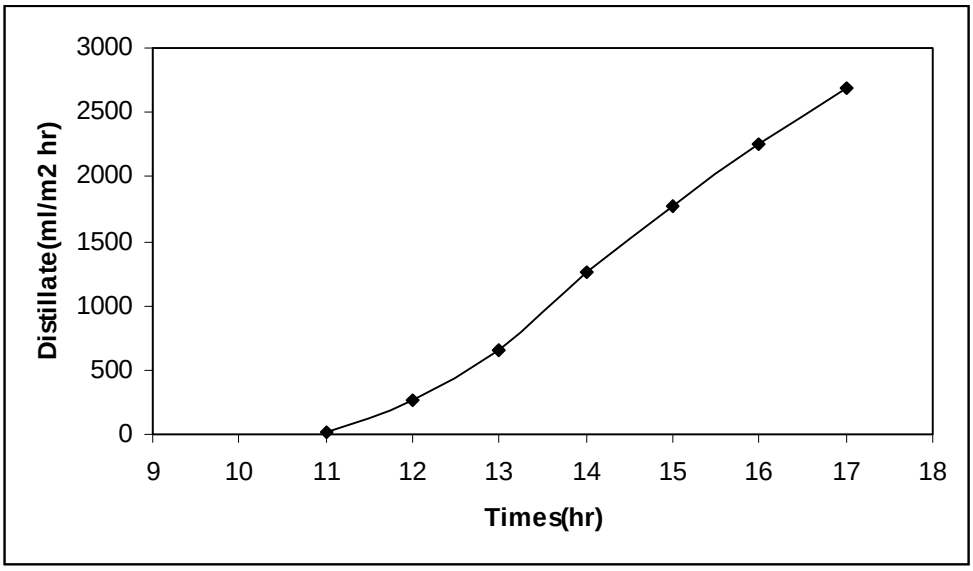

Figure E.34. Hourly variation of cumulative distillate output for 02.05.2003

Table E.11. Experimental Results for 09.05.2003

09.05.2003 **Without reflector** **Total Production:3615 ml**

Time(hr)	Tbottom	Tmoistair	Tinterface	Tglass	Tambient	Distillate(ml)
10	31,5	28,1	32,6	28	24	x
11	55,2	47,5	56,5	41,5	25	20
12	68	63,8	69,1	55,4	28	260
13	77,2	79,7	78,6	64,9	31	570
14	78,3	85,7	77,5	71,4	32	495
15	76,6	87,4	76,8	70,8	36	510
16	74,2	87,1	74,9	66,1	35	620
17	71,5	85,2	72,9	59,9	30	580
18	x	x	x	x	x	380
19	x	x	x	x	x	180

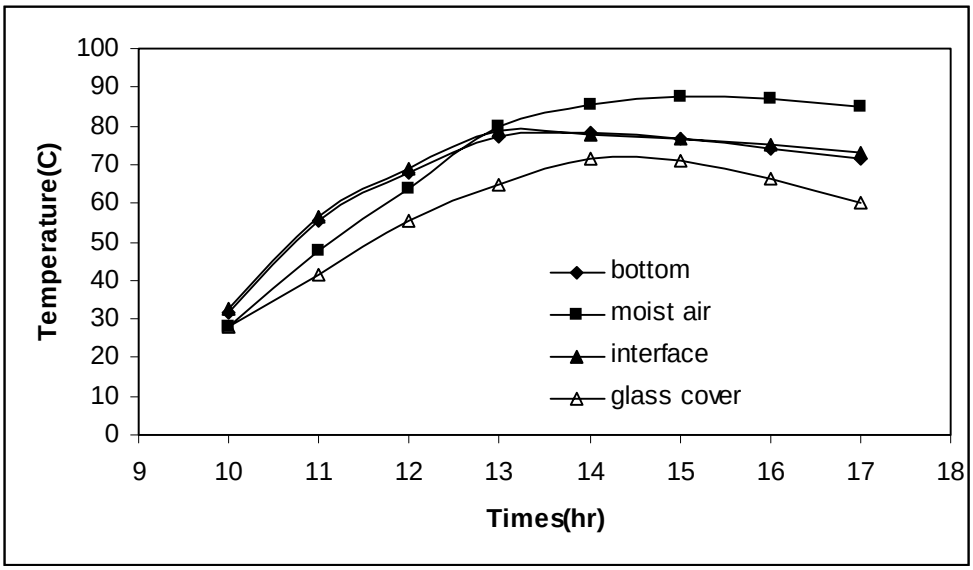

Figure E.35. Hourly variation of temperature values for 09.05.2003

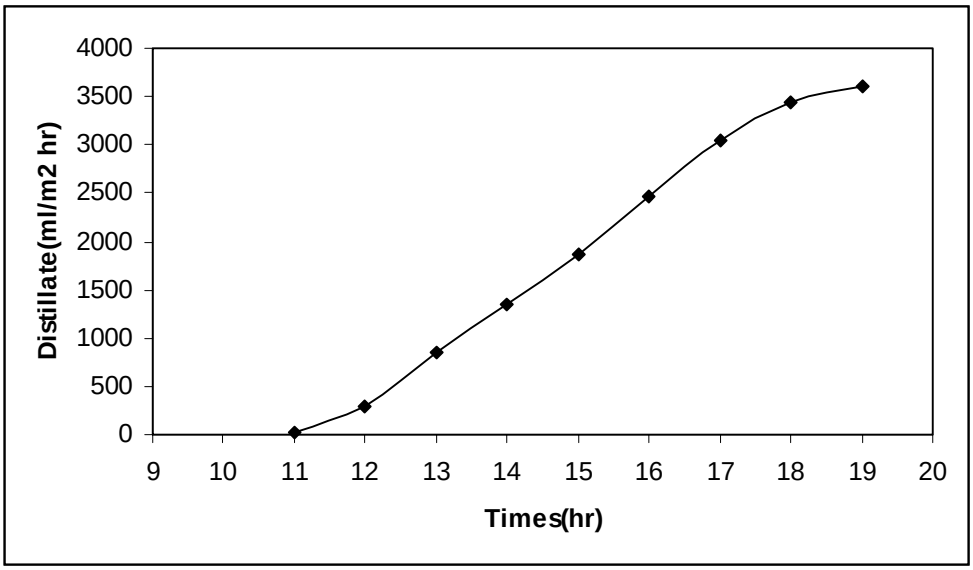

Figure E.36. Hourly variation of cumulative distillate output for 09.05.2003

Table E.12. Experimental Results for 12.05.2003

12.05.2003 Without reflector			Total Production:2540 ml			
Time(hr)	**Twater(C)**	**Tmoistair(C)**	**Tinterface(C)**	**Tglass**	**Tambient**	**Distillate(ml)**
10	28,8	27	30,3	29,1	24	x
11	55,1	47,6	53,8	46,1	27	10
12	72,3	68,5	71,4	58	30	250
13	78,6	79,1	78,1	68,2	30	310
14	80	85,7	80,8	69,2	30	480
15	77	85,3	75,2	65,3	34	750
16	71,8	83,3	72,5	64,1	33	420
17	68,1	80,2	68	62,1	30	320

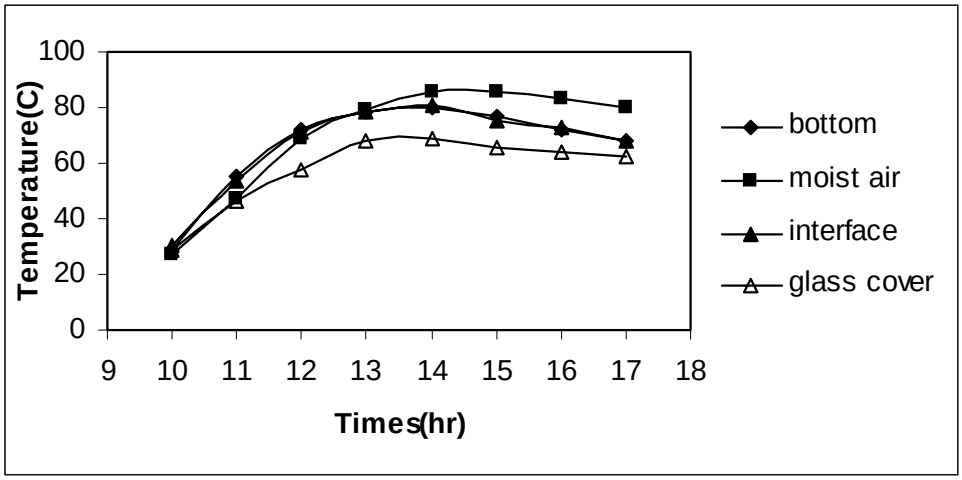

Figure E.37. Hourly variation of temperature values for 12.05.2003

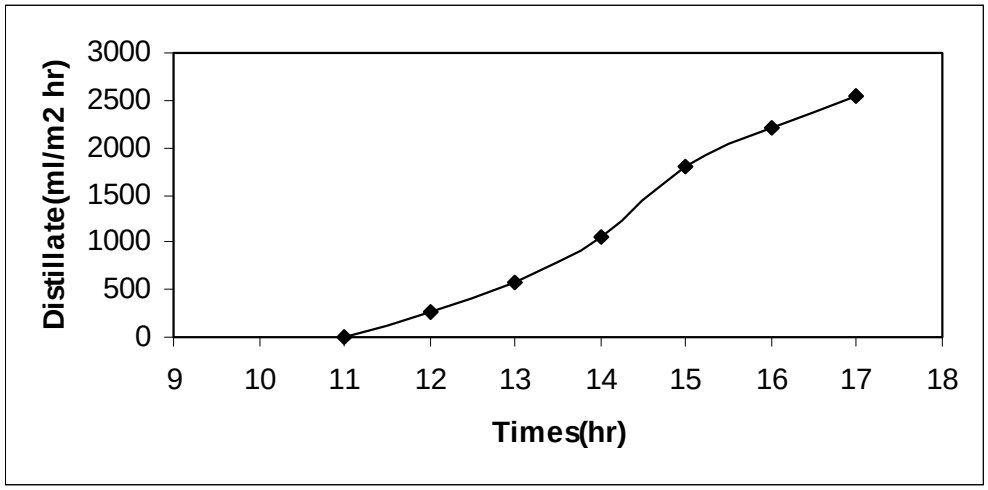

Figure E.38. Hourly variation of cumulative distillate output for 12.05.2003

APPENDIX F

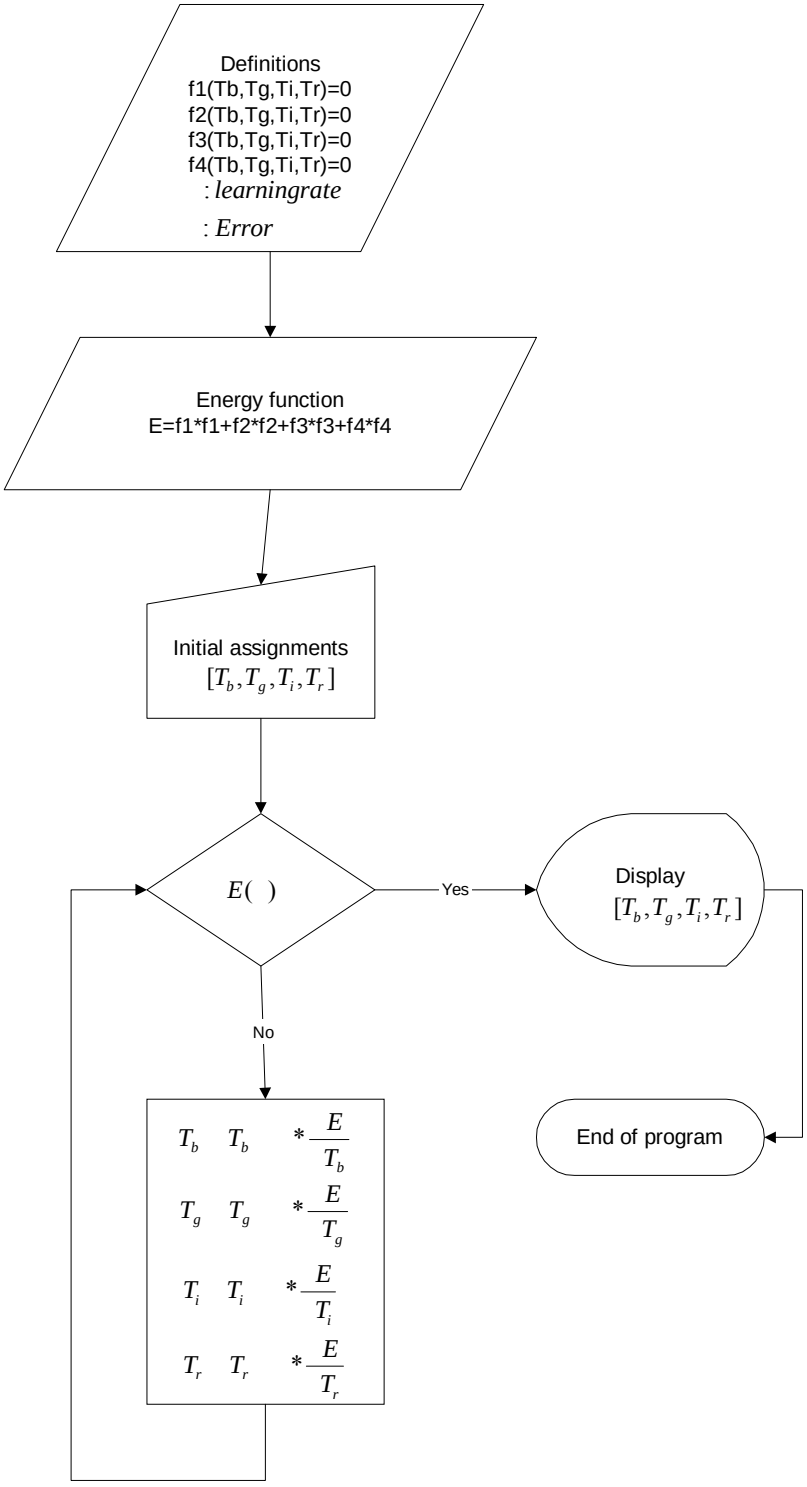

Figure F1. Flowchart of the Computer Program 2

APPENDIX G

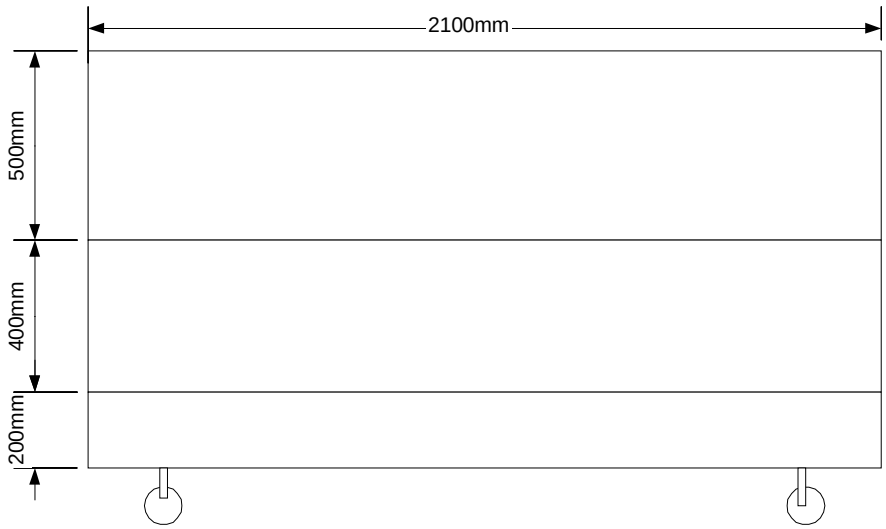

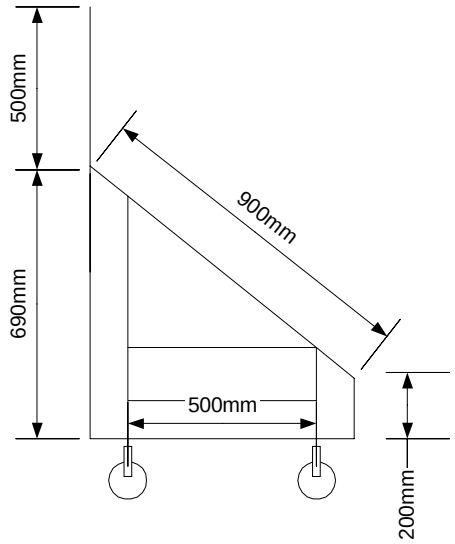

Figure G.1. Shematic view of the solar still